Gesellschaft für Anlagen- und Reaktorsicherheit (GRS) mbH

Values required for the simulation of CO2-storage in deep aquifers

GRS - 236

Gesellschaft für Anlagen- und Reaktorsicherheit (GRS) mbH

Values required for the simulation of CO2-storage in deep aquifers

Klaus-Peter Kröhn

May 2008

Remark:

This report was prepared under contract No. 03 G 0622 B with the German Federal Ministry for Economics and Technology (BMWi).

The work was conducted by the Gesellschaft für Anlagen- und Reaktorsicherheit (GRS) mbH.

The author is responsible for the content of this report.

GRS - 236
ISBN 978-3-939355-10-6

Keywords:
brine, CO^2-storage, deep aquifers, fluid properties, phase state, supercritical CO^2

Abstract

The mathematical description of the flow of supercritical carbon dioxide in deep saline aquifers is rather complex even if only the basic processes are considered. In the light of these complexities it is of vital importance to know the parameters and their dependencies as precise as possible. The present report compiles therefore the parameters and the referring approaches from the literature. For each parameter the source, the range of validity, at least one meaningful figure, a comment where necessary and conclusions with a view to the applicability of the formulation are also given. All required coefficients and auxiliary functions including the underlying dimensions are listed, too.

With this compilation an up-to-date set of mathematical formulations for fluid parameters to be used for modelling CO_2-storage in deep aquifers is available allowing immediate application. Moreover, it gives information about their dependencies on temperature, pressure and salinity.

Searching the literature it became apparent that there are still gaps in the knowledge of those formulations. This report includes therefore a short discussion of the state of knowledge referring to each constant and indicating where further research appears to be necessary.

Table of contents

1 Introduction

1.1 Motivation

The mathematical description of the movement of carbon dioxide in deep aquifers is rather complex even considering only the basic processes involved. These basic processes comprise

– multi-phase multi-component flow of water, carbon dioxide and salt,
– transport of dissolved components,
– heat flow, and
– phase changes.

The complexity originates from different reasons. Already the well-known mathematical description of a simple two-phase flow involves two coupled highly non-linear mass balance equations. In case of CO_2-storage in the underground an energy transport equation is to be solved, too. Temperature effects are primarily introduced by injecting the supercritical CO_2 at a temperature different from the surroundings, by phase changes and by the geothermal gradient. Non-isothermal conditions mean that the temperature-dependence of the parameters used in the equations must be taken into account. By this, several parameters introduce additional non-linearities into the mathematical description. The same applies also to the dependence on pressure and on the salt concentration of the groundwater.

While these complexities concern only the parameters in the equations, different sets of equations are to be used in case of changes of the phase state. When a phase appears or disappears the referring balance equation must be switched to comply with the physical problem. And to control the phase state additional parameters must be monitored.

In the light of all these complexities it is of vital importance to know the parameters and their dependencies as precise as possible. The present report compiles the required quantities and some of the referring approaches in order to provide a set of mathematical formulations. Despite the great effort that has gone into the task of getting a complete set containing only the most accurate formulations it must be acknowledged

that firstly, there are a lot more mathematical formulations in the literature than can possibly got hold of or even assessed within a reasonable period of pure research. Secondly, it became apparent, that there are still gaps of knowledge. What is given here, however, should more or less reflect the present state of the art in terms of CO_2-storage in the underground. The parameters addressed in this report are listed in Tab. 1.1.

Tab. 1.1 Processes and parameters of the CO_2 migration in the deep underground.

Process	Effect	Constant/Equation of state	Chapters
flow	advection	permeability relative permeability-saturation relation porosity viscosity density	2.3 3.2 2.2 4.3/5.4 4.2/5.3/6.1
	capillary pressure	capillary pressure-saturation relation	3.2
	phase changes	solubility vapour pressure	4.7/5.8 4.1/5.1
transport	diffusion	diffusion coefficient porosity tortuosity	4.8/5.9 2.2 2.3
	dispersion	(presently not enough knowledge [6])	-
heat flow	conduction	heat capacity thermal conductivity enthalpy geothermal gradient	4.6/5.7/6.3 0/5.5 4.5/5.6/6.2 2.5

The parameters concerning the matrix are generally described in chapter 2 but no values for a specific host rock are provided. In chapters 4, 5 and 6 the parameters and their formulations for water, carbon dioxide, and sodium chloride, respectively, are described and shortly evaluated. Chapter 7 begins with a discussion of the possible phase states of H_2O and CO_2. Criteria for phase changes and additional for this purpose required quantities are given further more. A discussion of the appropriateness of the described parameters and an appraisal of a possible need for research are given in chapter 8.

1.2 Conventions

The non-isothermal three-phase three-component system in a porous matrix is addressed in this report. The components are

– water,
– carbon dioxide, and
– salt.

The components will be denoted by the latin symbols i, j, etc. These components constitute phases that are dominated by one of the components. The greek symbols α, β, etc. will indicate these phases. Latin as well as greek symbols thus denote H_2O, CO_2, or NaCl, respectively, but have a different meaning.

If not stated otherwise component i is related to the α-phase, j to the β-phase and so on.

A phase dominated by the component i will be called the α-phase.

A quantity Q – the partial pressure for instance – of a component i in the phase β is written as Q_β^i, the superscript denoting the component and the subscript denoting the phase. This convention does not show the state of aggregation of the phase and thus includes the supercritical state.

If not specified otherwise the expression “water” refers to liquid water while “vapour” is used synonymeously for gaseous water.

For the conversion between bar and MPa 1 bar = 0.1 MPa is assumed if a more precise value not stated otherwise.

The formulations listed in this report are taken from a variety of sources. It has been tried to standardise the sections for each constant by giving them the following structure:

– source
– formulation including an explanation of the equations
– range of validity

– graphical plot
– comments
– conclusions

The dimension of input and output quantities may differ from section to section. The valid range of input data is hinted in the concerning paragraph “range of validity” while the dimension of the calculated quantity is given in the explanation of the variables. Since chapters 3 to 6 are exclusively devoted to properties of one component no special indices for the variables indicating the reference to the component are used if not necessary. The range of validity for a constant is considered to cover the relevant range for CO_2-sequestration if the following conditions are met:

pressure:	$0.1 < p < 30$ [MPa]
temperature:	$10 < T < 100$ [°C]
salinity:	$0 < m_{H_2O}^{NaCl} < 6.0$ [mol/kg]
CO_2 mass fraction:	$0 < m_{H_2O}^{CO_2} < 1.0$ [mol/kg]

(1.1)

p	-	pressure [MPa]
T	-	temperature [°C]
$m_{H_2O}^{NaCl}$	-	molality of NaCl in the water phase [mol/kg]
$m_{H_2O}^{CO_2}$	-	molality of CO_2 in the water phase [mol/kg]

2 Properties of the matrix

2.1 Preceding remark

While sequestration of CO_2 involves carbon dioxide and brine in any case the type of host rock envisaged will be site-specific. For this reason all parameters referring to a host rock will only be described in general. No specific data or functions will be given in this respect.

2.2 Porosity

Generally, the porosity Φ is given by the ratio of the pore volume V_p and the total volume V:

$$\Phi = \frac{V_p}{V} \qquad (2.1)$$

Φ - porosity [-]

V_p - pore volume [m³]

V - total volume [m³]

Care and attention are necessary with regard to the pore volume. Some processes take place everywhere in the pore space like diffusive solute transport. For other processes like fluid flow or advective solute transport only parts of the total pore volume are accessible. It is therefore advisable to define effective porosities for each process considered.

Other processes lead to changes of the pore volume. This can either be the result of changes of the matrix volume as in swelling clay particles, or the pore volume is changed by precipitation or dissolution. A third cause can be changes in the mechanical stress of the matrix. Porosity changes relating to the precipitated/dissolved mass can be described by

$$\Delta\Phi = -\frac{\Delta m_s}{\rho_s V} \qquad (2.2)$$

$\Delta\Phi$ - porosity change due to precipitation/dissolution [-]

Δm_s - change of solid mass due to precipitation/dissolution [-]

ρ_s - density of the solid mass [kg/m³]

2.3 Tortuosity

On the pore scale the coefficient of molecular diffusion suffices to correctly describe the process of diffusion. But for practical purposes modelling can only be done on a macroscopic scale. Averaging the diffusional fluxes in an REV (Representative Elementary Volume) lets appear a second-rank tensor for the tortuosity which accounts for the fact that there is no straight-line diffusional flow due to the solid matrix. Assuming an isotropic porous medium the tensor can be reduced to the well-known scalar tortuosity τ that takes into consideration the twisting of the flow paths. The tortuosity is theoretically a property of the porous medium. However, a value cannot even vaguely be assigned to a specific situation and so the tortuosity is rather a fit constant than a known quantity. It cannot exceed the value of 1 which means no solid matrix is present, but it can theoretically reach any value between 0 and 1.

2.4 Permeability

The permeability is generally assumed to be a function of the porosity:

$$k = k(\Phi) \qquad (2.3)$$

k - permeability [m²]

Φ - porosity [-]

Several models exist for the theoretical derivation of a permeability-porosity relation:

– Capillary bundle model
– Empirical model with porosity and permeability limits
– A simple model considering piecewise constant but changing flow path cross-section

All these models yield an exponential relation between permeability and porosity. In the capillary bundle model permeability becomes zero when the porosity reaches zero. In the other two models, though, permability vanishes already at a critical porosity $\Phi_c > 0$.

The third model has been used to simulate salt precipitation [45]. For the sake of simplicity it is assumed here that the flow channels consist of cylindrical sections with two different cross-section areas. The section with the large cross-section area A_1 represents the pore, and the section with the small cross-section area A_2 represents the bottleneck between two pores. In order to develop a model the sections are arranged in such a way that all sections with the same size are put together as indicated in Fig. 2.1. The total length of the flow path l is then subdivided into two segments l_1 und l_2.

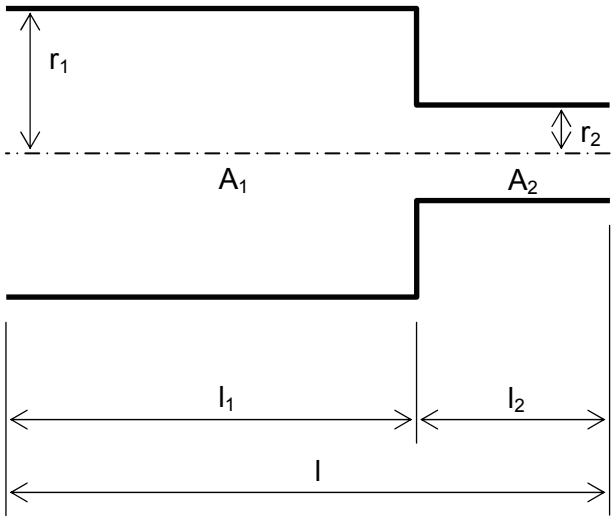

Fig. 2.1 Idealised model of a flow channel with varying cross-section area.

Using the standardised length ξ

$$\xi = \frac{l_1}{l} \qquad (2.4)$$

ξ - standardised length for the wider segment [-]

l_1 - length of the wider segment [m]

l - total length of the flow path [m]

the ratio of the cross-sectional areas ω

$$\omega = \frac{A_1}{A_2} \qquad (2.5)$$

ω - ratio of the cross-sectional areas [-]

A_1 - cross-section area of the wider segment [m²]

A_2 - cross-section area of the smaller segment [m²]

and the standardised porosity φ

$$\varphi = \frac{\Phi - \Phi_c}{\Phi_0 - \Phi_c} \qquad (2.6)$$

φ - standardised porosity [-]

Φ_0 - initial porosity [-]

Φ_c - critical porosity [-]

the permeability can be expressed as a function of porosity [45]:

$$\frac{k}{k_0} = \varphi^2 \frac{\frac{\xi}{\omega^2} + 1 - \xi}{\xi\left(\frac{\varphi}{\omega + \varphi - 1}\right)^2 + 1 - \xi} \qquad (2.7)$$

k_0 - initial permeability [m²]

2.5 Depth-dependent temperature

Due to heat flow from earth's interior the temperature in the earth crust rises with depth. This increase is approximately linear from the surface down to a few kilometres depth except for the upper 10 metres where seasonal temperature changes can be detected. For a formulation for the depth-dependent temperature information on the mean surface temperature and the temperature gradient is required.

In Germany the mean temperature at 10 m depth amounts to 8 °C to 10 °C [51] and the mean geothermal gradient to 30 °C/km [47]. The mean global thermal gradient is specified by [51] to be 25 °C/km. The gradient depends on the local geology and can therefore deviate considerably from the mean value. With appropriate caution the value of 30 °C/km will be adopted for a generic site in Germany.

3 Properties depending on matrix and fluids at the same time

3.1 General remarks

The mathematical description of two-phase flow in a porous medium requires additional equations of state (EOS) referring to the effect of capillarity and to the mutual impediment of flow of one phase by the other phase. Both can be formulated as a function of the saturation S_α of the α-phase meaning the volumetric fraction of pore space that is occupied by the α-phase. The resulting capillary pressure-saturation relation and the relative permeability-saturation relation make the mathematical formulation highly non-linear. Reliable predictions of two-phase flow depend therefore particularly on a good representation of the flow system by these two EOS.

Note: In case of CO_2 flowing upward to the surface a three-phase state with water, liquid and gaseous CO_2 is likely to evolve [35]. We are not aware of equations of state for this specific problem and will therefore restrict the following discussion to two-phase flow problems.

3.2 Two-phase flow equations of state

According to the Young-Laplace-equation

$$p_c = \frac{2\sigma \cos \alpha}{r} \qquad (3.1)$$

p_c - capillary pressure [Pa]

σ - interfacial tension [N/m]

r - curvature radius [m]

α - wetting angle between solid surface and phase interface [-]

capillary pressure at a phase boundary depends on interfacial tension σ and on

– the radius r of a bubble or droplet,

– the radius r of a cylindrical flow channel or

– half of the aperture d of a planar flow regime.

Even without considering the wetting angle between solid surface and phase interface, which is often neglected, properties of the fluids as well as properties of the matrix are involved in an equation of state for the capillary pressure. The interfacial tension depends on the combination of fluids that have contact at the interface, on pressure and on temperature. In case of the combination brine-CO_2 the interfacial tension increases with increasing temperature, with increasing water salinity and with decreasing pressure [3].

On pore size scale capillary pressure can fairly well be calculated. But for modelling purposes a formulation on the macroscopic scale is required. Though there exist several theoretical approaches to explain the effect of capillary pressure - best known are the formulations by Brooks and Corey [8] or by van Genuchten [18], a reliable formulation can be derived only empirically from measurements. The geometry of the pore space as well as the characteristic pore size distribution for a certain rock type are generally more complex than the rather simple conceptual models underlying the theoretically derived formulations. For the same reason it is necessary to measure relative permeability-data, too, even if theory allows to derive permeability-saturation relations using the same parameters as in the referring capillary pressure-saturation.

Measurements for the two EOS are often not available for the porous medium in question. In such a situation Leverett's dimensionless J-function [29]

$$J(S_w) = \frac{p_c(S_w)\sqrt{\frac{k}{\Phi}}}{\sigma \cos \alpha} \qquad (3.2)$$

J - Leverett's J-function [-]

p_c - capillary pressure [Pa]

k - permeability [m²]

Φ - porosity [-]

is often used to transform a capillary pressure-relation for a known porous medium to a new relation for another one. Only permeability and porosity of the unknown medium must be identified. This method is quite popular since two-phase flow measurements are expensive. But it has some severe limitations. Leveretts scaling method is not valid for

certain ranges of wetting angles, and, additionally, the wetting angle itself is dependent on the interfacial tension [22].

Furthermore, Leveretts approach yields only qualitatively similar EOS. But especially in case of CO_2 storage where the storage strata can be located in a wide range of depths the in-situ conditions referring to pressure, temperature and salinity may vary significantly from the conditions applied during the laboratory measurements. This means differences in the interfacial tension which in turn can not only change the scale of the EOS considerably but also the values for the residual saturation of brine and of CO_2 [3]. Trapping of CO_2 in isolated bubbles at the residual CO_2-saturation happens in the wake of a CO_2-plume after shutdown of injection and strongly influences further movement of the plume. Leverett's scaling method may therefore cause misleading model results in the end.

For all these reasons, the EOS for two-phase flow are ideally measured in the laboratory and under in-situ conditions at that. If such data are not available - as is mostly the case - conclusions by analogy referring to the EOS should be drawn with extreme caution.

3.3 Hydrodynamic dispersion

The phenomenon of dispersion is well known in the context of single-phase transport problems. It is introduced by switching from a microscopic to a macroscopic observation level. Dispersion describes the spreading of transported matter by the splitted and tortuous flow channels on the microscopic level. For single-phase modelling the approach of [36] is generally used.

Contrary to single-phase flow and transport this phenomenon states a serious problem for two-phase flow. Approaches as well as referring parameters are scarce [6] and hard to come by since a saturation-dependent tortuosity has to be considered. It is therefore often neglected in two-phase flow simulations.

4 Properties of water

4.1 Vapour pressure

4.1.1 Vapour pressure of pure water

Source: [23]

Formulation:

$$\frac{p_s}{p*} = \left[\frac{2C}{-B + (B^2 - 4AC)^{1/2}} \right]^4 \qquad (4.1)$$

p_s - vapour saturation pressure [MPa]

$p*$ - reference pressure (c.f. Appendix B)

A, B, C - ansatz functions (q.v. eq. (4.2))

$$\begin{aligned} A &= \vartheta^2 + n_1\vartheta + n_2 \\ B &= n_3\vartheta^2 + n_4\vartheta + n_5 \\ C &= n_6\vartheta^2 + n_7\vartheta + n_8 \end{aligned} \qquad (4.2)$$

ϑ - ansatz function (q.v. eq. (4.3))

n_1 to n_6, - constants (c.f. Appendix B)

$$\vartheta = \frac{T}{T*} + \frac{n_9}{\left(\frac{T}{T*}\right) - n_{10}} \qquad (4.3)$$

T - temperature [K]

T^* - reference temperature (c.f. Appendix B)

n_9, n_{10}, - constants (c.f. Appendix B)

Range of validity:

temperature: 273.15 K < T ≤ 647.096 K

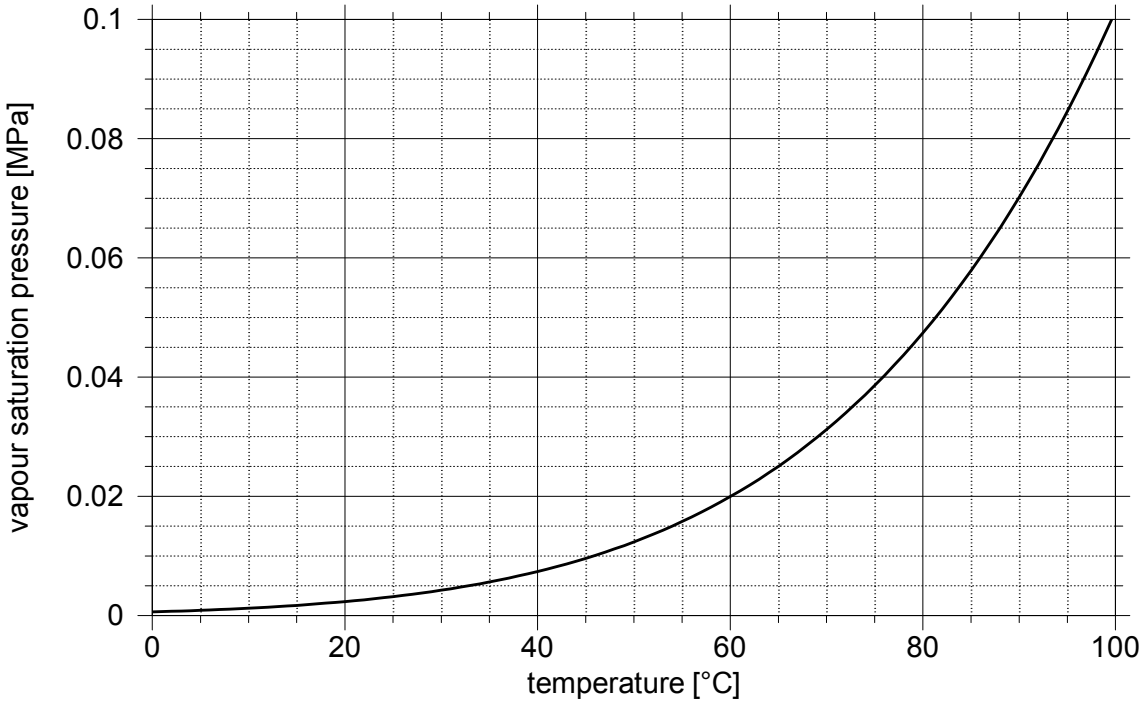

Fig. 4.1 Vapour pressure of pure water; after [23].

Conclusions: Eq. (4.1) is a reliable formulation within the ranges (1.1).

4.1.2 Vapour pressure of water with dissolved NaCl

Source: [21], [4]

Formulation:

$$\ln p_s = e_0 + \frac{e_1}{z} + \frac{e_2 w}{z} + \left[10^{(e_3 w^2)} - 1\right] + e_4 10^{(e_5 y^{1.25})} \qquad (4.4)$$

p_s - vapour saturation pressure [bar]

e_0 to e_5 - constants (c.f. Appendix B)

y - ansatz function (q.v. eq. (4.5))

z - ansatz function (q.v. eq. (4.6)

w - ansatz function (q.v. eq. (4.7))

$$y = 647.27 - T_0 \qquad (4.5)$$

T_0 - temperature of pure water (referring to brine temperature via eq. (4.8)) [K]

$$z = T_0 + 0.01 \qquad (4.6)$$

$$w = z^2 - e_6 \qquad (4.7)$$

e_6 - constant (c.f. Appendix B)

$$\ln T_0 = f \ln T \qquad (4.8)$$

T - brine temperature [K]

f - ansatz function (q.v. eq. (4.9))

$$f = \frac{1}{(a + bT)} \qquad (4.9)$$

a - ansatz function (q.v. eq. (4.10))

b - ansatz function (q.v. eq. (4.11))

$$a = 1 + a_1 m + a_2 m^2 + a_3 m^3 \qquad (4.10)$$

m - molality of NaCl in the water-phase [mol/kg]

a_i - constants (c.f. Appendix B)

$$b = 0 + b_1 m + b_2 m^2 + b_3 m^3 + b_4 m^4 + b_5 m^5 \qquad (4.11)$$

b_i - constants (c.f. Appendix B)

Range of validity:

temperature: 353.15 K < T ≤ 647.096 K for eq. (4.4)

and 262.15 K < T < 623.15 K for eq. (4.8)

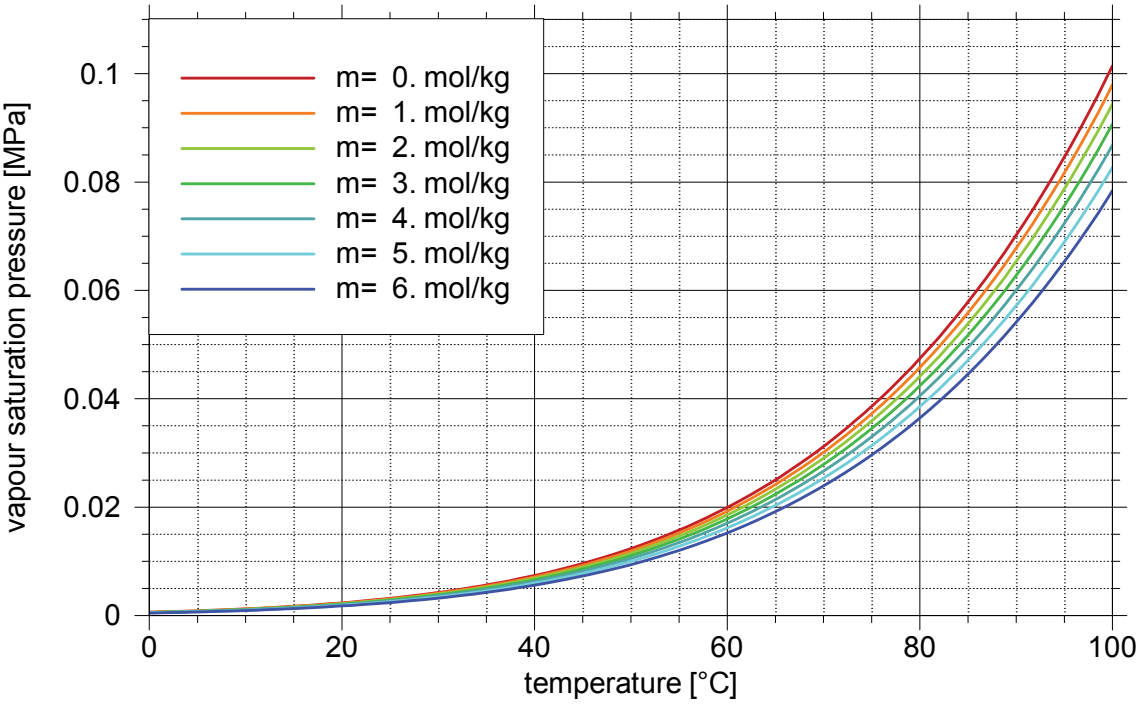

Fig. 4.2 Vapour saturation pressure of brine; after [21].

Comments:
The formulation for the vapour pressure of brine from [21] contains the physically meaningful constant T_0. This constant is the temperature of pure water and is related to the brine temperature T_x at the same vapour saturation pressure by eq. (4.8).

For two reasons this approach is not entirely satisfying in the framework of CO_2-sequestration. Firstly, it is valid only in a temperature range that is clearly beyond the range of interest. Secondly, the calculated vapour pressure with a salt concentration of 0 and a temperature of 100 °C should result in a value of about 0.1 MPa but instead yields about 0.25 MPa.

An improvement is suggested by [4] starting with eq. (4.8) but subsequently using the formulations of [25] for the vapour pressure of pure water. Fig. 4.3 shows a comparison of the formulation of [21] and the equivalent vapour pressure using the approach of [23][1]. The results with the equivalent vapour pressure appear to be more credible than

[1] Note that the formulations in [23] are an updated version of the formulations suggested in [25].

the approach of [21]. It has to be mentioned, though, that [21] as well as [4] claim that the computed vapour saturation pressures are in good agreement with measured data despite the significant differences in the sets of curves shown in Fig. 4.3.

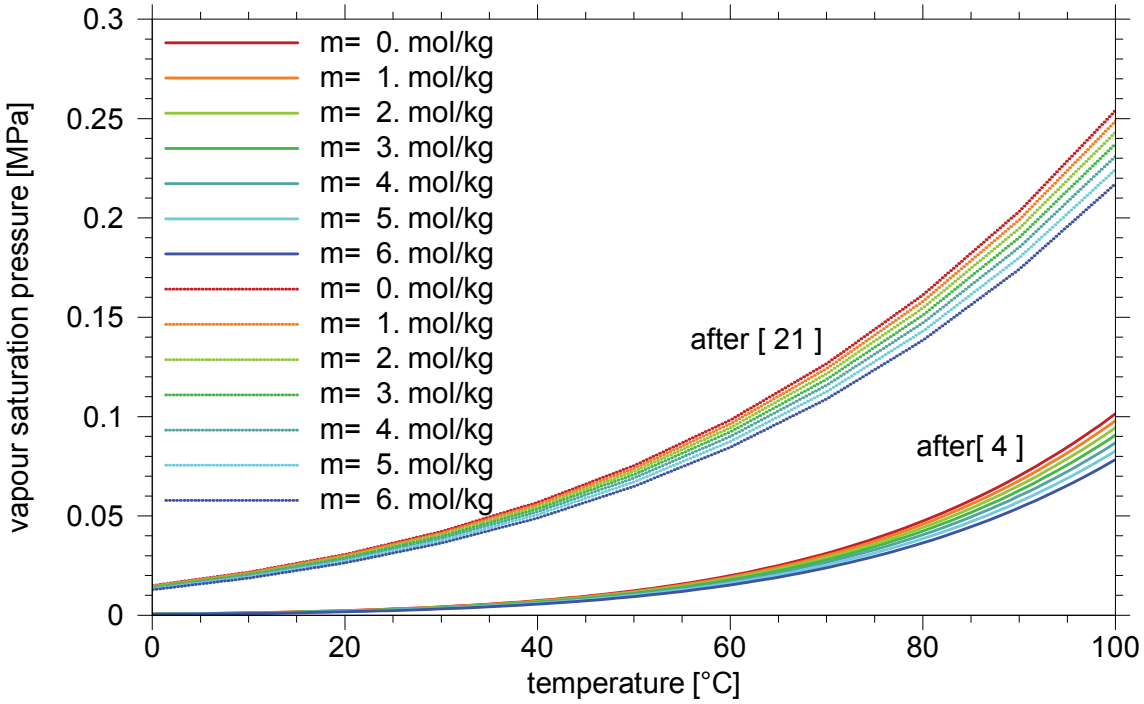

Fig. 4.3 Vapour saturation pressure after [21] and the equivalent pure water vapour pressure after [4].

Conclusions: Eq. (4.8) in combination with eq. (4.1) seems to be a reliable formulation within the ranges (1.1). It should be checked against measured data, though.

4.1.3 Vapour pressure of water with dissolved CO_2

Comments: We are not aware of formulations concerning vapour pressure of water with dissolved CO_2.

4.1.4 Vapour pressure of water with dissolved NaCl and CO_2

Comments: We are not aware of formulations concerning vapour pressure of water with dissolved NaCl and CO_2.

4.2 Density

4.2.1 Density of pure water

The approaches for the water density presented in the next two sections are given in [23]. They actually provide data for the specific volume of pure liquid water as well as of water vapour. The specific volume is the reciprocal of the density.

4.2.1.1 Density of liquid water

Source: [23]

Formulation:

$$\rho = \frac{1}{\nu} \qquad (4.12)$$

ρ - water density [kg/m³]

ν - specific volume [m³/kg]

$$\nu \frac{p}{R_{H_2O} T} = \pi \gamma_\pi \qquad (4.13)$$

p - pressure [MPa]

T - temperature [K]

R_{H_2O} - specific gas constant for water vapour (c.f. Appendix B)

π - standardised pressure (q.v. eq. (4.14)) [-]

γ_π - ansatz function (q.v. eq. (4.15))

$$\pi = \frac{p}{p*} \qquad (4.14)$$

p^* - reference pressure (c.f. Appendix B)

$$\gamma_\pi = \sum_{i=1}^{34} -n_i I_i (7.1-\pi)^{I_i - 1} (\tau - 1.222)^{J_i} \qquad (4.15)$$

τ - standardised temperature (q.v. eq. (4.16) [-]

n_i, I_i, J_i - constants (c.f. Appendix B)

$$\tau = \frac{T^*}{T} \qquad (4.16)$$

T^* - reference temperature (c.f. Appendix B)

Range of validity:

temperature: 273.15 K < T < 623.15 K

pressure: $p_s(T) < p <$ 100 MPa

$p_s(T)$ - vapour saturation pressure [MPa] (q.v. eq. (4.1))

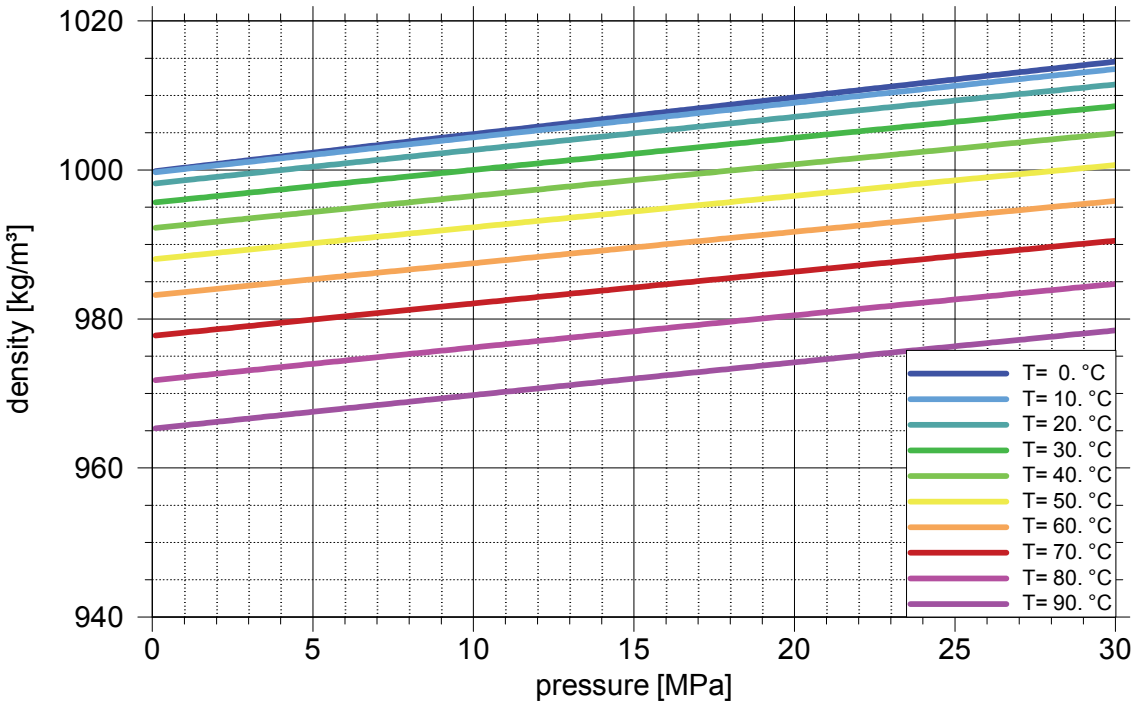

Fig. 4.4 Density of pure liquid water; after [23].

Conclusions: Eq. (4.13) is a reliable formulation within the ranges (1.1).

4.2.1.2 Density of water vapour

Source: [23]

Formulation:

$$\nu \frac{p}{R_{H_2O} T} = \pi\left(\gamma_\pi^0 + \gamma_\pi^r\right) \qquad (4.17)$$

ν - specific volume [m³/kg] (q.v. eq. (4.12))

p - pressure [MPa]

T - temperature [K]

R_{H_2O} - specific gas constant for water vapour (c.f. Appendix B)

γ_π^0 - ansatz function (q.v. eq. (4.18)) [-]

γ_π^r - ansatz function (q.v. eq. (4.19))

$$\gamma_\pi^0 = \frac{1}{\pi} \qquad (4.18)$$

π - standardised pressure (c.f. eq. (4.14)) [-]

p^* - reference pressure (c.f. Appendix B)

$$\gamma_\pi^r = \sum_{i=1}^{43} n_i I_i \pi^{I_i - 1} (\tau - 0.5)^{J_i} \qquad (4.19)$$

τ - standardised temperature (q.v. eq. (4.16)) [-]

T^* - reference temperature (c.f. 0)

n_i, I_i, J_i - constants (c.f. Appendix B)

Range of validity:

temperature: 273.15 K $\leq T \leq$ 623.15 K

pressure: 0 MPa < p < $p_s(T)$

Comments: Eq.s (4.12), (4.14) and (4.16) are needed again for calculating the vapour density from the specific volume.

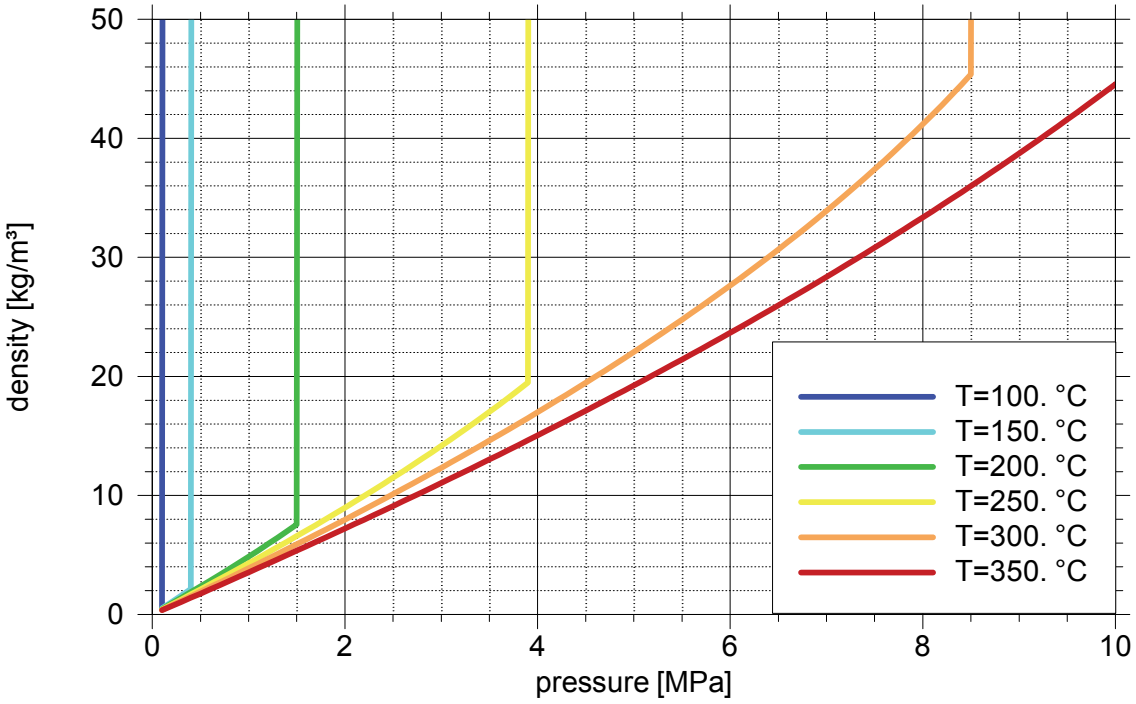

Fig. 4.5 Density of water vapour; after [23].

Water with a pressure above 0.1 MPa and a temperature below 100 °C exists only in the liquid form as shown in Fig. 4.4. For temperatures above 100 °C the vapour saturation pressure $p_s(T)$ exceeds 0.1 MPa (c.f. Fig. 4.1) thus allowing water to take the vaporous form as long as pressures stay below $p_s(T)$. In Fig. 4.5 the change from the vaporous to the liquid phase is indicated by the vertical segment of a density curve.

Conclusions: Eq. (4.17) is a reliable formulation. However, water vapour as the only water phase is not to be expected within the ranges (1.1).

4.2.2 Density of water with dissolved NaCl

Sources: [21], [31]

Formulation:

$$\rho = A + Bf + Cf^2 + Df^3 \qquad (4.20)$$

ρ - density of water with dissolved NaCl [g/cm³]

A, B, C, D - constants (c.f. Appendix B)

f - ansatz function (q.v. eq. (4.21))

$$f = c_1 e^{a_1 m} + c_2 e^{a_2 T} + c_3 e^{a_3 p} \qquad (4.21)$$

m - molality of NaCl in the water-phase [mol/kg]

T - Temperature [°C]

p - pressure [bar]

a_i, c_i - constants (c.f. Appendix B)

Range of validity:

salinity: 0.25 mol/kg < m < 5 mol/kg

temperature: 10 °C ≤ T ≤ 350 °C

pressure: $p_s(T)$ < p < 50 MPa

$p_s(T)$ - vapour saturation pressure [MPa] (q.v. eq. (4.1))

Accuracy: ± 2% in the range of validity

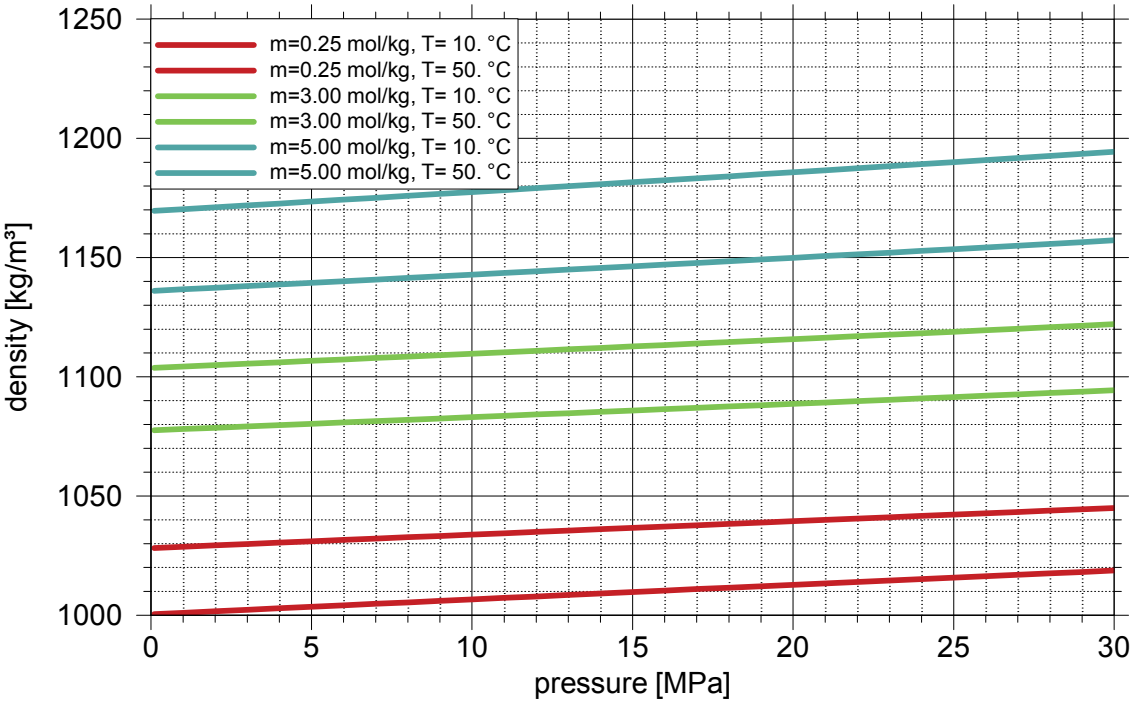

Fig. 4.6 Density of brine; after [21].

Comments: The formulations given above can be found in [21] and in [31]. An approach for a wider range of application in terms of temperature and pressure is provided by [32], but temperature dependent coefficients are given only for discrete temperatures and thus are only conditionally useful for modelling purposes.

[4] states that the compressibility of brine is almost the same as of pure water regardless of the salinity up to a temperature of 250 °C.

An algorithm comparison with other formulations has been performed in [2]. Here, the approach of [31] was discarded because of deviation from several other formulations. However, these other formulations yield somewhat dubious values for high NaCl-concentrations, namely 1230 kg/m³ at atmospheric pressure, a temperature of 25 °C and a salinity of about 5 mol/kg.

Conclusions: Eq. (4.20) appears to be a reliable formulation within the ranges (1.1) except for the extreme values of the salinity. There are alternative formulations but presently no definite conlusion about the validity of any of the approaches is possible.

4.2.3 Density of water with dissolved CO_2

Source: [16]

Formulation:

$$\rho = \rho_{H_2O} + M_{CO_2} c - c \rho_{H_2O} V_\Phi \qquad (4.22)$$

ρ - density of water with dissolved carbon dioxide [kg/m³]

M_{CO_2} - molecular weight of CO_2 [kg/mol] (c.f. Appendix B)

ρ_{H_2O} - density of pure water [kg/m³] (q.v. eq. (4.13))

c - concentration of dissolved CO_2 [mol CO_2/m³ H_2O]

V_Φ - molar volume of dissolved CO_2 [m³/mol] (q.v. eq. (4.23))

$$V_\Phi = 37.51 - 9.585\,10^{-2} T + 8.740\,10^{-4} T^2 - 5.044\,10^{-7} T^3 \qquad (4.23)$$

T - temperature [°C]

Range of validity:

The range of validity is not presented in [16]. The plots in [16] suggest:

temperature: $0\ °C \le T \le 300\ °C$

pressure: $p_s(T) < p < 30$ MPa (see Comments);

$p_s(T)$ - (q.v. eq. (4.1))

CO_2-concentration: c'[mol/mol]: $0 < c' < 0.05$ mol/mol

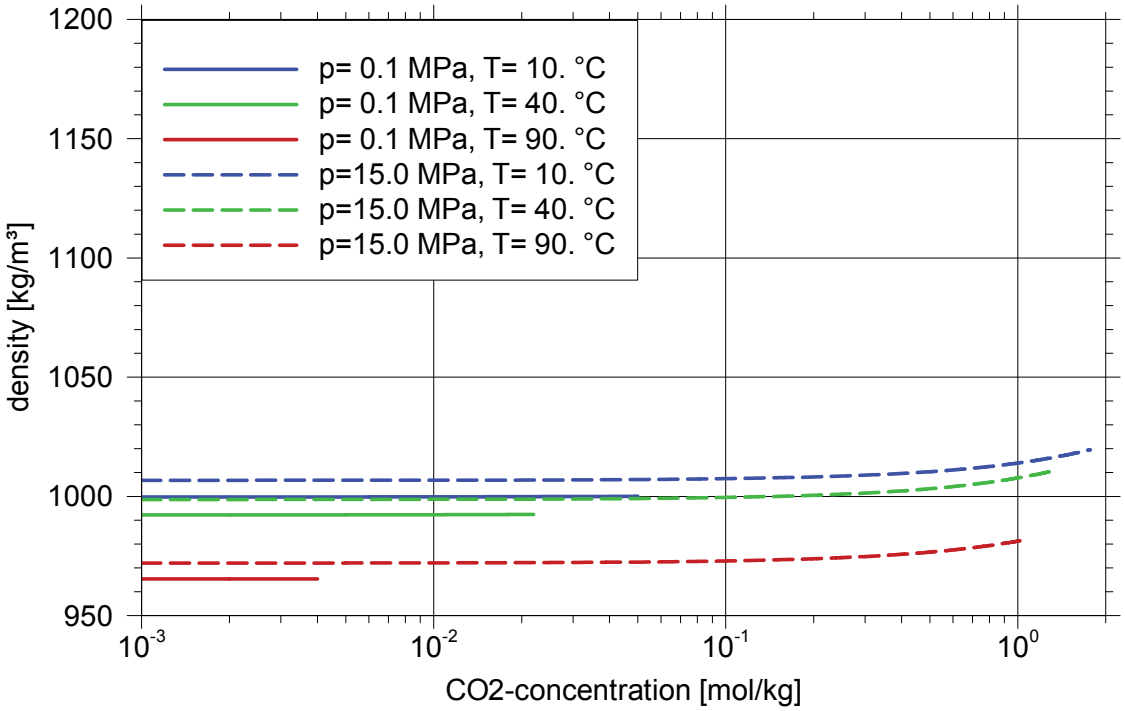

Fig. 4.7 Density of pure water with dissolved CO_2 up to CO_2-solubility; after [16].

Comments: The influence of dissolved carbon dioxide on the water density has been ignored in multiphase flow modelling for a long time (e.g. in [34] und [4]). The reason for that is “that the density increase due to salinity can be up to almost 20 % whereas carbon dioxide content produces an increase in aqueous phase density on the order of at most 2 to 3 %” [16]. Maximum density changes due to solution of CO_2 is estimated in [27] to be less than 0.6 % at temperatures between 0° and 5°C. However, for CO_2-sequestration the density effects may play a vital role for the final fate of injected CO_2.

Along with the pure water density (see section 4.2.1) this approach requires a second equation for the molar volume V_Φ of dissolved CO_2 which is the volume occupied by one mole of a CO_2 at a given temperature and pressure. According to [16] the molar volume

is only weakly dependent on the CO_2-concentration and does not depend on pressure for temperatures below 300 °C. The influence of salinity on the molar volume may be negligible [16].

Note that pressure enters this formulation only via the density of pure water which can reliably be calculated using eq. (4.13) up to 100 MPa.

Conclusions: Eq. (4.22) is a reliable formulation within the ranges (1.1).

4.2.4 Density of water with dissolved NaCl and CO_2

Source: [17]

Formulation:

$$\rho = \rho_b + M_{CO_2} c - c \rho_b V_\Phi \qquad (4.24)$$

ρ - brine density including dissolved CO_2 [kg/m³]

ρ_b - brine density without dissolved CO_2 [kg/m³]

M_{CO_2} - molecular weight of CO_2 [kg/mol] (c.f. 0)

c - concentration of dissolved CO_2 [mol CO_2/m³ solution]

V_Φ - molar volume of dissolved CO_2 [m³/mol] (q.v. eq. (4.23))

Range of validity: The range of validity is not presented in [17]. Presumably, the ranges given in section 4.2.3 apply.

Comments: Apparently, little is known about the density of a solution containing CO_2 as well as NaCl. [4] neglects the influence of CO_2 on the brine density on account of the low solubility of the CO_2. In [17] an ad hoc approach based on the formulation in section 4.2.3 for pure water and CO_2 is used without justification that simply exchanges the pure water density with the brine density:

Note: Neither eq. (4.20) nor eq. (4.22) offer a formulation including 0% salt content or 0% CO_2-content, respectively. The brine density for a salt molality below 0.25 is therefore calculated as a linear interpolation between the value of eq. (4.20) with

m=0.25 and the value for pure water according to eq. (4.13). In case of low CO_2-concentrations the lower limit for the applicability of eq. (4.22) is ignored.

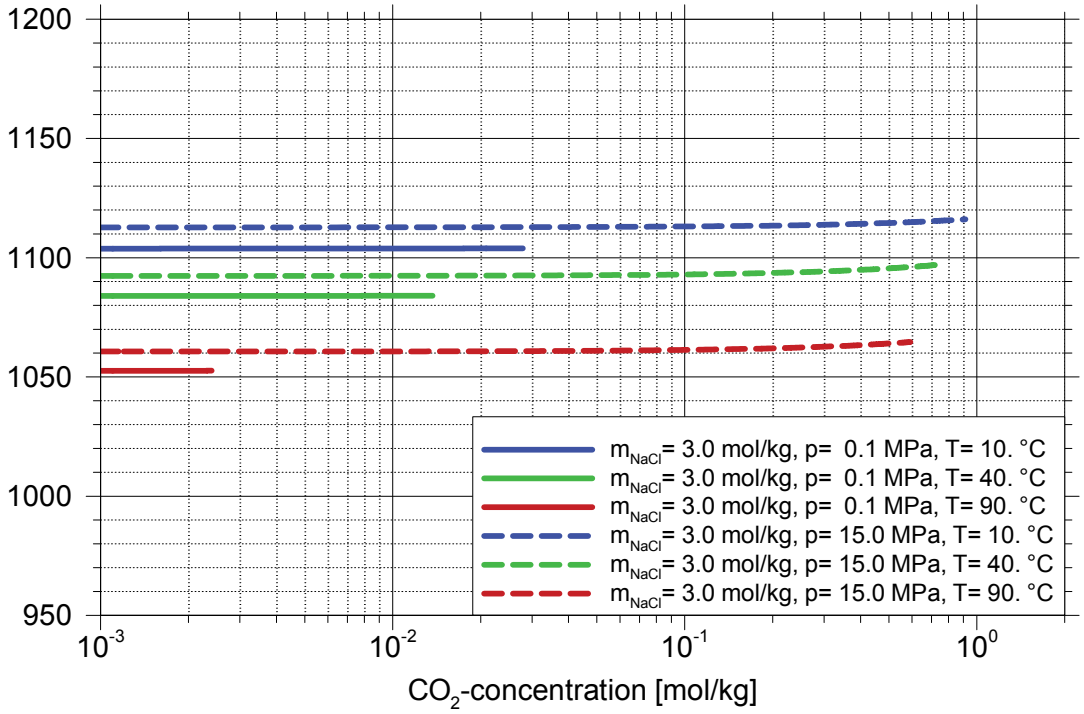

Fig. 4.8 Density of brine with 3 mol/kg NaCl and CO_2 up to CO_2-solubility; after [17].

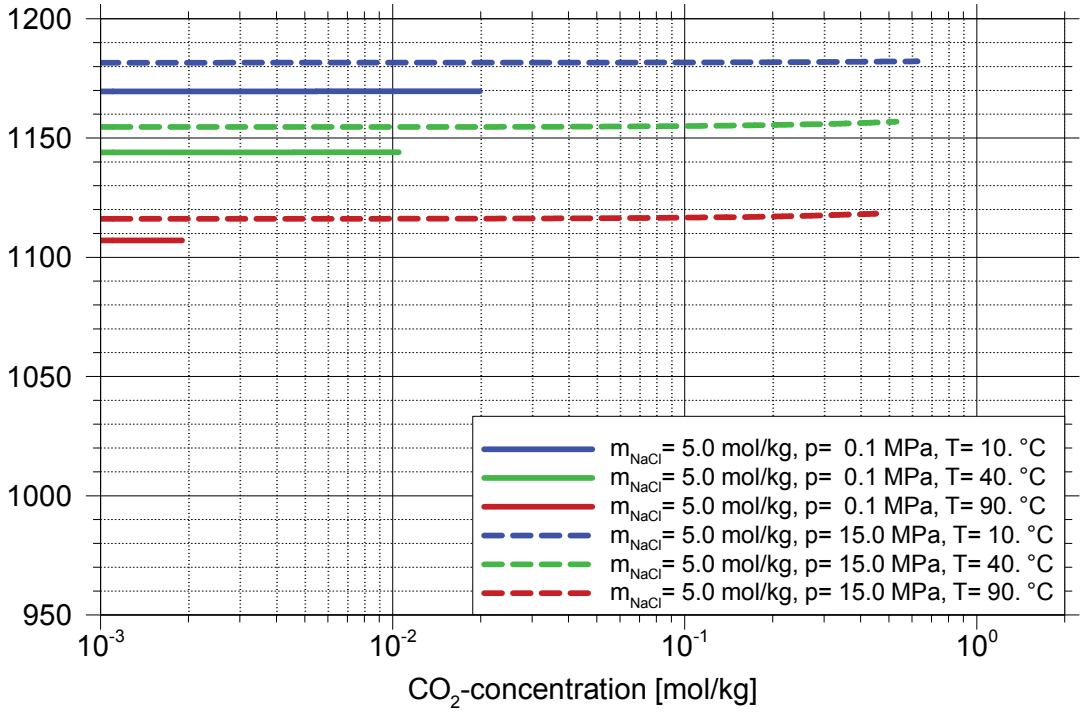

Fig. 4.9 Density of brine with 5 mol/kg NaCl and CO_2 up to CO_2-solubility; after [17].

Conclusions: Eq. (4.24) is probably a good approximation but still has to be validated. The ranges (1.1) referring to NaCl- and CO_2-concentrations are not fully covered.

4.3 Viscosity

4.3.1 Viscosity of pure water

Source: [24]

Formulation:

$$\overline{\eta} = \overline{\eta}_0(\overline{T}) \cdot \overline{\eta}_1(\overline{T}, \overline{\rho}) \cdot \overline{\eta}_2(\overline{T}, \overline{\rho}) \qquad (4.25)$$

$\overline{\eta}$ - standardised viscosity (q.v. eq.s (4.26) [-]

$\overline{T}$ - standardised temperature (q.v. eq.s (4.26) [-]

$\overline{\rho}$ - standardised density (q.v. eq.s (4.26) [-]

$\overline{\eta}_0, \overline{\eta}_1, \overline{\eta}_2$ - ansatz functions [-] (q.v. eq.s (4.27) to (4.29))

$$\overline{T} = \frac{T}{T^*}, \quad \overline{\rho} = \frac{\rho}{\rho^*}, \quad \overline{\eta} = \frac{\eta}{\eta^*} \qquad (4.26)$$

T - temperature [K]

ρ - density [kg/m³]

η - viscosity [Pa s]

T^*, p^*, ρ^*, η^* - reference values (c.f. Appendix B)

$$\overline{\eta}_0 = \frac{\sqrt{\overline{T}}}{\sum_{i=0}^{3} \frac{H_i}{\overline{T}^i}} \qquad (4.27)$$

H_i - constants (c.f. Appendix B)

$$\overline{\eta}_1 = e^{\left[\overline{\rho} \sum_{i=0}^{5} \sum_{j=0}^{6} H_{ij} \left(\frac{1}{\overline{T}} - 1\right)^i (\overline{\rho} - 1)^j\right]} \qquad (4.28)$$

H_{ij} - constants (c.f. Appendix B)

$$\overline{\eta}_2 = 1 \qquad (4.29)$$

Range of validity:

pressure: p < 500 MPa for 0 °C < T < 150 °C

p < 350 MPa for 150 °C < T < 600 °C

p < 300 MPa for 600 °C < T < 900 °C

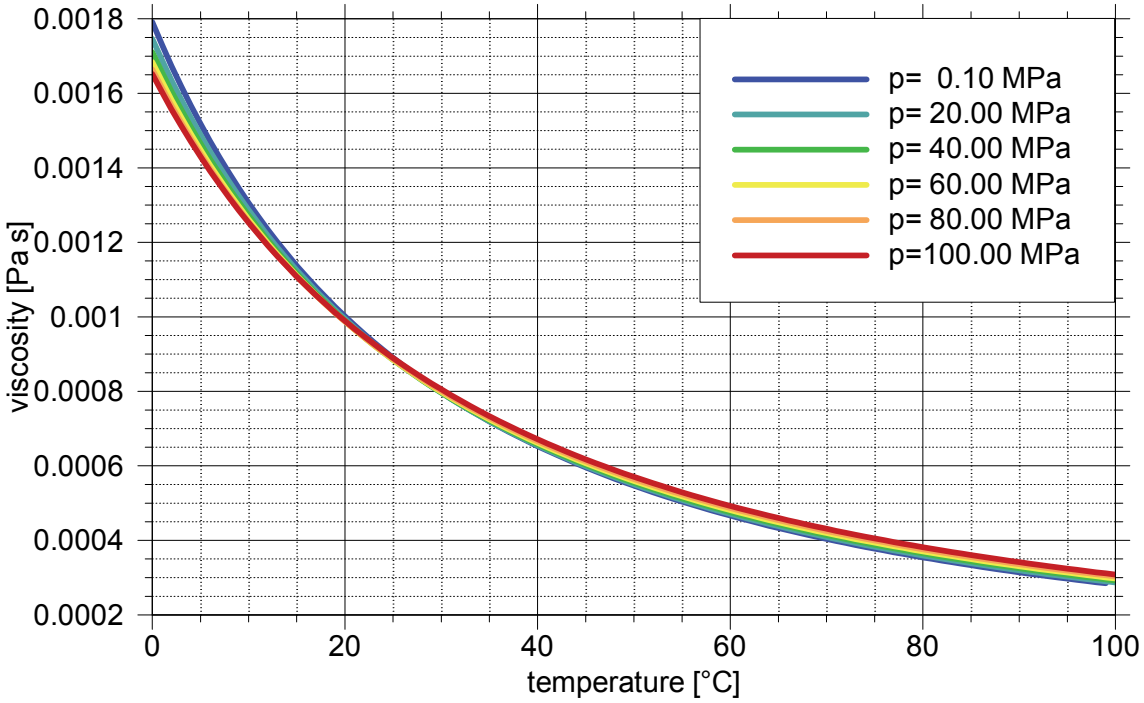

Fig. 4.10 Viscosity of pure water as a function of temperature; after [23].

Comments: For 'industrial' use eq. (4.29) may be used everywhere within the range of validity. For 'general and scientific use' it becomes considerably more complex. Generally, water (and brine) viscosity is almost negligibly dependent on pressure [2].

Conclusions: Eq. (4.25) is a reliable formulation within the ranges (1.1). The influence of pressure on the water viscosity is apparently negligible.

4.3.2 Viscosity of water with dissolved NaCl

Source: [31]

Formulation:

$$\frac{\eta}{\eta_w} = 1 + am + bm^2 + cm^3 + dT(1 - e^{km}) \qquad (4.30)$$

η - viscosity [Pa s]

η_w - viscosity of pure water [Pa s] (c.f. eq. (4.25))

T - temperature [°C]

m - molality of NaCl in the water-phase [mol/kg]

a, b, c, d, k - constants (c.f. Appendix B)

Range of validity:

temperature: 10 °C < T < 350 °C

pressure: 0.1 MPa < p < 50 MPa (for eq. (4.25))

salinity: 0 mol/kg < m < 5 mol/kg[2]

Accuracy:

Eq. (4.30) reproduces data to an average of ± 2% within the range of validity.

Comments: The approach of [31] provides a departure function that modifies the pure water viscosity by a factor according to the salinity. Note that there is a small influence of pressure which is introduced by the formulation (4.25) for the viscosity of pure water.

An algorithm comparison with other formulations has been performed in [2]. It appears that the differences between theses formulations were small.

[2] NaCl-saturated solution contains 359 g $_{NaCl}$ /l $_{H_2O}$ solution at 25 °C which equals 6.1 mol $_{NaCl}$ /kg $_{H_2O}$.

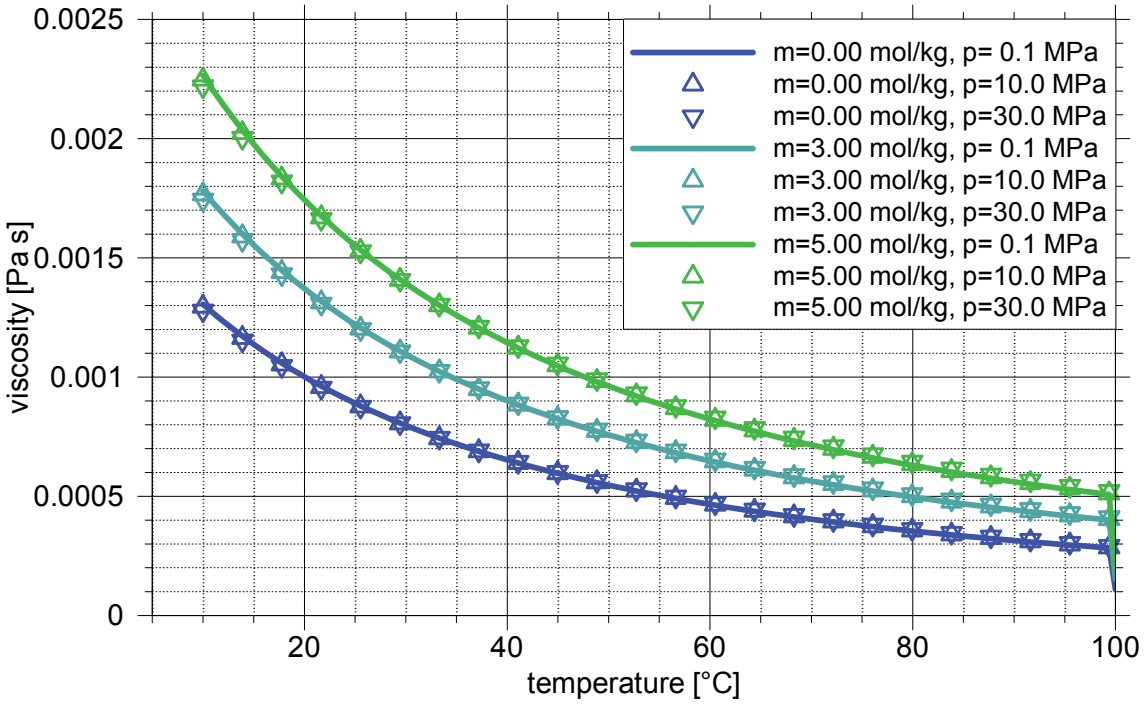

Fig. 4.11 Viscosity of water with dissolved NaCl as a function of temperature; after [31].

Conclusions: Eq. (4.30) is a reliable formulation within the ranges (1.1) except for very high salinities.

4.3.3 Viscosity of water with dissolved CO_2

Source: [4]

Comments: At the time we are not aware of formulations describing the viscosity of water with dissolved CO_2. [4] neglects the influence of CO_2 on the brine viscosity on account of the low solubility of the CO_2.

Conclusions: No reliable formulation is known. Possibly it is negligible.

4.3.4 Viscosity of water with dissolved NaCl and CO_2

Source: [27]

Formulation:

$$\eta = (a+bT)m_{H_2O}^{NaCl} + (c+dT)\sqrt{m_{H_2O}^{NaCl}} + (e+fT)m_{H_2O}^{CO_2} + (g+hT)\left(m_{H_2O}^{CO_2}\right)^2 + i(p-0.1) + \eta^{H_2O}(T, p=0.1) \quad (4.31)$$

η	-	viscosity [m(Pa s)]
η^{H_2O}	-	viscosity of pure water at T and p=0.1 MPa [m(Pa s)]
T	-	temperature [K]
$m_{H_2O}^{NaCl}$	-	molality referring to NaCl [mol/kg]
$m_{H_2O}^{CO_2}$	-	molality referring to CO_2 [mol/kg]
p	-	pressure [MPa]
a to i	-	constants (c.f. Appendix B)

Range of validity:

temperature:	0 °C < T < 5 °C
pressure:	0.1 MPa < p < 30 MPa
salinity:	0 mol/kg < $m_{H_2O}^{NaCl}$ < 0.856 mol/kg
CO_2-concentration:	0 mol/kg < $m_{H_2O}^{CO_2}$ < 0.913 mol/kg

Comments: The approach of [27] provides a departure function that modifies the pure water viscosity at 0.1 MPa by adding a summand according to salt- and CO_2-molality. Note that there is a small influence of pressure which is introduced by the formulation (4.25) for the viscosity of pure water.

According to [17] in 2003 the only source for data concerning the viscosity in the three-component-system of water, NaCl and CO_2 was [27]. No other could be found in the meantime. But this literature aims at deep disposal in the ocean and thus provides only a formulation for these specific conditions.

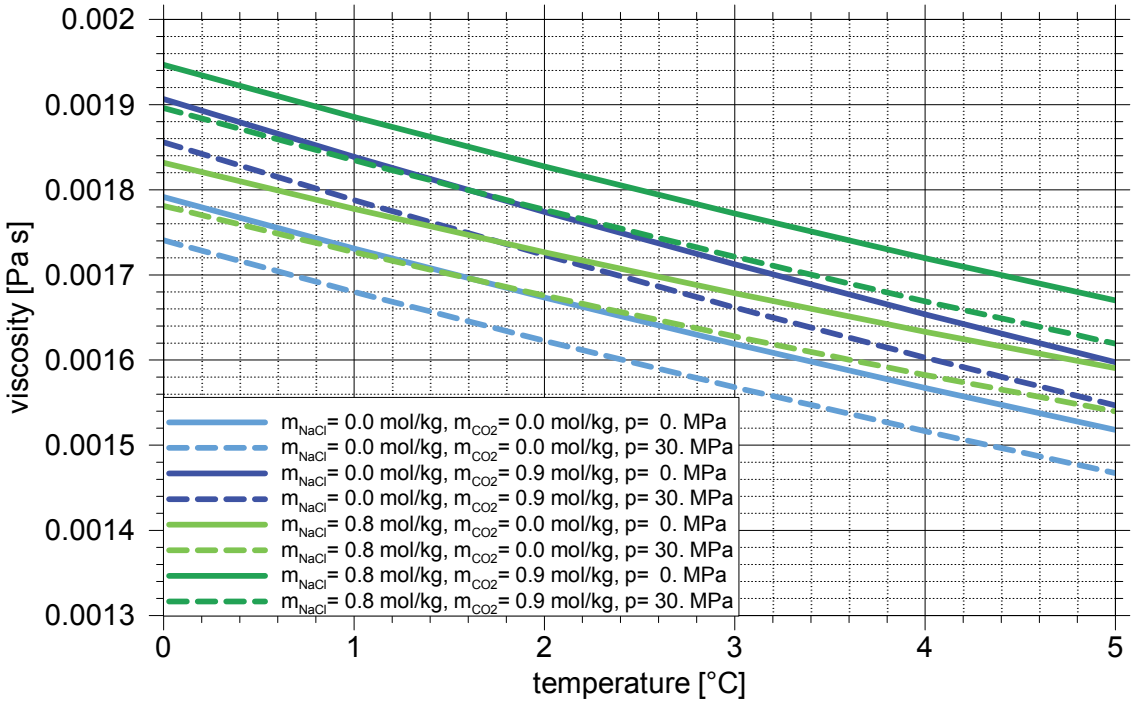

Fig. 4.12 Viscosity of water with dissolved NaCl and CO_2; after [27].

Conclusions: In Fig. 4.12 it seems as if the influence of dissolved CO_2 on the brine viscosity decreases with temperature compared to the influence of NaCl. The pressure induced increase of viscosity in the three-component mixture is not significantly different from the increase in pure water. This may justify the assumption of negligible changes of the viscosity with the CO_2-content especially in high-salinity brines.

The temperature range valid for eq. (4.31) actually excludes a use for CO_2-sequestration in underground aquifers because these aquifers show temperatures above at least 10 °C. However, this formulation might be used anyway for a lack of better data. Therefore it is important to know the error that follows from an extrapolation in the temperature direction. Fig. 4.13 shows such extrapolations for a brine without dissolved CO_2 in comparison to the formulations from [31]. Apparently, the calculated curves are not reliable for higher temperature and salinities. They cross the pure water curve as well as each other and some even fall below zero. The approach should certainly not be used above 40 °C for low up to medium salinities and not above 20 °C for medium up to high salinities.

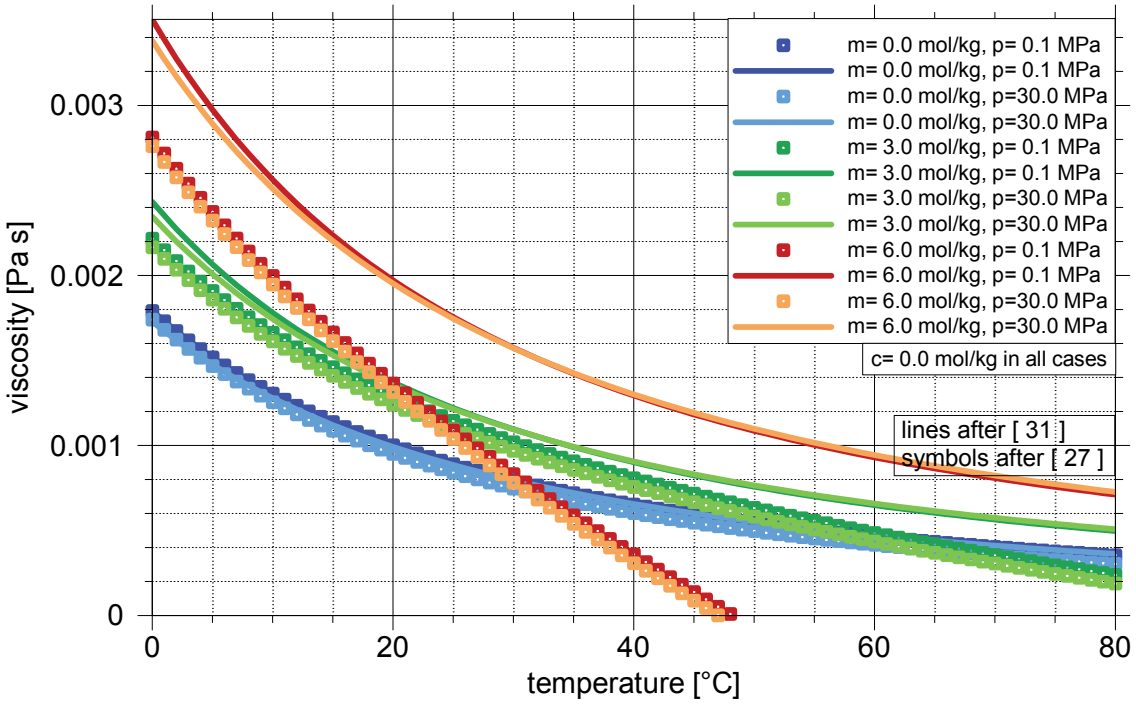

Fig. 4.13 Viscosity of water with dissolved NaCl; after [27] and after [31].

4.4 Thermal conductivity

4.4.1 Thermal conductivity of pure water

Source: [49] (cited in [31])

Formulation:

$$\lambda = -0.92247 + 2.8395\,T' - 1.8007\,T'^2 + 0.52577\,T'^3 - 0.07344\,T'^4 \qquad (4.32)$$

λ - thermal conductivity of pure water [J/(m K s)]

T' - normalised temperature [-]

$$T' = \frac{T + 273.15}{273.15} \qquad (4.33)$$

T - temperature [°C]

Range of validity:

temperature: 20 °C < T < 330 °C

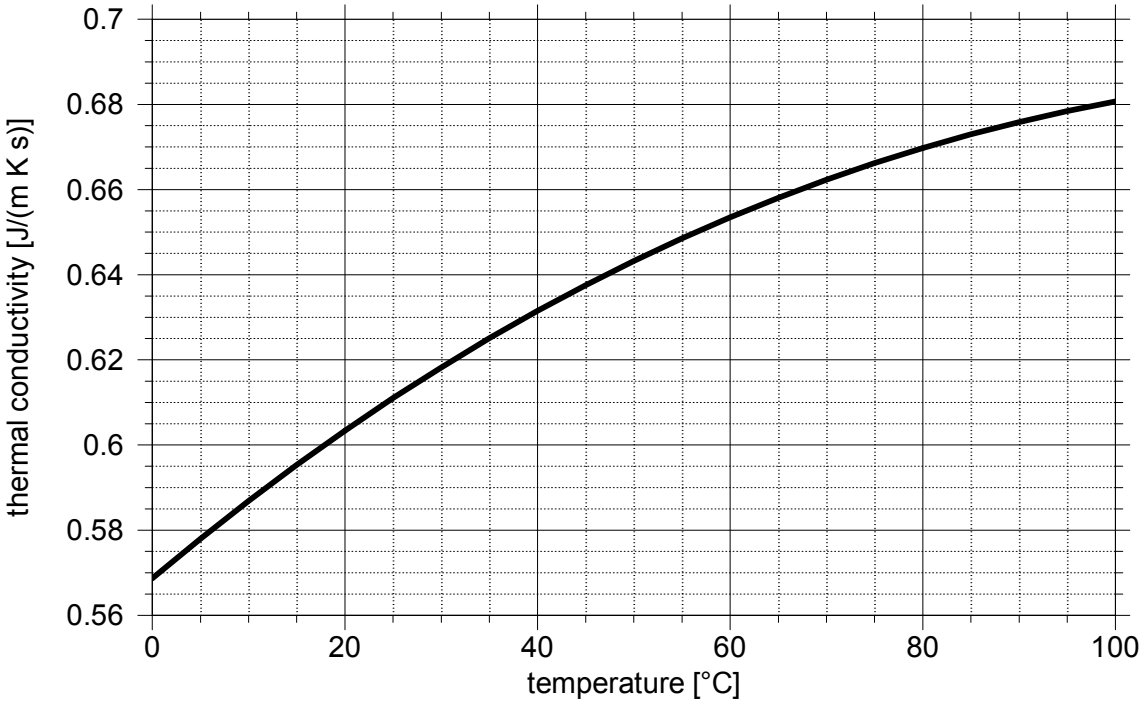

Fig. 4.14 Thermal conductivity of pure water; after [49], cited in [31].

Comments: The formulation (4.32) is based on a comparison with laboratory data. Additional data given in [31] apparently confirm this approach especially for the temperature range between 20 °C and 80 °C.

Conclusions: Eq. (4.32) is a reliable formulation within the ranges (1.1) except for low temperatures.

4.4.2 Thermal conductivity of water with dissolved NaCl

Source: [49] (cited in [31])

Formulation:

$$\frac{\lambda}{\lambda_w} = 1.0 - \left[2.3434\,10^{-3} - 7.924\,10^{-6}T + 3.924\,10^{-8}T^2\right]S + \left[1.06\,10^{-5} - 2\,10^{-8}\,T - 1.2\,10^{-10}T^2\right]S^2 \qquad (4.34)$$

λ - thermal conductivity of water with dissolved NaCl [J/(m K s)]

λ_ω - thermal conductivity of pure water [J/(m K s)] (q.v. eq. (4.32))

T - temperature [°C]

S - ansatz function [-] (q.v. eq. (4.35))

$$S = \frac{5844.3m}{1000 + 58.443m} \qquad (4.35)$$

m - molality of NaCl in the water-phase [mol/kg]

Range of validity:

temperature: 20 °C < T < 330 °C

pressure: 0 mol/kg < m< 5 mol/kg

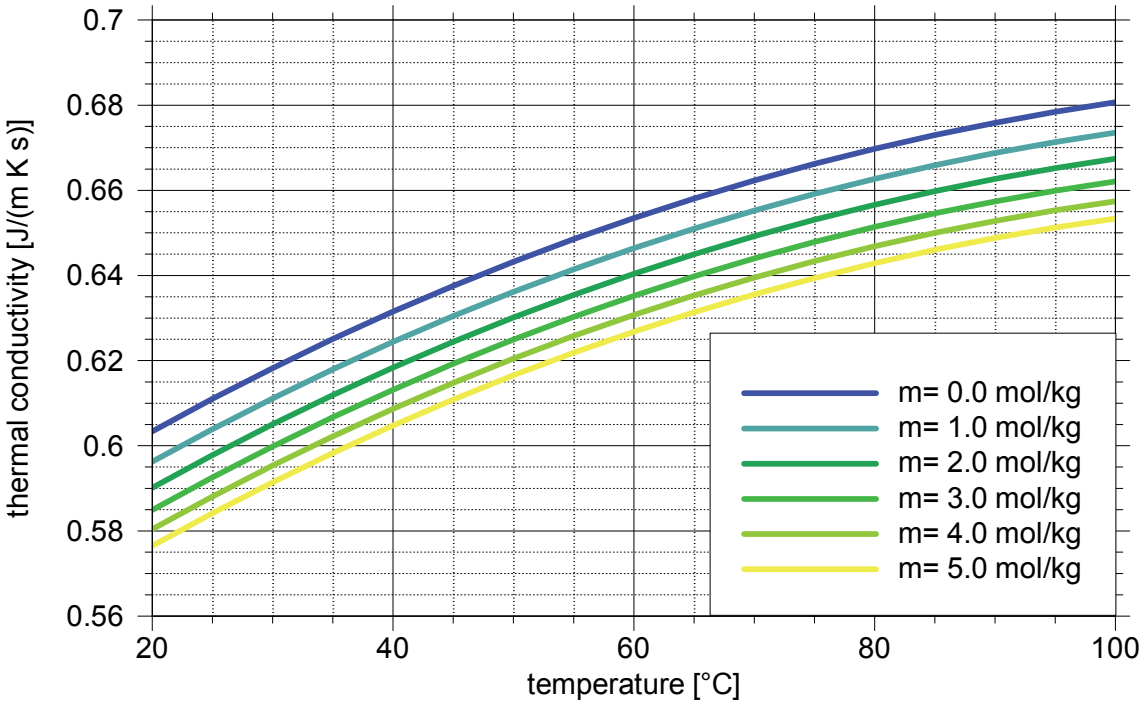

Fig. 4.15 Thermal conductivity of water and dissolved NaCl; after [49], cited in [31].

Comments: The formulation (4.34) is based on a comparison with laboratory data. Additional data given in [31] apparently confirm this approach especially for the temperature range between 20 °C and 80 °C.

Conclusions: Eq. (4.34) is a reliable formulation within the ranges (1.1) except for low temperatures and for very high salinities.

4.4.3 Thermal conductivity of water with dissolved CO_2

Comments: We are not aware of formulations concerning the thermal conductivity of water with dissolved CO_2.

4.4.4 Thermal conductivity of water with dissolved NaCl and CO_2

Comments: We are not aware of formulations concerning the thermal conductivity of water with dissolved NaCl and CO_2.

4.5 Enthalpy

4.5.1 Enthalpy of pure water

Source: [23]

Formulation:

$$\frac{h}{R_{H_2O}T} = \tau\gamma_\tau \qquad (4.36)$$

h - enthalpy [kJ/kg]

R_{H2O} - specific gas constant for water vapour (c.f. Appendix B)

T - temperature [K]

γ_τ - ansatz function (q.v. eq. (4.38))

τ - standardised temperature (q.v. eq. (4.37)) [-]

$$\tau = \frac{T*}{T} \qquad (4.37)$$

T^* - reference temperature (c.f. Appendix B)

$$\gamma_\tau = \sum_{i=1}^{34} n_i \left(7.1 - \pi\right)^{I_i} J_i (\tau - 1.222)^{J_i - 1} \qquad (4.38)$$

n_i, I_i, J_i - constants (c.f. Appendix B)

π - standardised pressure [-]

$$\pi = \frac{p}{p*} \qquad (4.39)$$

p^* - reference pressure (c.f. Appendix B)

p - pressure [MPa]

Range of validity:

temperature: 273.15 K < T < 623.15 K

pressure: $p_s(T)$ < p < 100 MPa

$p_s(T)$ - vapour saturation pressure [MPa] (q.v. eq. (4.1))

Comments: A formulation for the enthalpy can be derived from the specific Gibbs free energy (eq. (4.40)):

$$h = g - T\left(\frac{\partial g}{\partial T}\right)_p \qquad (4.40)$$

g - specific Gibbs free energy [kJ/kg]

Conclusions: Eq. (4.36) is a reliable formulation within the ranges (1.1).

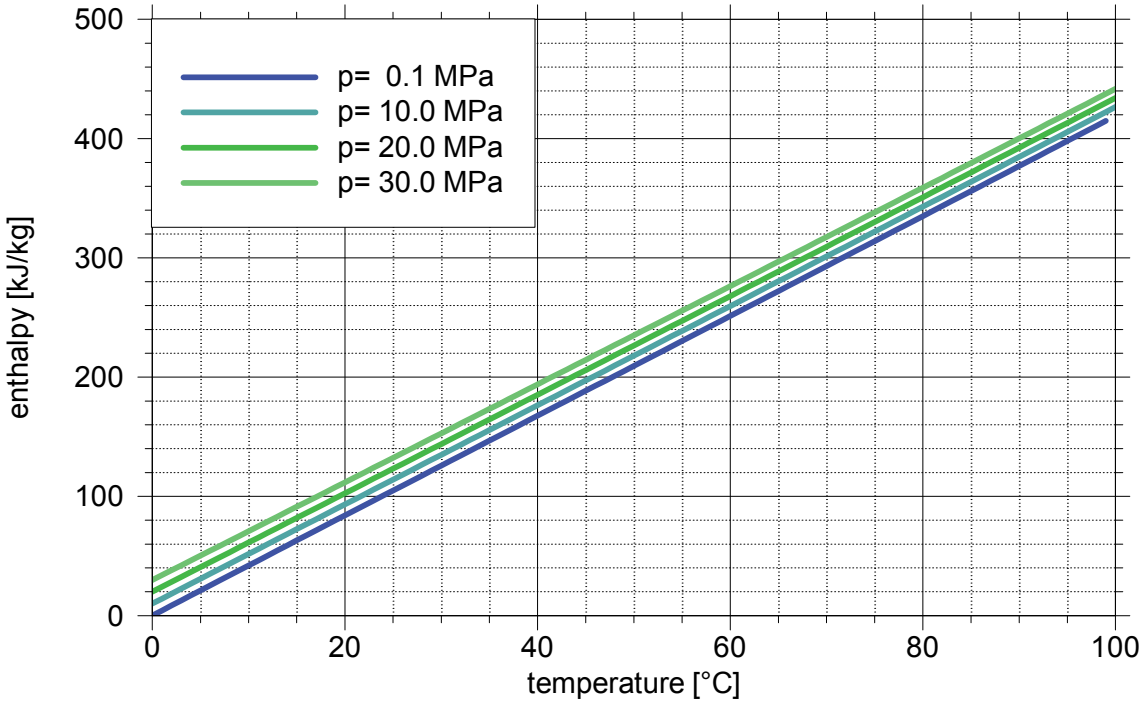

Fig. 4.16 Enthalpy of pure water; after [23].

4.5.2 Enthalpy of water with dissolved NaCl

Source: [30]

Formulation:

$$h = X_{H_2O}^{H_2O} h_{H_2O} + X_{H_2O}^{NaCl} h_{NaCl} + m\Delta h_{H_2O}^{NaCl} \qquad (4.41)$$

h	-	enthalpy of water with dissolved NaCl [kJ/kg]
$X_{H_2O}^{H_2O}$	-	mass fraction of water [-] (q.v. eq. (4.42))
$X_{H_2O}^{NaCl}$	-	mass fraction of salt [-] (q.v. eq. (4.43))
h_{H_2O}	-	enthalpy of pure water [kJ/kg] (q.v. eq.s (4.36) or (4.45))
h_{NaCl}	-	enthalpy of pure salt [kJ/kg] (q.v. eq. (6.3))
$\Delta h_{H_2O}^{NaCl}$	-	enthalpy of mixing [kJ/kg] (q.v. eq. (4.44))
T	-	temperature [°C]
m	-	molality of NaCl in the water-phase [mol/kg]

$$X_{H_2O}^{H_2O} = \frac{1000}{1000 + 58.44m} \qquad (4.42)$$

$$X_{H_2O}^{NaCl} = \frac{58.44m}{1000 + 58.44m} \qquad (4.43)$$

$$\Delta h_{H_2O}^{NaCl} = \frac{4.184}{1000 + 58.44m} \sum_{i=0}^{3} \sum_{j=0}^{2} a_{ij} T^i m^j \qquad (4.44)$$

a_{ij} - constants (c.f. Appendix B)

$$h_{H_2O} = 0.12453\,10^{-4} T^3 - 0.4513710^{-2} T^2 + 4.81155\,T - 29.578 \qquad (4.45)$$

Range of validity is not specified, but secondary literature gives hints:

temperature: 0 °C < T < 350 °C

salinity: 0 to full NaCl saturation (as in the tabulated data from [21])

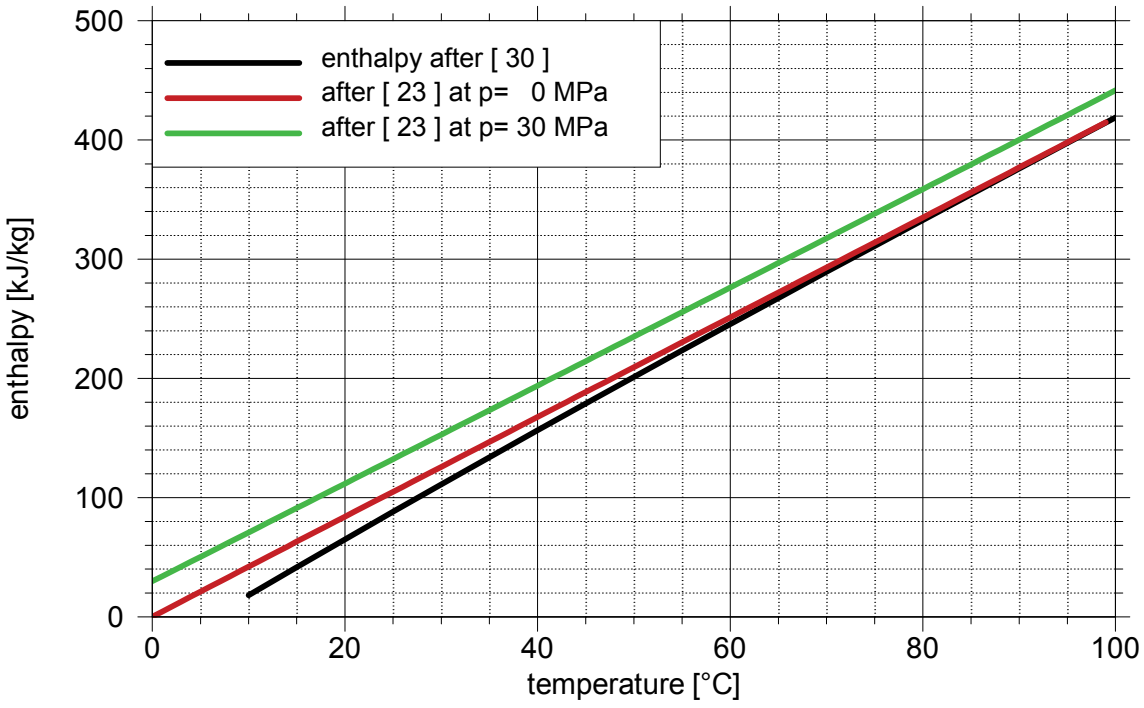

Fig. 4.17 Enthalpy of pure water; after [30] and after [23].

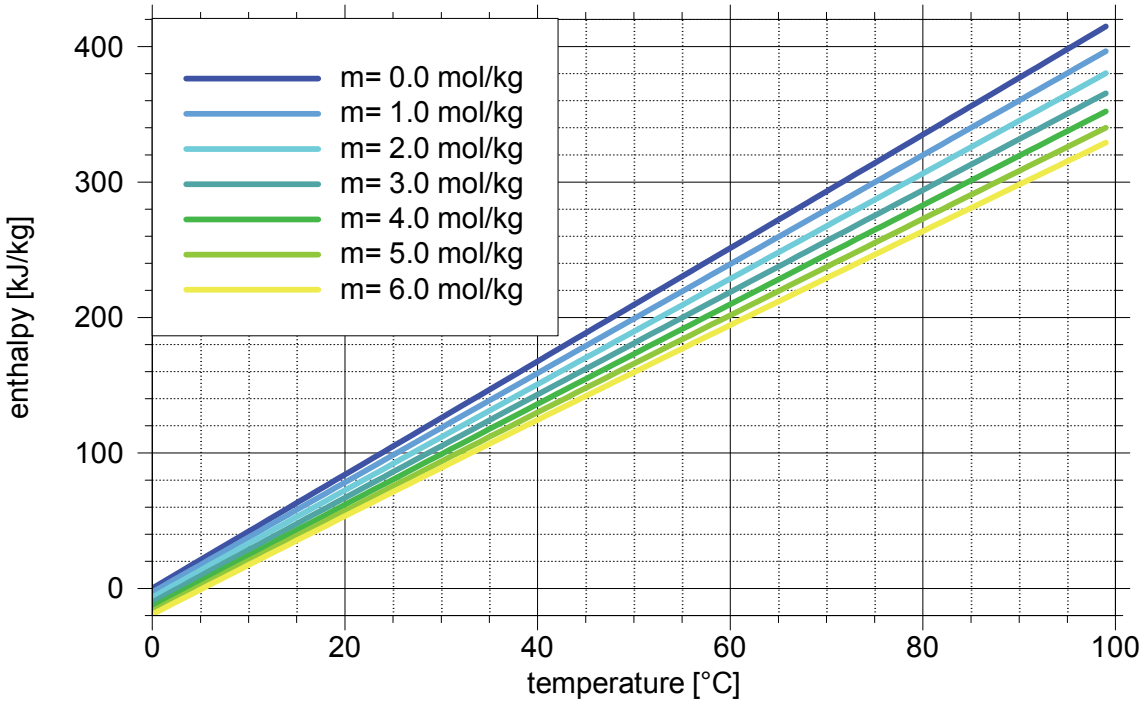

Fig. 4.18 Enthalpy of water with dissolved NaCl at 0.1 MPa; after [30], using the modifications described in the text.

Comments:

– Formulation (4.41) is derived from tabulated data from [21] and [37]. The approach follows the general principle that the enthalpies of the components of a solution add proportionally to the mass of the components. An additional term for the heat of dissolution is considered, too.

– Formulation (4.45) for the enthalpy of pure water h_{H_2O} is less extensive than eq. (4.36) but it does not include the admittedly small effect of pressure. Additionally, it appears to be optimised for higher temperatures as has already been observed in [20]. For pure water there are noticeable deviations in the lower temperature range from the more accurate data of [23] as shown in Fig. 4.17. The curves in Fig. 4.18 are therefore calculated using eq. (4.36) instead of eq. (4.45).

– Problems with the correlation for the enthalpy of salt h_{NaCl} after [30] are discussed in section 6.2.

– Finally, the summands in eq. (4.41) are not consistent in terms of dimensions. In the definitions (4.45), (6.2) and (4.44) all three enthalpies are given in [kJ/kg] but in eq. (4.41) the enthalpies h_1 and h_2 are multiplied by the referring mass fraction

while the enthalpy of mixing is multiplied by the molality of the solution. So either correlation (4.44) for the enthalpy of mixing contains another error, or it is not given in the right dimensions, or the enthalpy of mixing is multiplied in (4.41) by the salt mass fraction instead of the molality. The first two assumptions are rather hard to check. The curves in Fig. 4.18 are thus calculated using salt mass fractions instead of the molalities in (4.41) as has been done for practical model calculations described in [6].

Conclusions:

– Formulation (4.41) is valid within the ranges (1.1). However, the approach of [30] is obviously not too reliable - neither related to the single enthalpies of pure water h_1, of pure salt h_2 as well as of mixing Δh nor related to the formulation as such. A big problem here is that data to check the formulations are hard to come by.
– The formulations for the enthalpies h_1 and h_2 from [30] can be replaced by eq.s (4.45) and (6.3), respectively. But the formulation for the enthalpy of mixing introduces an inconsistency. The reason for that is unknown and must be checked since the different explanations to resolve these inconsistencies lead to a highly different relevance of this term for the enthalpy of brine.

4.5.3 Enthalpy of water with dissolved CO_2

Source: adapted from [14]

Formulation:

$$h = X_{H_2O}^{H_2O} h_{H2O} + X_{H_2O}^{CO_2} h_{CO_2} + X_{H_2O}^{CO_2} \Delta h_{H_2O}^{CO_2} \qquad (4.46)$$

h	-	enthalpy of water with dissolved CO_2 [kJ/kg]
$X_{H_2O}^{H_2O}$	-	mass fraction of water [-]
$X_{H_2O}^{CO_2}$	-	mass fraction of CO_2 [-]
h_{H_2O}	-	enthalpy of pure water [kJ/kg] (q.v. eq. (4.36))
h_{CO_2}	-	enthalpy of pure CO_2 [kJ/kg] (q.v. eq. (5.52))
$\Delta h_{H_2O}^{CO_2}$	-	enthalpy of dissolution [kJ/kg] (q.v. eq. (4.47))

$$\Delta h_{H_2O}^{CO_2} = (-RT^2)\cdot \left(c_2 - \frac{c_3}{T^2} + 2c_4 T + \frac{c_5}{(630-T)^2} + \frac{c_7 p}{T} - \frac{c_8 p}{T^2} + \frac{c_9 p}{(630-T)^2} + \frac{2c_{10}p^2}{(630-T)^3} \right) \quad (4.47)$$

p - Druck der Wasserphase [bar]

T - temperature [K]

R - universal gas constant [J/(K mol)]

c_i - constants (c.f. Appendix B)

Range of validity:

temperature: 0 °C < T < 260 °C

pressure: 0 MPa < p < 200 MPa

salinity: 0 mol/kg < m < 4.87 mol/kg

Comments:

– Formulation (4.46) can be regarded as a simplified version of formulation (4.48).
– Due to the mass proportionality of the three contributory enthalpies the range of validity for formulation (4.46) is equal to the common range of validities of all these three enthalpies. For the range of validity: see Comments in section 4.7.3.

Conclusions: Formulation (4.46) is valid within the ranges (1.1).

4.5.4 Enthalpy of water with dissolved CO_2 and NaCl

Source: [4], [14]

Formulation:

$$h = (1 - X_{H_2O}^{CO_2})h_b + X_{H_2O}^{CO_2} h_{CO_2} + X_{H_2O}^{CO_2} \Delta h_{H_2O}^{CO_2} \quad (4.48)$$

h - enthalpy of water with dissolved NaCl and dissolved CO_2 [kJ/kg]

h_b - enthalpy of water with dissolved NaCl [kJ/kg] (q.v. eq. (4.41))

h_{CO_2} - enthalpy of pure CO_2 [kJ/kg] (q.v. eq. (5.52))

$\Delta h_{H_2O}^{CO_2}$ - enthalpy of dissolution [kJ/kg] (q.v. eq. (4.49))

$X_{H_2O}^{CO_2}$ - mass fraction of CO_2 [-]

$$\left(\frac{\partial \ln K_{hb}}{\partial T}\right)_p = -\frac{\Delta h_s}{R(T+273.15)^2 M_{CO_2}} \qquad (4.49)$$

K_{hb} - Henry's constant for brine and gaseous CO_2 [Pa] (q.v. eq. (4.50))

T - temperature [°C]

R - universal gas constant [J/(mol K)]

M_{CO_2} - molecular weight of CO_2 [kg/mol]

$$K_{hb} = K_h 10^{(m\,k_b)} \qquad (4.50)$$

K_{hb} - Henry's constant for brine and gaseous CO_2 [Pa]

K_h - Henry's constant for pure water [Pa] (q.v. eq. (4.51))

k_b - salting-out coefficient [kg/mol] (q.v. eq. (4.52))

m - molality of NaCl in the water-phase [mol/kg]

$$K_h = \sum_{i=0}^{5} B(i) T^i \qquad (4.51)$$

$B(i)$ - constants (c.f. Appendix B)

$$k_b = \sum_{i=0}^{4} C(i) T^i \qquad (4.52)$$

$C(i)$ - constants (c.f. Appendix B)

As a kind of validation of the approach (4.49) formulation (4.46) for the enthalpy of dissolution for pure water from [14] was checked against the approach from [4] as shown in Fig. 4.20.

Range of validity:

temperature: 0 °C < T < 300 °C

salinity: 0 mol/kg < m < halite saturation

further clues: (see section 4.5.2)

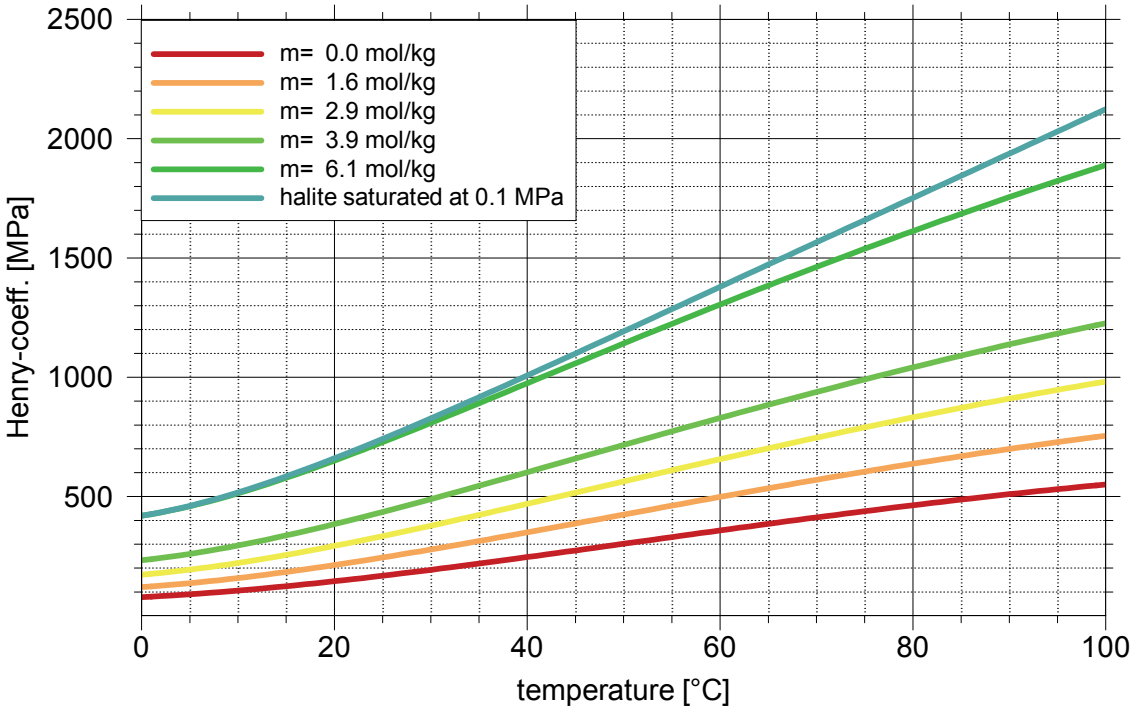

Fig. 4.19 Henry's constant for different salinities, after [4].

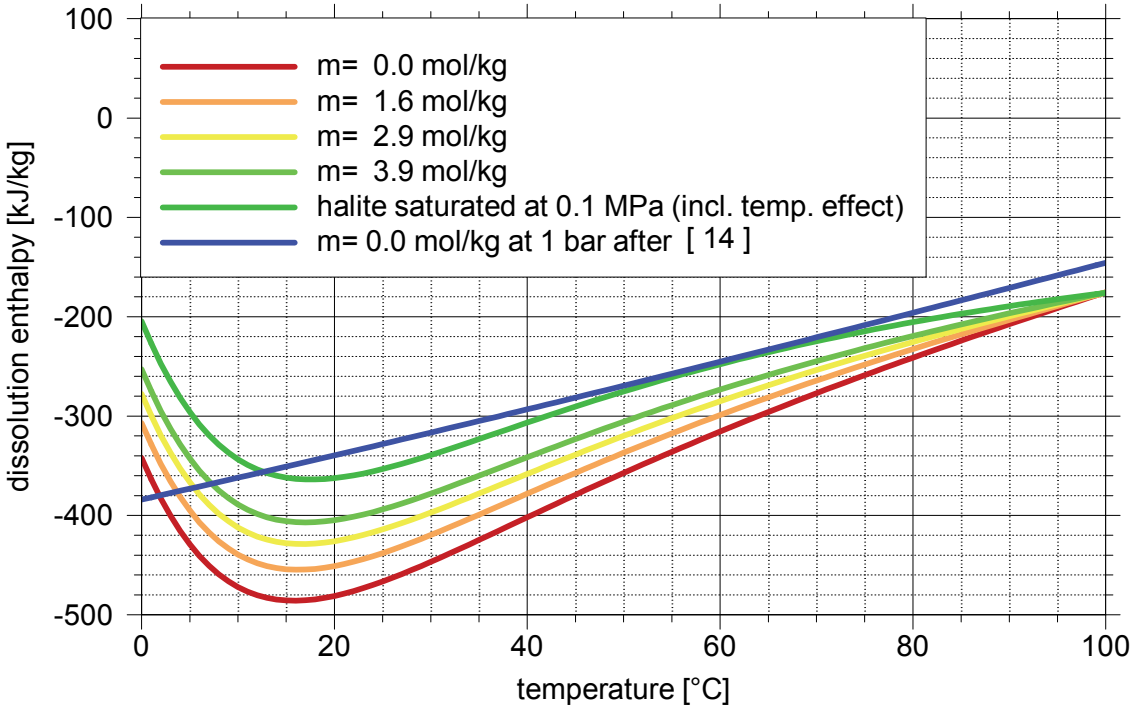

Fig. 4.20 Dissolution enthalpy of CO_2; after [4], approach for pure water after [14].

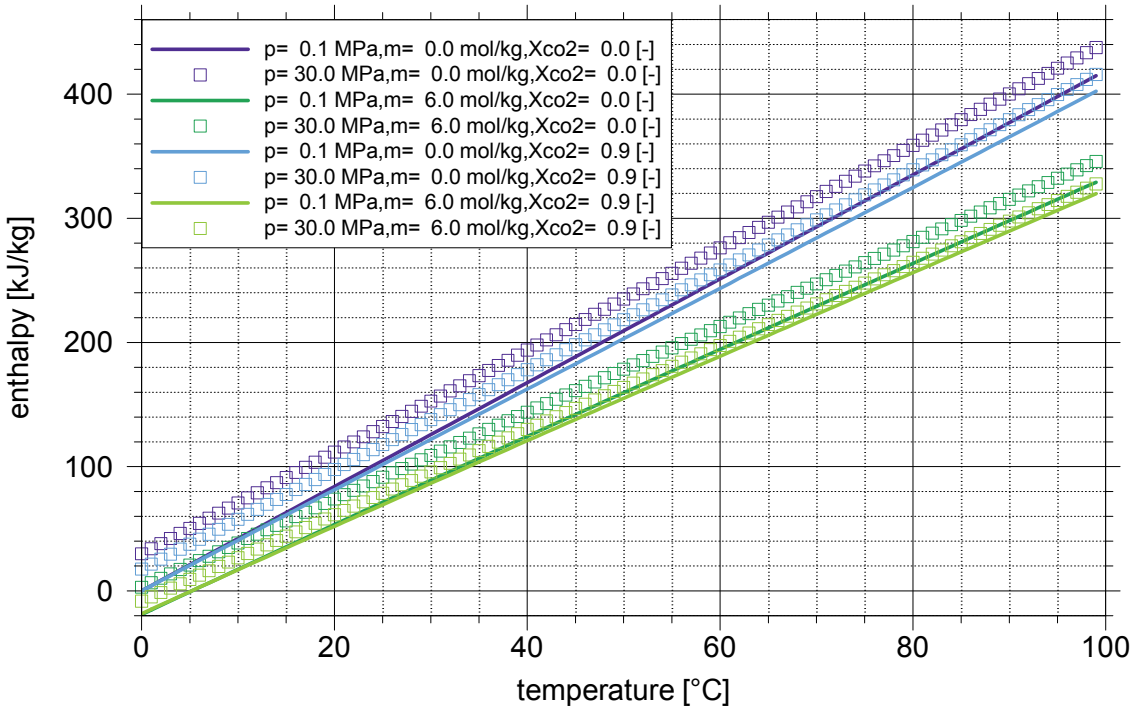

Fig. 4.21 Enthalpy of water with dissolved NaCl and dissolved CO_2; after [4].

Comments: Formulation (4.48) is based on an already known brine enthalpy as well as the mass proportionality of the enthalpies of brine and of CO_2.

The enthalpy of dissolution of gaseous CO_2 is not given directly in [4] but as a function of the temperature- and salinity-dependent Henry's constant as well as on the exclusively temperature-dependent salting-out coefficient. It is fitted to data in the temperature range of 100 °C up to 350 °C. Considering this, the sharp bendig of the curves below 20 °C in Fig. 4.20 looks suspicious, especially so, because the formulation in [14] for fresh water looks almost linear in this range. The additional data used in [14] confirms a more or less linear trend even down to 30 °C.

No comparison with measured data under any salinity is given in [4].

Conclusions: The only quantity in eq. (4.48) not already evaluated in other sections is the dissolution enthalpy $\Delta h_{H_2O}^{CO_2}$. Since the enthalpy of dissolution is multiplied by the mass fraction of CO_2 in brine it has no significant meaning for practical purposes. The referring formulations (4.49) or (4.46) appear to be reliable and valid within the ranges

(1.1) except for temperatures below 20 °C where the formulations differ strongly. Here, it cannot be decided which formulation is more realistic. Otherwise the conclusions concerning brine enthalpy from section 4.5.2 apply.

4.6 Heat capacity

Heat capacity can be derived from the enthalpy as the partial derivative with respect to temperature:

$$c = \frac{\partial h}{\partial T} \qquad (4.53)$$

c - heat capacity [kJ/(kg K)]
h - enthalpy [kJ/kg]
T - temperature [K]

4.6.1 Heat capacity of pure water

Source: [23], [30]

Formulation after [23]:

$$\frac{c_p}{R} = -\tau^2 \gamma_{\tau\tau} \qquad (4.54)$$

c_p - isobaric heat capacity [kJ/(kg K)]
R - specific gas constant for water vapour [kJ/(kg K)] (c.f. Appendix B)
$\gamma_{\tau\tau}$ - ansatz function
τ - standardised temperature [-] (q.v. eq. (4.16))

$$\gamma_{\tau\tau} = \sum_{i=1}^{34} n_i (7.1 - \pi)^{I_i} J_i (J_i - 1)(\tau - 1.222)^{(J_i - 2)} \qquad (4.55)$$

π - standardised pressure [-] (q.v. eq. (4.13))
n_i, I_i, J_i - constants for eq. (4.38) (c.f. Appendix B, eq. (4.15))

Range of validity:

temperature: 273.15 K < T < 623.15 K

pressure: $p_s(T) < p <$ 100 MPa

$p_s(T)$ - vapour saturation pressure [MPa] (q.v. eq. (4.1))

Another formulation for the heat capacity can be derived starting with eq. (4.45) from [30] for the enthalpy of pure water. The temperature derivative of this approach reads as follows:

$$c_w = \frac{\partial h_1}{\partial T} = 0.37359 \cdot 10^{-4} T^2 - 0.90274 \cdot 10^{-2} T + 4.81155 \qquad (4.56)$$

c_w - heat capacity of pure water [kJ/(kg °C)]

h_1 - enthalpy of pure water (q.v. eq. (4.45))

T - temperature [°C]

Range of validity:

(see section 4.5.2)

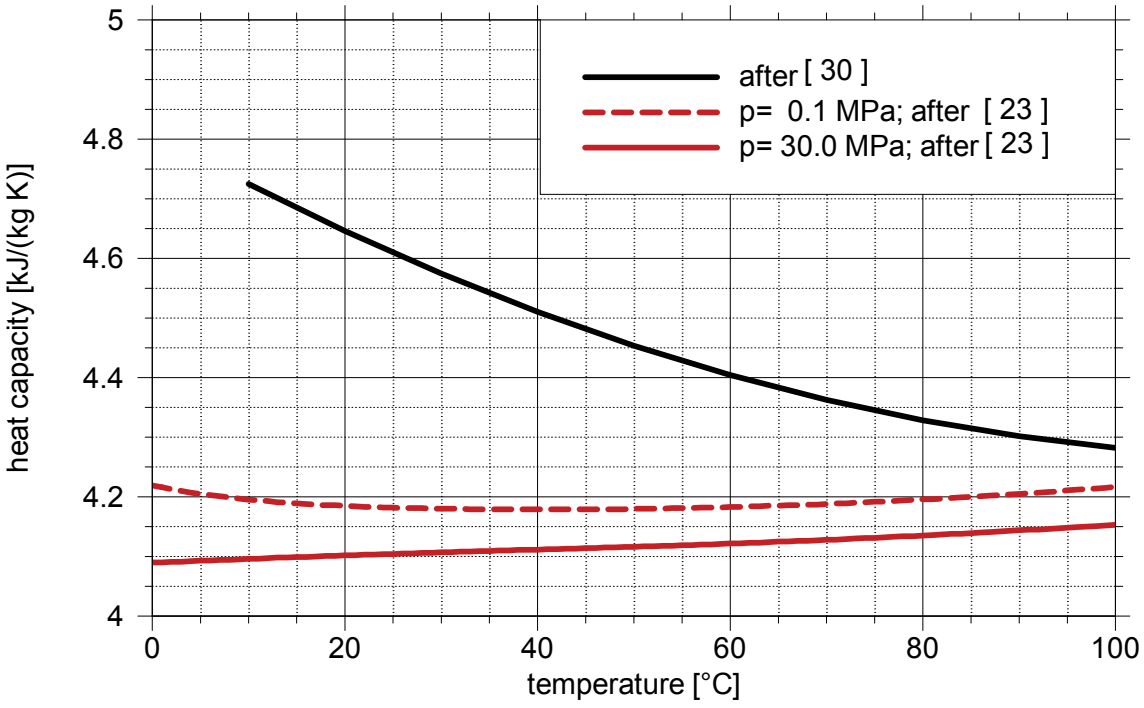

Fig. 4.22 Heat capacity of pure water; after [23] and [30].

Comments: Following the formulation from [23] for the heat capacity the effects of pressure and temperature appear to be negligible in the constant range of interest. In contrast the approach based on the enthalpy of pure water provided by [30] shows a clear dependency on temperature while the effect of pressure is not included.

Conclusions: Eq. (4.54) is a reliable formulation within the ranges (1.1). Instead of using the approach (4.56) a representative constant value based on eq. (4.54) should be considered.

4.6.2 Heat capacity of water with dissolved NaCl

Source: [23], [30]

Formulation:

$$\begin{aligned} c &= X_{H_2O}^{H_2O}\frac{\partial h_1}{\partial T} + X_{H_2O}^{NaCl}\frac{\partial h_2}{\partial T} + X_{H_2O}^{NaCl}\frac{\partial(\Delta h_m)}{\partial T} \\ &= X_{H_2O}^{H_2O}c_w + X_{H_2O}^{NaCl}c_{NaCl} + X_{H_2O}^{NaCl}\frac{\partial(\Delta h_m)}{\partial T} \end{aligned} \qquad (4.57)$$

c	-	heat capacity of water with dissolved NaCl [kJ/(kg K)]
c_w	-	heat capacity of pure water [kJ/(kg K)] (q.v. eq. (4.54))
c_{NaCl}	-	heat capacity of NaCl [kJ/(kg K)] (q.v. eq. (6.4))
$X_{H_2O}^{H_2O}$	-	mass fraction of water [-] (q.v. eq. (4.42))
$X_{H_2O}^{NaCl}$	-	mass fraction of salt [-] (q.v. eq. (4.43))
h_1	-	enthalpy of pure water [kJ/kg] (q.v. eq. (4.36))
h_2	-	enthalpy of pure salt [kJ/kg] (q.v. eq. (6.3))
Δh	-	enthalpy of mixing [kJ/kg] (q.v. eq. (4.44))
T	-	temperature [°C]

$$\frac{\partial(\Delta h)}{\partial T} = \frac{4.184}{1000 + 58.44m}\sum_{i=0}^{3}\sum_{j=0}^{2} a_{ij} i T^{(i-1)} m^j \qquad (4.58)$$

m	-	molality of NaCl in the water-phase [kg/mol]

Range of validity:

(see section 4.5.2)

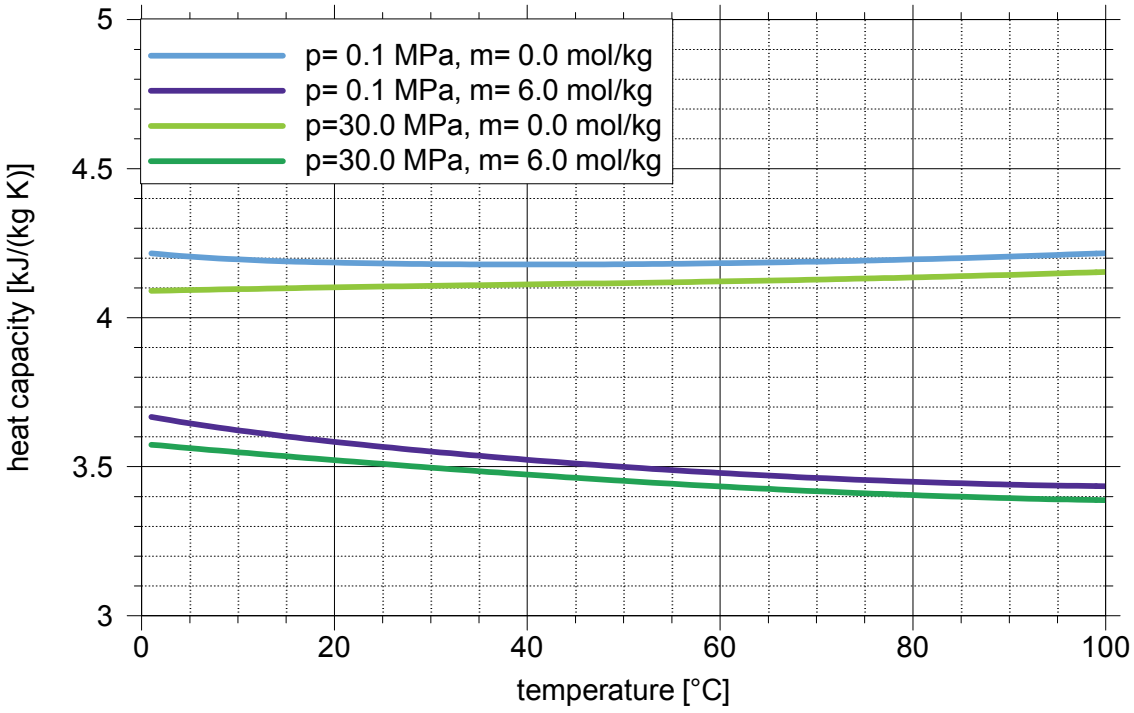

Fig. 4.23 Heat capacity of water with dissolved NaCl; derived from [30].

Comments: Analogously to the enthalpy the heat capacity for water with dissolved NaCl is the mass weighted sum of the single heat capacities plus enthalpy of mixing and/or enthalpy of dissolution. Formulation (4.41) for the enthalpy of water with dissolved NaCl is inserted in eq. (4.53) including the modifications described in the comments in section 4.5.2. The approach consists of three summands that can be differentiated separately.

Conclusions:

(see section 4.5.2)

4.6.3 Heat capacity of water with dissolved CO_2

Source: -

Formulation:

$$c = (1 - X_{H_2O}^{CO_2})\frac{\partial h_{H2O}}{\partial T} + X_{H_2O}^{CO_2}\frac{\partial h_{CO_2}}{\partial T} + X_{H_2O}^{CO_2}\frac{\partial \Delta h_{H_2O}^{CO_2}}{\partial T} \qquad (4.59)$$

c	-	heat capacity of water with dissolved NaCl [kJ/(kg K)]
$X_{H_2O}^{CO_2}$	-	mass fraction of CO_2 [-]
h_{H_2O}	-	enthalpy of pure water [kJ/kg] (q.v. eq. (4.36))
h_{CO_2}	-	enthalpy of pure CO_2 [kJ/kg] (q.v. eq. (5.52))
$\Delta h_{H_2O}^{CO_2}$	-	enthalpy of dissolution [kJ/kg] (q.v. eq. (4.47))

Comments: The heat capacity given here is derived from the enthalpy (4.46) using (4.53).

Conclusions: Formulation (4.59) is valid within the ranges (1.1).

4.6.4 Heat capacity of water with dissolved NaCl and CO_2

Source: [4]

Formulation: Approach (4.53) using eq. (4.48) can be used. Since a special formulation would be very complex, the partial derivative of eq. (4.48) with respect to temperature is calculated numerically.

Range of validity:

(see section 4.5.3)

Comments: -

Conclusions: (see section 4.5.3)

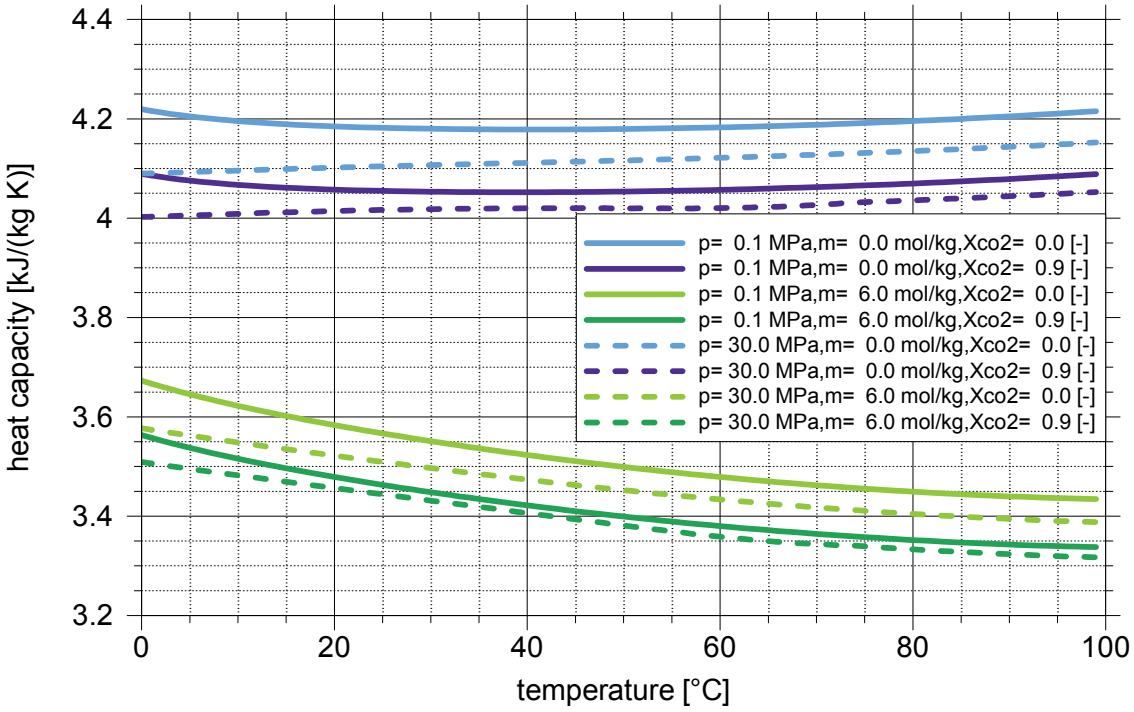

Fig. 4.24 Heat capacity of water with dissolved NaCl and CO_2; derived from [4].

4.7 Solubility[3]

4.7.1 Solubility of NaCl in water

4.7.1.1 Solubility of NaCl in liquid water

Source: [33] cited in [9]

Formulation:

$$\overline{L}_{water}^{NaCl} = 26.218 + 0.0072\,T + 0.000106\,T^2 \qquad (4.60)$$

[3] Solubility is essentially the ratio of the mass of solute to the mass of solvent. However, solubility can be given in different units like [g/100g solvent], [kg/kg], [mol/mol], [mol/kg], etc..

$\overline{L}_{water}^{NaCl}$ - solubility of NaCl in liquid water[4] [kg/kg] (q.v. eq. (4.61))

T - temperature [°C]

Conversion to molality:

$$L_{water}^{NaCl} = \frac{\overline{L}_{water}^{NaCl}}{\left(1 - \overline{L}_{water}^{NaCl}\right) M^{NaCl}} \qquad (4.61)$$

L_{water}^{NaCl} - solubility of NaCl in liquid water [mol/kg]

M^{NaCl} - molecular weight of NaCl [kg/mol] (c.f. Appendix B)

Range of validity:

temperature: $0 < T < 800$°C claimed by [33]

$0 < T < 400$°C recommended by [9]

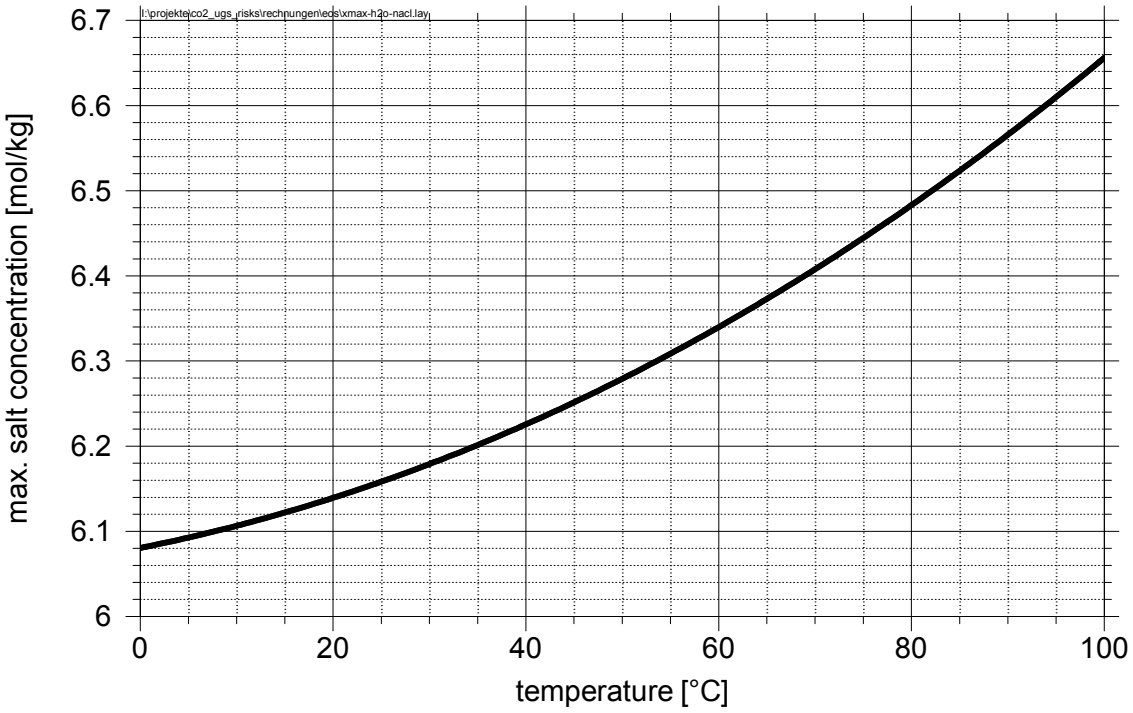

[4] In order to differentiate the phase state of H_2O the term 'water' will be used for liquid H_2O and vapour for a H_2O–rich gas-phase.

Fig. 4.25 Solubility of NaCl in water; after [33].

Comments: Tabulated data also in [31].

Conclusions: Eq. (4.60) is a reliable formulation within the ranges (1.1).

4.7.1.2 Solubility of NaCl in water vapour

Source: [21]

Formulation :

$$L_{vapour}^{NaCl} \cong 0 \qquad (4.62)$$

L_{vapour}^{NaCl} - solubility of NaCl in water vapour [mol/kg]

Comments: The concentration of salt in water vapour amounts to $8 \cdot 10^{-4}$ mol percent at 350 °C [21]. Within the temperature range (1.1) it is even lower.

Conclusions: Solubility of NaCl in water vapour is negligible within the ranges (1.1).

4.7.2 Solubility of CO_2 in water

Source: [41]

Formulation:

$$\hat{L}_{H_2O(p)}^{CO_2} = B\left(1 - \hat{L}_{CO_2}^{H_2O}\right) \qquad (4.63)$$

$\hat{L}_{H_2O(p)}^{CO_2}$ - Solubility of CO_2 in pure water [mol/mol]

$\hat{L}_{CO_2}^{H_2O}$ - Solubility of H_2O in CO_2-phase [mol/mol] (q.v. eq. (4.65))

B - constant (q.v. eq. (4.69))

Conversion of solubility $\hat{L}_{H_2O}^{CO_2}$ to molality:

$$L_{H_2O(p)}^{CO_2} = \frac{\hat{L}_{H_2O(p)}^{CO_2}}{\left(1 - \hat{L}_{H_2O(p)}^{CO_2}\right) M^{H_2O}} \quad (4.64)$$

$L_{H_2O(p)}^{CO_2}$ - Solubility of CO_2 in pure water [mol/kg]

M^{H_2O} - molecular weight of H_2O [kg/mol] (c.f. Appendix B)

$$\hat{L}_{CO_2}^{H_2O} = \frac{1 - B}{\left(\frac{1}{A}\right) - B} \quad (4.65)$$

A,B - ansatz functions (q.v. eq. (4.67))

Conversion of solubility $\hat{L}_{CO_2}^{H_2O}$ to molality:

$$L_{CO_2}^{H_2O} = \frac{\hat{L}_{CO_2}^{H_2O}}{\left(1 - \hat{L}_{CO_2}^{H_2O}\right) M^{CO_2}} \quad (4.66)$$

$L_{H_2O}^{CO_2}$ - Solubility of H_2O in the CO_2-phase [mol/kg]

M^{CO_2} - molecular weight of CO_2 [kg/mol] (c.f. 0)

$$A = \frac{K_0^{H_2O}}{\Phi^{H_2O} p} e^{\left(\frac{(p - p_0)\overline{V}^{H_2O}}{RT}\right)} \quad (4.67)$$

$K_0^{H_2O}$ - equilibrium constant [bar], (q.v. eq. (4.68))

Φ^{H_2O} - fugacity coefficient for water [-] (q.v. eq. (4.71))

p - total pressure [bar]

p_0 - reference pressure [bar], here: $p_0 = 1$ bar

$\overline{V}^{H_2O}$ - partial molar volume of CO_2 in water at infinite solution [cm³/mol] (c.f. Appendix B)

T - temperature [K]

R - universal gas constant [(bar cm³)/(K mol)]

$$K_0^{H_2O} = a + bT + cT^2 + dT^3 + eT^4 \qquad (4.68)$$

a,b,c,d,e - constants (c.f. Appendix B)

$$B = \frac{\Phi^{CO_2} p}{55.508 K_0^{CO_2}} e^{\left(\frac{(p-p_0)\overline{V}^{CO_2}}{RT}\right)} \qquad (4.69)$$

Φ^{CO_2} - fugacity coefficient for carbon dioxide [-] (q.v. eq. (4.71))

$K_0^{CO_2}$ - equilibrium constant [bar] , (q.v. eq. (4.70))

$\overline{V}_{CO_2}$ - partial molar volume of CO_2 in water at infinite solution [cm³/mol] (c.f. Appendix B)

$$K_0^{CO_2} = a + bT + cT^2 \qquad (4.70)$$

a,b,c - constants (c.f. Appendix B)

$$\ln \Phi^k = \ln\left(\frac{V}{V-b_{mix}}\right) + \left(\frac{b_k}{V-b_{mix}}\right) - \left(\frac{2\sum_{i=1}^{n} x_{CO_2}^i a_{ik}}{RT^{1.5} b_{mix}}\right) \ln\left(\frac{V+b_{mix}}{V}\right) + \left(\frac{a_{mix} b_k}{RT^{1.5} b_{mix}^2}\right)\left[\ln\left(\frac{V+b_{mix}}{V}\right) - \left(\frac{b_{mix}}{V+b_{mix}}\right)\right] - \ln\left(\frac{pV}{RT}\right)$$

for k=CO_2: (4.71)

$$\ln \Phi^{CO_2} = \ln\left(\frac{V}{V-b_{mix}}\right) + \left(\frac{b_{CO_2}}{V-b_{mix}}\right) - \left(\frac{2x_{CO_2}^{H_2O} a_{H_2O-CO_2} + 2x_{CO_2}^{CO_2} a_{CO_2}}{RT^{1.5} b_{mix}}\right) \ln\left(\frac{V+b_{mix}}{V}\right) + \left(\frac{a_{mix} b_{CO_2}}{RT^{1.5} b_{mix}^2}\right)\left[\ln\left(\frac{V+b_{mix}}{V}\right) - \left(\frac{b_{mix}}{V+b_{mix}}\right)\right] - \ln\left(\frac{pV}{RT}\right)$$

for k= H_2O:

$$\ln \Phi^{H_2O} = \ln\left(\frac{V}{V-b_{mix}}\right)+\left(\frac{b_{H_2O}}{V-b_{mix}}\right) - \left(\frac{2x_{CO_2}^{CO_2}a_{H_2O-CO_2}+2x_{CO_2}^{H_2O}a_{H_2O}}{RT^{1.5}b_{mix}}\right)\ln\left(\frac{V+b_{mix}}{V}\right) + \left(\frac{a_{mix}b_{H_2O}}{RT^{1.5}b_{mix}^2}\right)\left[\ln\left(\frac{V+b_{mix}}{V}\right)-\left(\frac{b_{mix}}{V+b_{mix}}\right)\right]-\ln\left(\frac{pV}{RT}\right)$$

Φ^k - fugacity coefficient of component k in mixtures with other components i [-]

V - partial molar volume of the gas phase [cm³/mol] (q.v. eq. (4.75))

a_i - measure for attractive molecular force of component i [bar cm^6 K$^{0.5}$ mol^{-2}]; (q.v. eq. (4.74))

b_k - measure for molecular size of component k [cm³/mol] (c.f. Appendix B)

a_{mix} - constant a for mixtures [bar cm^6 K$^{0.5}$ mol^{-2}] (q.v. eq. (4.72))

b_{mix} - constant b for mixtures [cm³/mol] (q.v. eq. (4.73))

$x_{CO_2}^i$ - mole fraction of component i in the CO_2-phase [-]

a_{ik} - measure for attractive molecular force of components i and k [bar cm^6 K$^{0.5}$ mol^{-2}] (c.f. Appendix B)

n - number of involved components [-]

i - index standing for H_2O and CO_2

$$a_{mix} = \left(x_{CO_2}^{H_2O}\right)^2 a_{H_2O} + 2x_{CO_2}^{H_2O}x_{CO_2}^{CO_2}a_{H_2O-CO_2} + \left(x_{CO_2}^{CO_2}\right)^2 a_{CO_2} \qquad (4.72)$$

$$b_{mix} = x_{CO_2}^{H_2O}b_{H_2O} + x_{CO_2}^{CO_2}b_{CO_2} \qquad (4.73)$$

$$a_{CO_2} = 7.54\,10^7 - 4.02\,10^4\ T \qquad (a_{H_2O} \text{ is not required}) \qquad (4.74)$$

$$V^3 - V^2\left(\frac{RT}{p}\right) - V\left(\frac{RTb}{p} - \frac{a}{pT^{0.5}} + b^2\right) - \left(\frac{ab}{pT^{0.5}}\right) = 0 \qquad (4.75)$$

Eq. (4.75) can yield more than one solution for the Volume V for a given subcritical state expressed in temperature T and pressure p. Maximum root depicts the volume V_{gas} of a gas phase, minimum root the volume V_{liquid} of a liquid phase. Which phase state is actually stable can be decided from the criterium

$c > 0$ stable gas phase

$c = 0$ two-phase state (4.76)

$c < 0$ stable liquid state

c - criterium for a stable subcritical phase state [-] (q.v. eq. (4.77))

$$c = w_2 - w_1 \qquad (4.77)$$

w_1, w_2 - work expressions (q.v. eq.s (4.78) and (4.79))

$$w_1 = p\left(V_{gas} - V_{liquid}\right) \qquad (4.78)$$

V_{gas} - partial molar volume of the gas phase [cm³/mol]

V_{liquid} - partial molar volume of the liquid phase [cm³/mol]

$$w_2 = RT \ln\left(\frac{V_{gas} - b}{V_{liquid} - b}\right) + \frac{a}{T^{0.5} b} \ln\left(\frac{\left(V_{gas} + b\right) V_{liquid}}{\left(V_{liquid} + b\right) V_{gas}}\right) \qquad (4.79)$$

Range of validity:

temperature: 12 °C < T < 100 °C

pressure: 0 MPa < p < 60 MPa

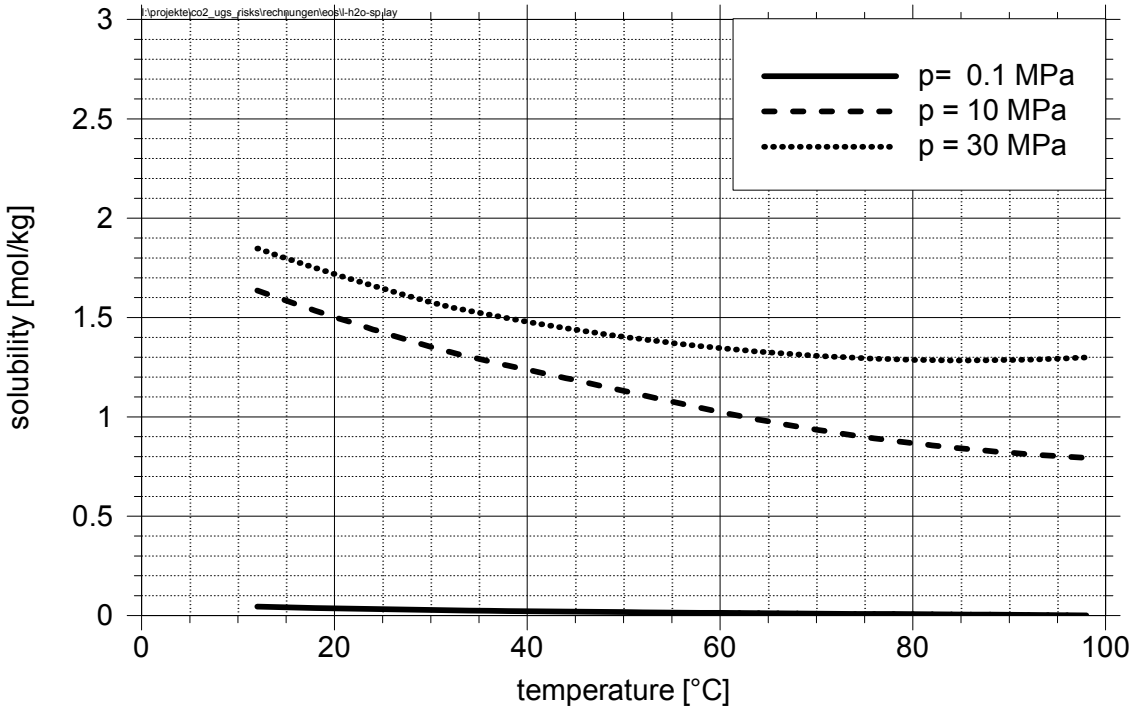

Fig. 4.26 Solubility of CO_2 in pure water; after [41].

Comments: Henry's law constitutes a simple linear relation between the mole fraction of dissolved gas in a solution and the partial pressure of this gas over the solution:

$$x_{CO_2}^{CO_2} p_{CO_2} = x_{H_2O}^{CO_2} K_{H\,H_2O}^{CO_2} \qquad (4.80)$$

The proportionality factor $K_{H\,H_2O}^{CO_2}$ in this equation is called Henry's constant. It is rather accurate for strongly diluted ideal solutions and ideal gases at constant temperature and pressures up to 10 MPa.

Apparently, this approach is not appropriate in the context of CO_2-sequestration because of varying temperature and rather high pressures. Additionally, the dissolved substance is not allowed to react with the solvent as in the case of carbon dioxide that partly becomes carbonic acid in water. Henry's law must therefore be substituted by a more accurate relation.

Conclusions: Eq. (4.63) is a reliable formulation within the ranges (1.1).

4.7.3 Solubility of CO_2 in water with dissolved NaCl

Source: [14], [40]

Formulation after [14]:

$$\ln \frac{L_{vapour}^{CO_2} p}{m_{H_2O}^{CO_2}} = \frac{\mu_{CO_2}^{1(0)}}{RT} - \ln \varphi_{CO_2} + 2\lambda_{CO_2-Na} m_{\text{water}}^{Na} + \zeta_{CO_2-Na-Cl} m_{\text{water}}^{Na} m_{\text{water}}^{Cl} \qquad (4.81)$$

$L_{vapour}^{CO_2}$ - solubility of CO_2 in the vapour phase [mol/kg]

p - total pressure [bar]

$m_{H_2O}^{CO_2}$ - molality of CO_2 in the water-phase [mol/kg]

$\mu_{CO_2}^{1(0)}$ - chemical potential

$\mu_{CO_2}^{1(0)} / RT$ - fitted quantity [-] (q.v. eq. (4.82))

φ_{CO_2} - fugacity coefficient for CO_2 [-]

λ_{CO_2-Na} - interaction constant [kg/mol](q.v. eq. (4.82))

$\zeta_{CO_2-Na-Cl}$ - interaction constant [(kg/mol)²] (q.v. eq. (4.82))

$m_{H_2O}^{Na}$ - molality of Na the water-phase [mol/kg]

$m_{H_2O}^{Cl}$ - molality of Cl the water-phase [mol/kg]

$$(quantity) = c_1 + c_2 T + \frac{c_3}{T} + c_4 T^2 + \frac{c_5}{630 - T} + c_6 p + c_7 p \ln T + c_8 \frac{p}{T} + c_9 \frac{p}{630 - T} + c_{10} \left(\frac{p}{630 - T} \right)^2 + c_{11} T \ln p \qquad (4.82)$$

$quantity$ - stands for $\mu_{CO_2}^{1(0)} / RT$, λ_{CO_2-Na} and $\zeta_{CO_2-Na-Cl}$

c_1 to c_{11} - 11 constants; different constants for different quantities (c.f. Appendix B)

T - temperature [K]

$$\ln\varphi = Z - 1 - \ln Z + \frac{a_1 + \frac{a_2}{T_r^2} + \frac{a_3}{T_r^3}}{V_r} + \frac{a_4 + \frac{a_5}{T_r^2} + \frac{a_6}{T_r^3}}{2V_r^2} + \frac{a_7 + \frac{a_8}{T_r^2} + \frac{a_9}{T_r^3}}{4V_r^4} + \frac{a_{10} + \frac{a_{11}}{T_r^2} + \frac{a_{12}}{T_r^3}}{5V_r^5} + \frac{a_{13}}{2T_r^3 a_{15}}\left[a_{14} + 1 - \left(a_{14} + 1 + \frac{a_{15}}{V_r^2}\right)e^{-\left(\frac{a_{15}}{V_r^2}\right)}\right] \quad (4.83)$$

Z - ansatz function [-] (q.v. eq. (4.86))

T_r - reduced temperature [-] (q.v. eq. (4.84))

V_r - reduced volume [-] (q.v. eq. (4.85))

a_1 to a_{15} - constants (c.f. Appendix B)

$$T_r = \frac{T}{T_c} \quad (4.84)$$

T_c - critical temperature of CO_2 [K]

$$V_r = \frac{RT_c}{p_c} \quad (4.85)$$

$$Z = \frac{p_r V_r}{T_r} = 1 + \frac{a_1 + \frac{a_2}{T_r^2} + \frac{a_3}{T_r^3}}{V_r} + \frac{a_4 + \frac{a_5}{T_r^2} + \frac{a_6}{T_r^3}}{V_r^2} + \frac{a_7 + \frac{a_8}{T_r^2} + \frac{a_9}{T_r^3}}{V_r^4} + \frac{a_{10} + \frac{a_{11}}{T_r^2} + \frac{a_{12}}{T_r^3}}{V_r^5} + \frac{a_{13}}{T_r^3 V_r^2}\left[a_{14} + \frac{a_{15}}{V_r^2}\right]e^{-\left(\frac{a_{15}}{V_r^2}\right)} \quad (4.86)$$

p_r - reduced pressure [-] (q.v. eq. (4.87))

$$p_r = \frac{p}{p_c} \qquad (4.87)$$

p_c - critical pressure of CO_2 [bar]

Formulation after [40]:

$$L_{H_2O}^{CO_2} = \frac{L_{H_2O(p)}^{CO_2}}{\gamma^*} \qquad (4.88)$$

γ^* - activity coefficient after [14] [-]; (q.v. eq. (4.90))

$L_{H_2O(p)}^{CO_2}$ - solubility of CO_2 in pure water [mol/kg]; (q.v. eq. (4.89))

$L_{H_2O}^{CO_2}$ - solubility of CO_2 in the water-phase [mol/kg]

Conversion of $L_{H_2O}^{CO_2}$ to mole fraction:

$$\hat{L}_{H_2O}^{CO_2} = \frac{L_{H_2O}^{CO_2}}{\frac{1}{M^{H_2O}} + \upsilon\, m_{H_2O}^{NaCl} + L_{H_2O}^{CO_2}} \qquad (4.89)$$

$\hat{L}_{H_2O}^{CO_2}$ - solubility of CO_2 in the water-phase [mol/mol]; (q.v. eq. (4.63))

M^{H_2O} - molecular weight of H_2O [kg/mol] (c.f. Appendix B)

$m_{H_2O}^{NaCl}$ - molality of NaCl in the water-phase [mol/kg]

υ - stoichiometric number of ions contained in the dissolved salt [-]; $\upsilon = 2$ in case of NaCl

$$\gamma^* = e^{\left(2\lambda_{CO_2-Na}\, m_{H_2O}^{Na} + \zeta_{CO_2-Na-Cl}\, m_{H_2O}^{Na} m_{H_2O}^{Cl}\right)} \qquad (4.90)$$

λ_{CO_2-Na} - interaction constant [kg/mol] (q.v. eq. (4.82))

$\zeta_{CO_2-Na-Cl}$ - interaction constant [(kg/mol)²] (q.v. eq. (4.82))

$m_{H_2O}^{Na}$ - molality of Na the water-phase [mol/kg]

$m_{H_2O}^{Cl}$ - molality of Cl the water-phase [mol/kg]

Range of validity:

	[14]:	[40]
temperature:	0 °C < *T* < 260 °C	12 °C < *T* < 100 °C
pressure:	0 MPa < p < 200 MPa	0 MPa < p < 60 MPa
salinity:	0 mol/kg < m < 4.3 mol/kg	0 mol/kg < m < 6 mol/kg

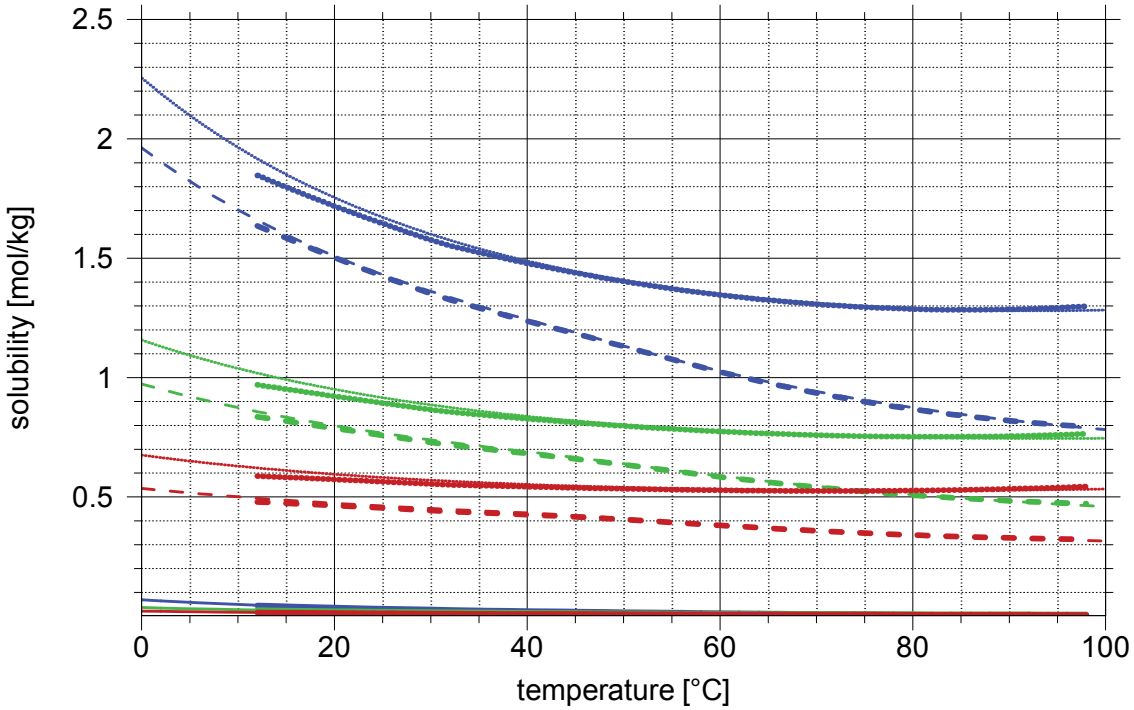

Fig. 4.27 Solubility of CO_2 in NaCl-solutions; line coding:
line thickness: thin lines - after [14], thick lines - after [40];
line type: solid - p=0.1 MPa, dashed - 10 MPa , dotted - 30 MPa;
line colour: blue - $m_{H_2O}^{NaCl}$ = 0 mol/kg, green - 3 mol/kg, red - 6 mol/kg.

Comments:

– V_r in eq. (4.86) is to be solved iteratively befor Z can be calculated.

– λ_{CO_2-Na} was set to zero bevor fitting parameters were calculated.

– While components of a gas mixture do not influence each other with respect to solubility, the solubility of gases in NaCl-solutions depends strongly on the salt concentration [10].

– The relation derived in [14] is fitted to an extensive lot of solubility experiments. Since it includes the salinity of the water phase it is presently one of the best adapted and most general formulations. However, they provide only solubility of CO_2 in aqueous salt solutions but not solubility of water in CO_2.

The formulations in [14] includes an iterative calculation of constant V_r. [17] and [40] state that calculating the iterative solution requires too much computational time. On the other hand, [40] seems to prefer another formulation for the activity coefficient γ'_x that is apparently of similar accuracy as the approach of [14] but requires an iterative procedure as well.

While [14] claims that their formulations are accurate up to 4.3 mol/kg NaCl, [40] attests even a sufficient accuracy up to 6 mol/kg NaCl if pressure and temperature are restricted to a range typical for CO_2-sequestration.

Conclusions: Eqs. (4.81) and (4.88) are reliable formulations within the ranges (1.1) up to 6 mol/kg NaCl.

4.8 Diffusivity

Sources: data: [28], [11]
formulation: present report

Formulation:

$$D_{H_2O}^{CO_2} = 10^{-9} + 7.8 \cdot 10^{-11} T - 4 \cdot 10^{-13} \left[T(100 - T)\right] \cdot \left(1 - 0.15 \frac{m_{H_2O}^{CO_2}}{L_{H_2O}^{CO_2}}\right) \qquad (4.91)$$

$D_{H_2O}^{CO_2}$ - Diffusion coefficient of CO_2 in water [m²/s]
T - Temperature [°C]
$m_{H_2O}^{CO_2}$ - molality of CO_2 in the water-phase [mol/kg]
$L_{H_2O}^{CO_2}$ - solubility of CO_2 in the water-phase [mol/kg] (q.v. eq. (4.64))

Range of validity:

temperature: 0 °C < T < 100 °C

pressure: 0 MPa < p < 100 MPa

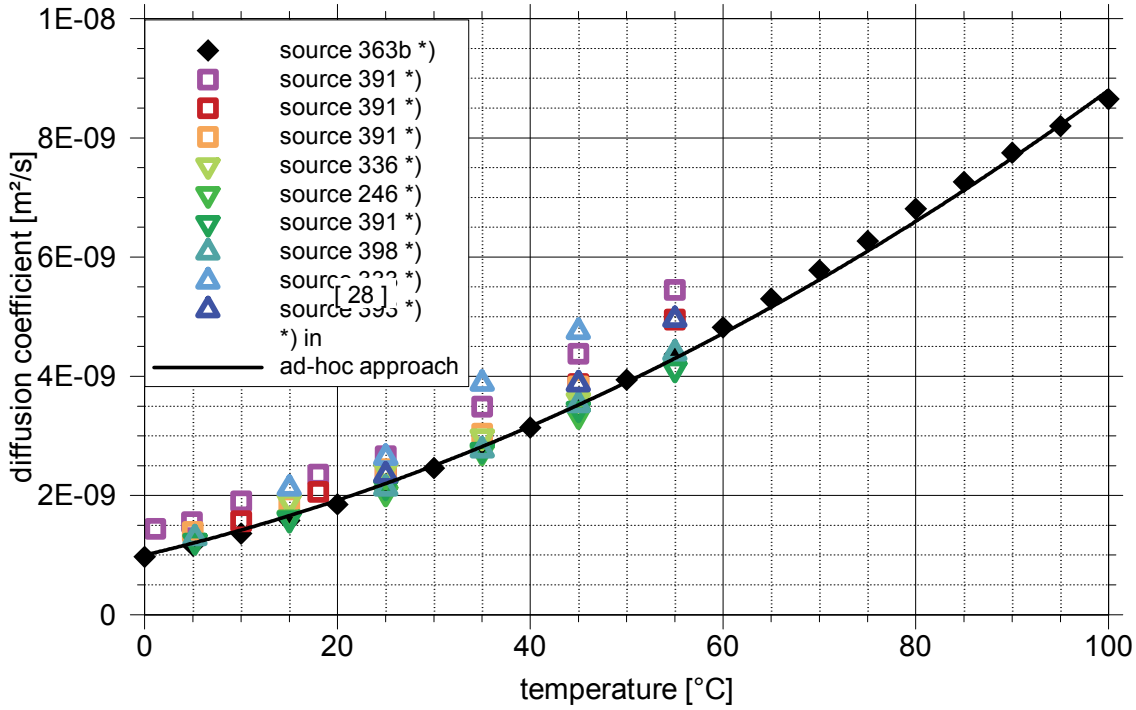

Fig. 4.28 Self-diffusivity of H_2O (probably at atmospheric pressure); data from [28].

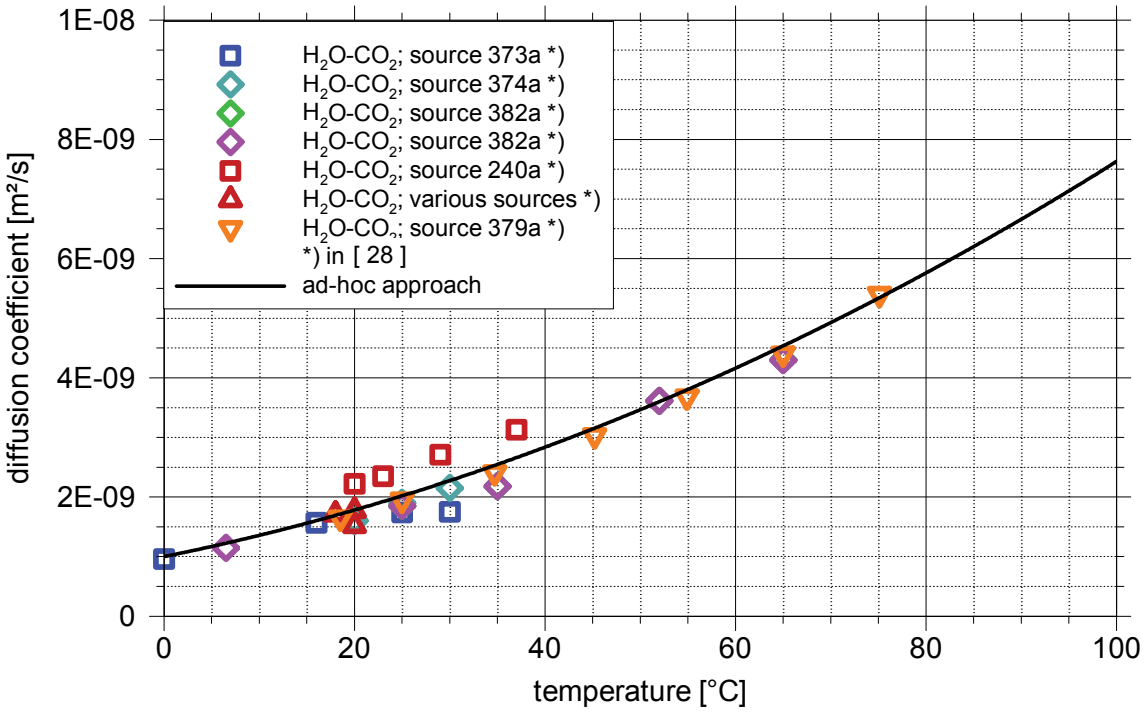

Fig. 4.29 Diffusivity of CO_2 in H_2O for different temperatures; data from [28].

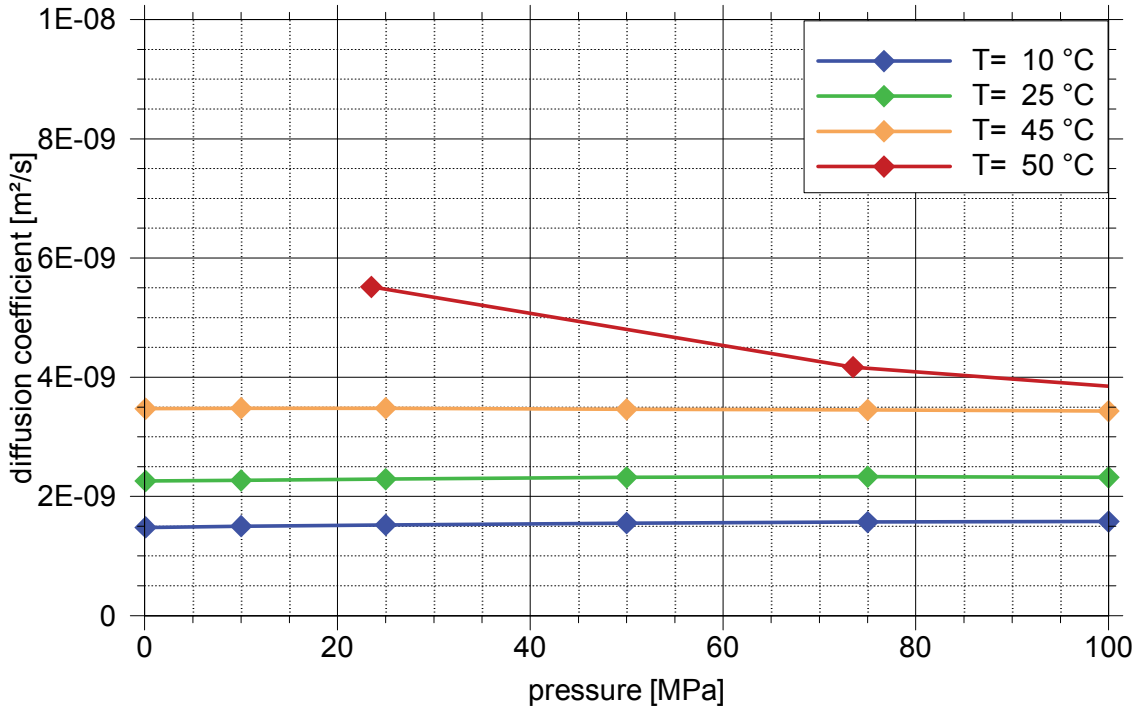

Fig. 4.30 Self-diffusivity of H_2O depending on pressure; data from [28], [11].

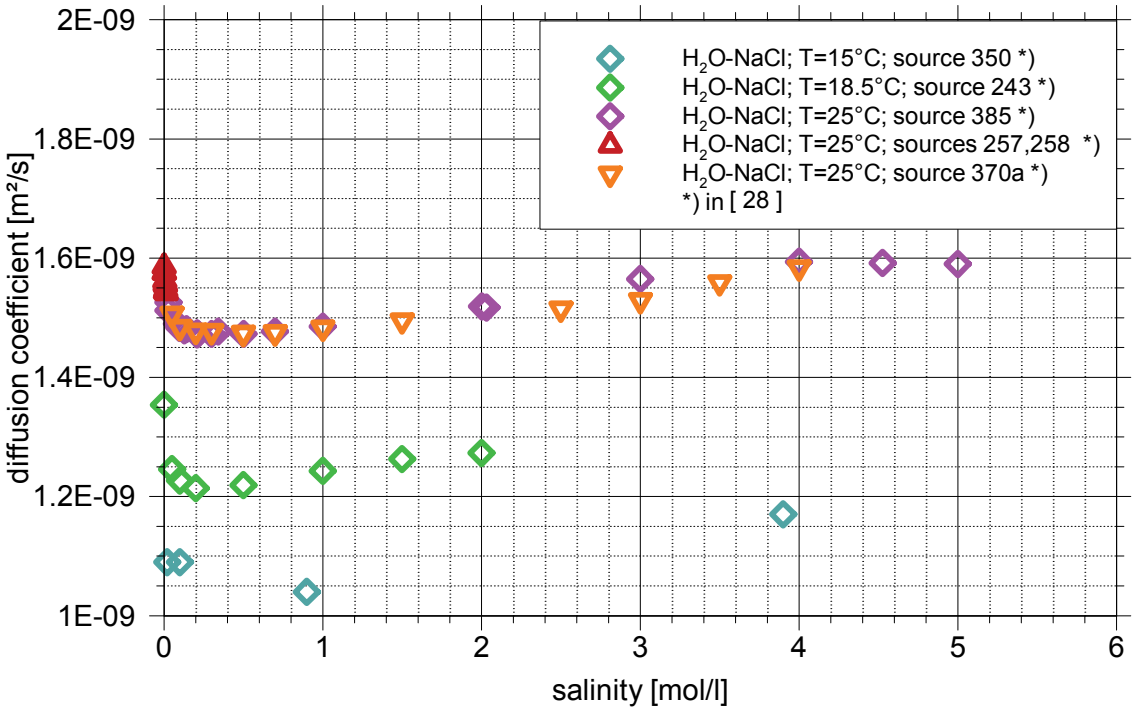

Fig. 4.31 Diffusivity of NaCl in H_2O for different temperatures; data from [28].

Comments:

– We are not aware of any formulations for the diffusivity in H_2O as a function of temperature, pressure and/or salinity. However, a good compilation of measured data exists.
– The formulation presented above is an ad hoc approach based on the data of [28] and [11] to provide a first approximation.
– Diffusivity of water is apparently neither significantly dependent on pressure nor on salinity in the ranges (1.1) (c.f. Fig. 4.30 and Fig. 4.31).
– Temperature, however, changes the diffusion coefficient considerably.
– The coefficient of self-diffusion is distinctly lowered by dissolved CO_2.

Conclusions: A rough estimate for the diffusivity in water can be concluded from the data. However, there is no data concerning the pressure-dependency of the diffusion of NaCl or CO_2 in water or CO_2 in brine.

5 Properties of carbon dioxide

5.1 Vapour pressure

5.1.1 Vapour pressure of pure CO_2

Source: [39]

Formulation:

$$\ln\left(\frac{p_s}{p_c}\right) = \frac{T_c}{T}\sum_{i=1}^{4} a_i \left(1 - \frac{T}{T_c}\right)^{t_i} \qquad (5.1)$$

p_s - vapour pressure of carbon dioxide [Pa]

T - temperature [K]

p_c - vapour pressure of CO_2 at the critical point [Pa] (c.f. Appendix B)

T_c - temperature of CO_2 at the critical point [K] (c.f. Appendix B)

a_i, t_i - parameters (c.f. Appendix B)

Range of validity:

temperature: 210 K < T < T_c

Comments: -

Conclusions: Eq. (5.1) is a reliable formulation within the ranges (1.1) up to the critical temperature.

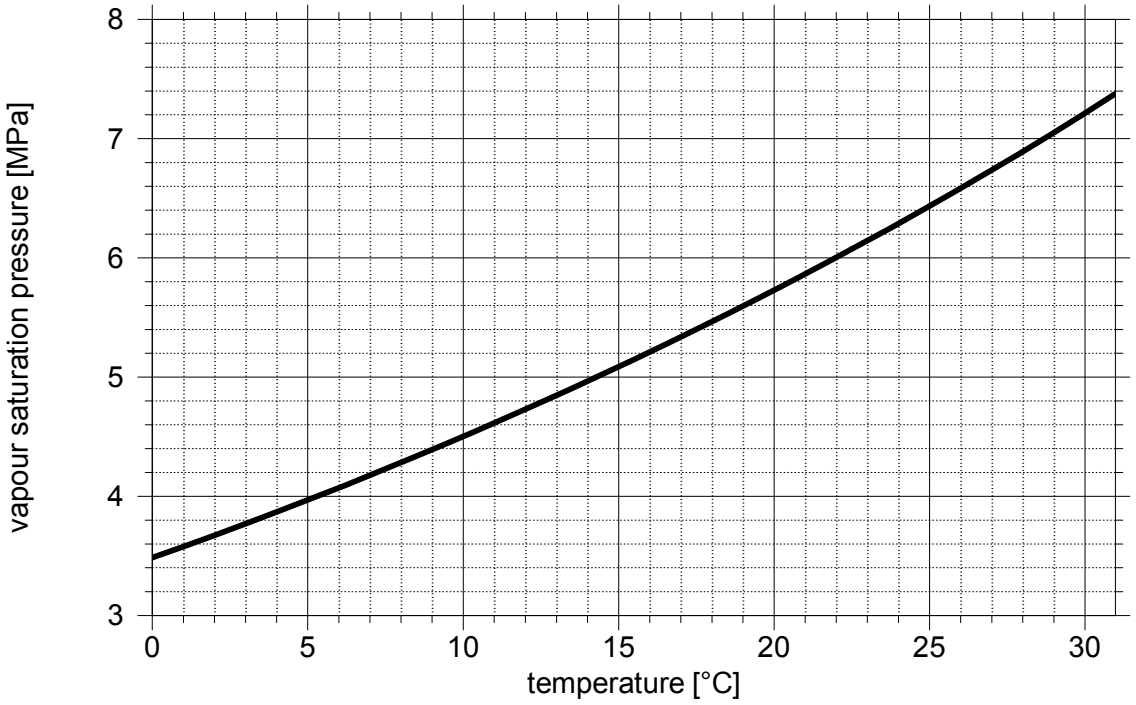

Fig. 5.1 Vapour saturation pressure of CO_2 [kg/m³]; after [39].

5.1.2 Vapour pressure of CO_2 with dissolved H_2O

Source: -

Comments: We are not aware of formulations concerning the vapour pressure CO_2 of with dissolved H_2O.

5.2 Helmholtz energy for CO_2

5.2.1 Approach

Several thermodynamic properties can be derived from the dimensionless Helmholtz energy Φ. An elaborate formulation is provided by [39].

$$\Phi = \frac{A}{R_{CO_2} T} \qquad (5.2)$$

A - specific Helmholtz energy [J/kg]

Φ - dimensionless Hemholtz energy [-]

R_{CO2} - specific gas constant for CO_2 [J/(kg K)] (c.f. Appendix B)

T - temperature [K]

$$\Phi = \Phi^0 + \Phi^r \qquad (5.3)$$

Φ^0 - dimensionless Helmholtz energy from ideal gas behaviour [-] (q.v. eq. (5.4))

Φ^r - dimensionless Helmholtz energy from residual fluid behaviour [-] (q.v. eq. (5.7))

$$\Phi^0 = \ln(\delta) + a_1^0 + a_2^0 \tau + a_3^0 \ln(\tau) + \sum_{i=4}^{8} a_i^0 \ln\left[1 - \exp\left(-\tau \theta_i^0\right)\right] \qquad (5.4)$$

a^0_i, θ^0_i - parameters (c.f. Appendix B)

δ - standardised density [-] (c.f. eq. (5.5))

τ - inverse standardised temperature [-] (c.f. eq. (5.6))

$$\delta = \frac{\rho}{\rho_c} \qquad (5.5)$$

ρ - density of carbon dioxide [kg/m³]

ρ_c - density of CO_2 at the critical point [kg/m³] (c.f. Appendix B)

$$\tau = \frac{T_c}{T} \qquad (5.6)$$

T_c - temperature at the critical point [K] (c.f. Appendix B)

$$\Phi^r = \sum_{i=1}^{7}\left(n_i\delta^{d_i}\tau^{t_i}\right) + \sum_{i=8}^{34}\left(n_i\delta^{d_i}\tau^{t_i}e^{-\delta^{c_i}}\right) + \sum_{i=35}^{39}\left(n_i\delta^{d_i}\tau^{t_i}e^{-\alpha_i(\delta-\varepsilon_i)^2-\beta_i(\tau-\gamma_i)^2}\right) + \sum_{i=40}^{42}\left(n_i\Delta^{b_i}\delta\Psi\right) \quad (5.7)$$

b_i, c_i, d_i, n_i, t_i, α_i, β_i, γ_i, ε_i - parameters of Helmholtz energy Φ (c.f. Appendix B)

Δ - distance function (q.v. eq. (5.8))

Ψ - exponential function (q.v. eq. (5.10))

$$\Delta = \theta^2 + B_i\left[(\delta-1)^2\right]^{a_i} \quad (5.8)$$

a_i, A_i, B_i - parameters of Helmholtz energy Φ (c.f. Appendix B)

θ - auxiliary function (q.v. eq. (5.9))

$$\theta = (1-\tau) + A_i\left[(\delta-1)^2\right]^{\frac{1}{2\beta_i}} \quad (5.9)$$

$$\Psi = e^{-C_i(\delta-1)^2 - D_i(\tau-1)^2} \quad (5.10)$$

C_i, D_i - parameters of Helmholtz energy Φ (c.f. Appendix B)

5.2.2 Derivatives

In [39] the writing convention

$$\left(\frac{\partial\Phi}{\partial x}\right)_y = \Phi_x \quad \text{with } x = \delta,\tau \text{ and } y = \tau,\delta \quad (5.11)$$

Φ - dimensionless Helmholtz energy [-] (q.v. eq. (5.3))

τ - inverse standardised temperature [-] (c.f. eq. (5.6))

δ - standardised density [-] (c.f. eq. (5.5))

is used. In the following, several derivatives of the dimensionless Helmholtz energy Φ are given that will be used in subsequent sections.

Derivative $\frac{\partial \Phi^0}{\partial \tau}$

$$\Phi_\tau^0 = a_2^0 + \frac{a_3^0}{\tau} + \sum_{i=4}^{8} a_i^0 \theta_i^0 \left[\left(1 - e^{-\theta_i^0 \tau}\right)^{-1} - 1 \right] \qquad (5.12)$$

$a^0{}_i$, $\theta^0{}_i$ - constants (c.f. Appendix B)

$$\Phi_{\tau\tau}^0 = -\frac{a_3^0}{\tau^2} - \sum_{i=4}^{8} a_i^0 \left(\theta_i^0\right)^2 e^{-\theta_i^0 \tau} \left(1 - e^{-\theta_i^0 \tau}\right)^{-2} \qquad (5.13)$$

Derivative $\frac{\partial \Phi^r}{\partial \delta}$

$$\begin{aligned} \Phi_\delta^r &= \sum_{i=1}^{7} n_i d_i \delta^{(d_i - 1)} \tau^{t_i} + \sum_{i=8}^{34} n_i e^{-\delta^{c_i}} \delta^{(d_i - 1)} \tau^{t_i} \left(d_i - c_i \delta^{c_i}\right) \\ &+ \sum_{i=35}^{39} n_i \delta^{d_i} \tau^{t_i} e^{-\alpha_i (\delta - \varepsilon_i)^2 - \beta_i (\tau - \gamma_i)^2} \left[\frac{d_i}{\delta} - 2\alpha_i \left(\delta - \varepsilon_i\right) \right] \\ &+ \sum_{i=40}^{42} n_i \left[\Delta^{b_i} \left(\Psi + \delta \frac{\partial \Psi}{\partial \delta} \right) + \frac{\partial \Delta^{b_i}}{\partial \delta} \delta \Psi \right] \end{aligned} \qquad (5.14)$$

a_i, b_i, c_i, d_i, n_i, t_i, α_i, β_i, γ_i, ε_i, A_i, B_i, C_i, D_i

- parameters of Helmholtz energy Φ (c.f. Appendix B)

Δ - distance function (q.v. eq. (5.8))

Ψ - exponential function (q.v. eq. (5.10))

$\frac{\partial \Delta^{b_i}}{\partial \delta}$ - auxiliary function (q.v. eq. (5.15))

$\frac{\partial \Psi}{\partial \delta}$ - auxiliary function (q.v. eq. (5.16))

$$\frac{\partial \Delta^{b_i}}{\partial \delta} = 2 b_i \Delta^{(b_i - 1)} \left(\delta - 1\right) * \left\{ \theta A_i \frac{1}{\beta_i} \left[(\delta - 1)^2 \right]^{\left(\frac{1}{2\beta_i} - 1\right)} + B_i a_i \left[(\delta - 1)^2 \right]^{(a_i - 1)} \right\} \qquad (5.15)$$

$$\frac{\partial \Psi}{\partial \delta} = -2 C_i \left(\delta - 1\right) \Psi \qquad (5.16)$$

Derivative $\frac{\partial^2 \Phi^r}{\partial \delta^2}$

$$\begin{aligned}\Phi^r_{\delta\delta} = &\sum_{i=1}^{7} n_i d_i (d_i - 1)\delta^{(d_i-2)}\tau^{t_i} \\ &+ \sum_{i=8}^{34} n_i e^{-\delta^{c_i}} \left[\delta^{(d_i-2)}\tau^{t_i}\left(\left(d_i - c_i\delta^{c_i}\right)\left(d_i - 1 - c_i\delta^{c_i}\right) - c_i^2\delta^{c_i}\right)\right] \\ &+ \sum_{i=35}^{39} n_i \tau^{t_i} e^{-\alpha_i(\delta-\varepsilon_i)^2 - \beta_i(\tau-\gamma_i)^2} \\ &\cdot\left[-2\alpha_i\delta^{d_i} + 4\alpha_i^2\delta^{d_i}(\delta-\varepsilon_i)^2 - 4d_i\alpha_i\delta^{(d_i-1)}(\delta-\varepsilon_i) + d_i(d_i-1)\delta^{(d_i-2)}\right] \\ &+ \sum_{i=40}^{42} n_i \left[\Delta^{b_i}\left(2\frac{\partial \Psi}{\partial \delta} + \delta\frac{\partial^2 \Psi}{\partial \delta^2}\right) + 2\frac{\partial \Delta^{b_i}}{\partial \delta}\left(\Psi + \delta\frac{\partial \Psi}{\partial \delta}\right) + \frac{\partial^2 \Delta^{b_i}}{\partial \delta^2}\delta\Psi\right]\end{aligned} \qquad (5.17)$$

$\frac{\partial^2 \Delta^{b_i}}{\partial \delta^2}$ - auxiliary function (q.v. eq. (5.18))

$\frac{\partial^2 \Psi}{\partial \delta^2}$ - auxiliary function (q.v. eq. (5.20))

$$\frac{\partial^2 \Delta^{b_i}}{\partial \delta^2} = b_i\left[\Delta^{(b_i-1)}\frac{\partial^2 \Delta}{\partial \delta^2} + {}_i(b_i - 1)\Delta^{(b_i-2)}\left(\frac{\partial \Delta}{\partial \delta}\right)^2\right] \qquad (5.18)$$

$\frac{\partial \Delta}{\partial \delta}$ - auxiliary function (q.v. eq. (5.19))

$$\frac{\partial \Delta}{\partial \delta} = (\delta - 1)\left\{A_i\theta\frac{2}{\beta_i}\left[(\delta-1)^2\right]^{\left(\frac{1}{2\beta_i}-1\right)} + 2B_i a_i\left[(\delta-1)^2\right]^{(a_i-1)}\right\} \qquad (5.19)$$

$$\frac{\partial^2 \Psi}{\partial \delta^2} = \left[-2C_i(\delta-1)^2 - 1\right]2C_i\Psi \qquad (5.20)$$

Derivative $\frac{\partial \Phi^r}{\partial \tau}$

$$\Phi_\tau^r = \sum_{i=1}^{7} n_i t_i \delta^{d_i} \tau^{(t_i-1)} + \sum_{i=8}^{34} n_i t_i \delta^{d_i} \tau^{(t_i-1)} e^{-\delta^{c_i}} + \sum_{i=35}^{39} n_i \delta^{d_i} \tau^{t_i} e^{-\alpha_i(\delta-\varepsilon_i)^2-\beta_i(\tau-\gamma_i)^2} \left[\frac{t_i}{\tau} - 2\beta_i(\tau-\gamma_i)\right] + \sum_{i=40}^{42} n_i \delta \left[\frac{\partial \Delta^{b_i}}{\partial \tau}\Psi + \Delta^{b_i}\frac{\partial \Psi}{\partial \tau}\right] \quad (5.21)$$

$\frac{\partial \Delta^{b_i}}{\partial \tau}$ - auxiliary function (q.v. eq. (5.22))

$\frac{\partial \Psi}{\partial \tau}$ - auxiliary function (q.v. eq. (5.23))

$$\frac{\partial \Delta^{b_i}}{\partial \tau} = -2\theta b_i \Delta^{(b_i-1)} \quad (5.22)$$

$$\frac{\partial \Psi}{\partial \tau} = -2D_i(\tau-1)\Psi \quad (5.23)$$

Derivative $\frac{\partial^2 \Phi^r}{\partial \tau^2}$

$$\Phi_{\tau\tau}^r = \sum_{i=1}^{7} n_i t_i (t_i-1)\delta^{d_i}\tau^{t_i} + \sum_{i=8}^{34} n_i t_i (t_i-1)\delta^{d_i}\tau^{(t_i-2)} e^{-\delta^{c_i}} + \sum_{i=35}^{39} n_i \delta^{d_i}\tau^{t_i} e^{-\alpha_i(\delta-\varepsilon_i)^2-\beta_i(\tau-\gamma_i)^2}\left[\left(\frac{t_i}{\tau} - 2\beta_i(\tau-\gamma_i)\right)^2 - \frac{t_i}{\tau^2} - 2\beta_i\right] + \sum_{i=40}^{42} n_i \delta \left[\frac{\partial^2 \Delta^{b_i}}{\partial \tau^2}\Psi + 2\frac{\partial \Delta^{b_i}}{\partial \tau}\frac{\partial \Psi}{\partial \tau} + \Delta^{b_i}\frac{\partial^2 \Psi}{\partial \tau^2}\right] \quad (5.24)$$

$\frac{\partial^2 \Delta^{b_i}}{\partial \tau^2}$ - auxiliary function (q.v. eq. (5.25))

$\frac{\partial^2 \Psi}{\partial \tau^2}$ - auxiliary function (q.v. eq. (5.26))

$$\frac{\partial^2 \Delta^{b_i}}{\partial \tau^2} = 2b_i \Delta^{(b_i-1)} + 4\theta^2 b_i (b_i - 1)\Delta^{(b_i-2)} \qquad (5.25)$$

$$\frac{\partial^2 \Psi}{\partial \tau^2} = \left[-2D_i(\tau-1)^2 - 1\right]2D_i\Psi \qquad (5.26)$$

Derivative $\frac{\partial^2 \Phi^r}{\partial \delta \partial \tau}$

$$\begin{aligned}\Phi^r_{\delta\tau} = &\sum_{i=1}^{7} n_i d_i t_i \delta^{(d_i-1)} \tau^{(t_i-1)} + \sum_{i=8}^{34} n_i e^{-\delta^{c_i}} \delta^{(d_i-1)} t_i \tau^{(t_i-1)} \left(d_i - c_i \delta^{c_i}\right) \\ &+ \sum_{i=35}^{39} n_i \delta^{d_i} \tau^{t_i} e^{-\alpha_i(\delta-\varepsilon_i)^2 - \beta_i(\tau-\gamma_i)^2} \left[\frac{d_i}{\delta} - 2\alpha_i(\delta-\varepsilon_i)\right]\left[\frac{t_i}{\tau} - 2\beta_i(\tau-\gamma_i)\right] \\ &+ \sum_{i=40}^{42} n_i \left[\Delta^{b_i}\left(\frac{\partial \Psi}{\partial \tau} + \delta \frac{\partial^2 \Psi}{\partial \delta \partial \tau}\right) + \delta \frac{\partial \Delta^{b_i}}{\partial \delta}\frac{\partial \Psi}{\partial \tau} + \frac{\partial \Delta^{b_i}}{\partial \tau}\left(\Psi + \delta \frac{\partial \Psi}{\partial \delta}\right) + \frac{\partial^2 \Delta^{b_i}}{\partial \delta \partial \tau}\delta\Psi\right]\end{aligned} \qquad (5.27)$$

$\frac{\partial^2 \Delta^{b_i}}{\partial \delta \partial \tau}$ - auxiliary function (q.v. eq. (5.28))

$\frac{\partial^2 \Psi}{\partial \delta \partial \tau}$ - auxiliary function (q.v. eq. (5.29))

$$\frac{\partial^2 \Delta^{b_i}}{\partial \delta \partial \tau} = -A_i b_i \frac{2}{\beta_i} \Delta^{(b_i-1)}(\delta-1)\left[(\delta-1)^2\right]^{\left(\frac{1}{2\beta_i}-1\right)} - 2\theta b_i (b_i-1)\Delta^{(b_i-2)}\frac{\partial \Delta}{\partial \delta} \qquad (5.28)$$

$$\frac{\partial^2 \Psi}{\partial \delta \partial \tau} = 4C_i D_i (\delta-1)(\tau-1)\Psi \qquad (5.29)$$

5.3 Density

5.3.1 Density of pure CO_2

Source: [39]

Formulation:

$$\frac{p}{\rho R_{CO_2} T} = 1 + \delta \frac{\partial \Phi^r}{\partial \delta} \qquad (5.30)$$

p - pressure of the carbon dioxide [Pa]

ρ - density of carbon dioxide [kg/m³]

R_{CO2} - specific gas constant for CO_2 [J/(kg K)] (c.f. Appendix B)

T - temperature [K]

δ - standardised density [-] (c.f. eq. (5.5))

Φ_δ^r - partial derivative of the Helmholtz energy Φ (q.v. eq. (5.14))

Range of validity:

temperature: 216 K < T < 1100 K

pressure: 0 MPa < p < 800 MPa

Comments: Pressure - usually a primary variable in a numerical scheme - is replaced by the density. Unfortunately, [39] does not provide an equation for the back calculation of the density as a function of temperature and pressure. The same problems are apparently encountered in [17] when it comes to application in a numerical model. There, the problem is solved by calculating the density of CO_2 at discrete points in the p-T-domain and linear interpolation during run time of the program. An iterative scheme to calculate the density from temperature and pressure is described in Appendix B.

Conclusions: Eq. (5.30) is a reliable formulation within the ranges (1.1).

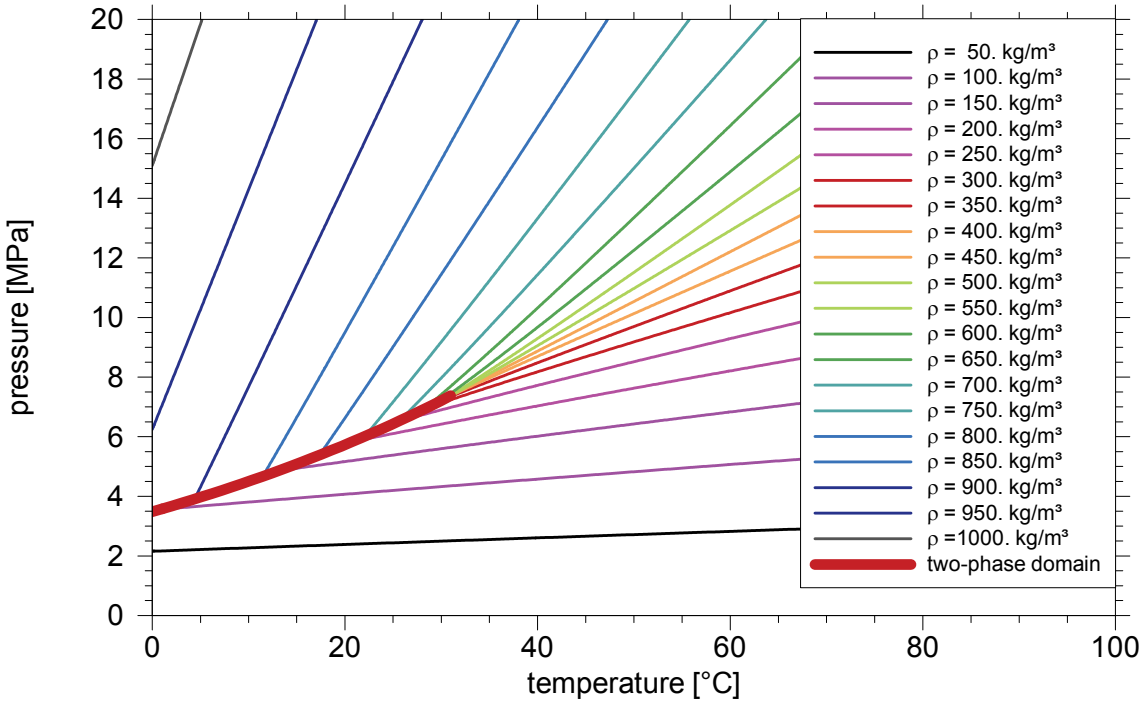

Fig. 5.2 Density of CO_2; after [39].

5.3.2 Density of CO_2 with H_2O

5.3.2.1 Density of gaseous CO_2

Source: e.g. [17]

Formulation:

$$\rho_{CO_2} = \rho_{CO_2}^{CO_2} + \rho_{CO_2}^{H_2O} \qquad (5.31)$$

ρ_{CO_2} - density of gaseous carbon dioxide [kg/m³]

$\rho_{CO_2}^{CO_2}$ - partial density of carbon dioxide in the gas phase [kg/m³]

$\rho_{CO_2}^{H_2O}$ - partial density of water vapour in the gas phase [kg/m³]

Range of validity:

temperature: 273.15 K ≤ T ≤ 623.15 K

pressure: 0 MPa < p < $p_s(T,m)$; p_s - vapour pressure of CO_2

Comments: In case of a gaseous CO_2-phase coexisting with a liquid water phase equilibrium of the water vapour in the gaseous CO_2-phase and the liquid water is assumed. The partial pressure of water vapour equals the vapour saturation pressure which is discussed in section 4.1.1 for pure water and in section 4.1.2 for water with dissolved NaCl. The partial density of water vapour can be calculated with the help of formulation (4.17) using the appropriate partial pressure of water vapour. The density of the gas mixture can finally be calculated as the sum of the partial gas densities.

Conclusions: Eq. (5.31) is a reliable formulation within the ranges (1.1).

5.3.2.2 Density of liquid CO_2

Source: [4], [17]

Comments: [4] and [17] assume that solution of water in liquid carbon dioxide can be described like an evaporation process. This leads to the same relation as in section 5.3.2.1, again with the additional assumption that the pressure of dissolved water equals the vapour saturation pressure.

Conlusions: Apparently, very little is known about the relation between CO_2-density and the amount of dissolved water in the CO_2-dominated phase.

5.4 Viscosity

5.4.1 Viscosity of pure CO_2

Source: [15], [46]

Formulation:

$$\eta = \eta_0 + \Delta\eta + \Delta\eta_c \qquad (5.32)$$

η - viscosity of carbon dioxide [µPa s]

η_0 - viscosity in the zero-density limit [µPa s] (q.v. eq. (5.33))

$\Delta\eta$ - excess viscosity [µPa s] (q.v. eq. (5.36))

$\Delta\eta_c$ - critical enhancement in the vicinity of the critical point [µPa s]

$$\eta_0 = \frac{1.00697\, T^{1/2}}{\sigma_\eta^*} \qquad (5.33)$$

σ_η^* - reduced effective cross-section (q.v. eq. (5.34))

T - Temperature [K]

$$\ln \sigma_\eta^* = \sum_{i=0}^{4} a_i \left(\ln T^*\right)^i \qquad (5.34)$$

T^* - reduced Temperature [K] (q.v. eq. (5.35))

a_i - constants (c.f. Appendix B)

$$T^* = \frac{T}{251.196} \qquad (5.35)$$

$$\Delta\eta = d_{11}\rho + d_{21}\rho^2 + \frac{d_{64}\rho^6}{\left(T^*\right)^3} + d_{81}\rho^8 + \frac{d_{82}\rho^8}{T^*} \qquad (5.36)$$

d_{ij} - constants (c.f. Appendix B)

ρ - density of carbon dioxide [kg/m³]

$$\Delta\eta_c = \sum_{i=1}^{4} e_i \rho^i \qquad (5.37)$$

e_i - constants (c.f. Appendix B)

Range of validity:

temperature: 200 K < T < 1500 K

pressure: p < 300 MPa for T < 1000 K

density: ρ < 1400 kg/m³

Accuracy is ±0.3% for the viscosity of dilute gas near room temperature and ±5% at the highest pressures.

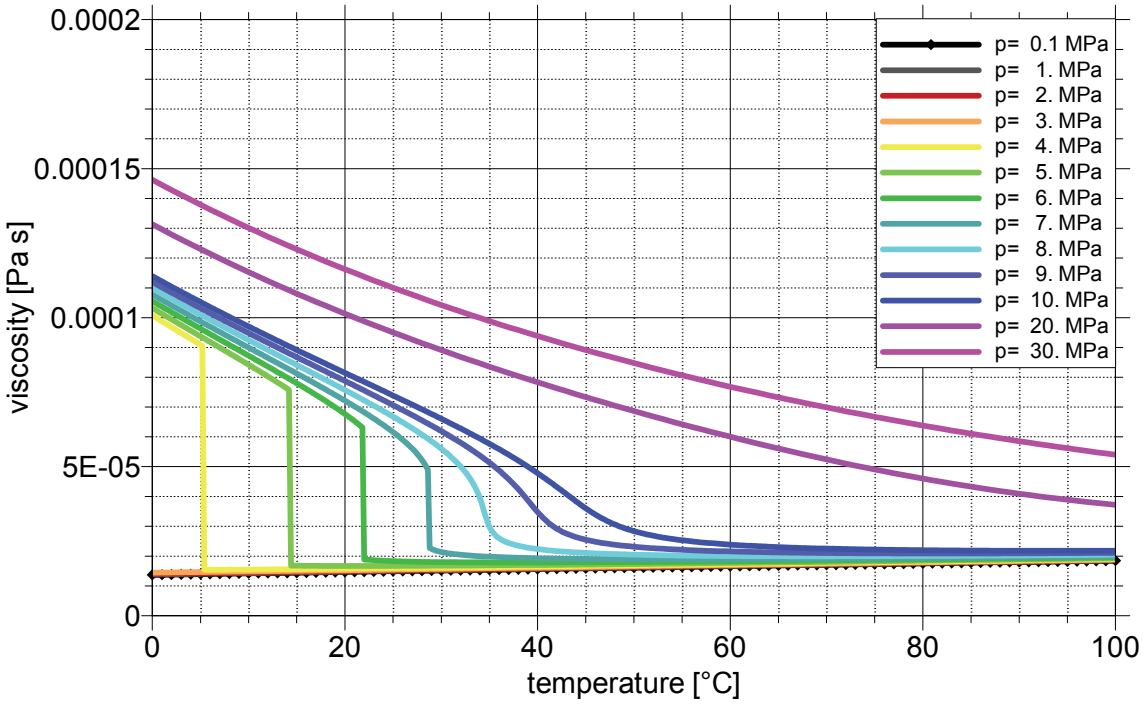

Fig. 5.3 Viscosity of CO_2; after [15].

Comments: The third summand of eq. (5.32) is effective only in the vicinity of the critical point. Vicinity is defined in [15] by 300 K < T < 310 K and 300 kg/m³ < ρ < 600 kg/m³. In this range the quotient $\Delta\eta_c/\eta$ exceeds 1%. $\Delta\eta_c$ is not given in [15] but the authors refer to [46] for formulation (5.37).

Values of the viscosity at specified temperatures, pressures and densities are given in [15] as well and can be found under in Appendix B.

An additional backup for the formulations from [15] comes from [17]. The correlations from [15] are compared with an approach from [1] which yields a maximum difference of less than 2%.

Conclusions: Eq. (5.32) is a reliable formulation within the ranges (1.1).

5.4.2 Viscosity of CO_2 with H_2O

5.4.2.1 Viscosity of gaseous CO_2

Source: [4]

Formulation:

$$\eta_g = X_g^{CO_2}\eta_g^{CO_2} + X_g^{H_2O}\eta_g^{H_2O} \qquad (5.38)$$

η_g - viscosity of the mixture of gaseous CO_2 and water vapour [Pa s]
η_g^{CO2} - viscosity of gaseous CO_2 [Pa s] (q.v. eq. (5.32))
η_g^{H2O} - viscosity of water vapour [Pa s] (q.v. eq. (4.25))
X_g^{CO2} - mass fraction of CO_2 in the gas phase [-]
X_g^{H2O} - mass fraction of water vapour in the gas phase [-]

Range of validity:

pressure: $p_g^{H_2O} < p_{sat}^{H_2O}$

Comments: At single gas phase conditions the viscosity of a mixture of water vapour and carbon dioxide is assumed to be mass proportional.

Conclusions: Apparently, no measurements are known to confirm approach (5.38).

5.4.2.2 Viscosity of liquid CO_2

Comments: At the time we are not aware of formulations describing the viscosity of liquid carbon dioxide with dissolved H_2O. A first approximation may be to neglect the influence of the dissolved water on the liquid CO_2 on account of the low solubility of water in carbon dioxide.

Conclusions: Apparently, no measurements are known to back up the suggested approach.

5.5 Thermal conductivity

5.5.1 Thermal conductivity of pure CO_2

Source: [46] including modifications from [38]

Formulation

$$\lambda = \lambda_0 + \Delta\lambda + \Delta\lambda_c \qquad (5.39)$$

λ - thermal conductivity [W/(m K)]

λ_0 - thermal conductivity of the ideal gas with negligible density [W/(m K)] (q.v. eq. (5.40))

$\Delta\lambda$ - correction for the influence of density [W/(m K)] (q.v. eq. (5.44))

$\Delta\lambda_c$ - critical enhancement [W/(m K)] (q.v. eq. (5.45))

$$\lambda_0 = \frac{0.475598\sqrt{T}\left(1+r^2\right)}{1000\,\sigma_\lambda^*} \qquad (5.40)$$

T - temperature [K]

r - ansatz function (q.v. eq. (5.41))

σ_λ^* - ansatz function (q.v. eq. (5.42))

$$r = \sqrt{\frac{2}{5}\left(1+e^{-\frac{183.5}{T}}\cdot\sum_{i=1}^{5}c_i\left(\frac{T}{100}\right)^{2-i}\right)} \qquad (5.41)$$

c_i - constants (c.f. Appendix B)

$$\sigma_\lambda^* = \sum_{i=0}^{7}\frac{b_i}{T^*} \qquad (5.42)$$

T^* - normalised temperature [-] (q.v. eq. (5.43))

b_i - constants (c.f. Appendix B)

$$T^* = \frac{T}{251.196} \qquad (5.43)$$

$$\Delta\lambda = \frac{1}{1000}\sum_{i=1}^{4} d_i \rho^i \qquad (5.44)$$

d_i - constants (c.f. Appendix B)

ρ - density [kg/m³]

$$\Delta\lambda_c = \rho\, c_p \frac{R^* k T}{6\pi\eta\xi}\left(\widetilde{\Omega} - \widetilde{\Omega}_0\right) \qquad (5.45)$$

c_p - isobaric heat capacity [J/(kg K)] (q.v. eq. (5.55))

R^* - constant; R^*=1.01 [-]

k - Boltzmann constant; k = 1.380662×10^{-23} [J/K]

π - Ludolph's number [-]

η - viscosity of carbon dioxide [Pa s] (q.v. eq. (5.32))

ξ - correlation length [m] (q.v. eq. (5.46))

$\widetilde{\Omega}$ - auxiliary function (q.v. eq. (5.50))

$\widetilde{\Omega}_0$ - auxiliary function (q.v. eq. (5.51))

$$\xi = \xi_0 \left(\frac{\Delta\widetilde{\chi}}{\Gamma}\right)^{\frac{\nu}{\gamma}} \qquad (5.46)$$

ξ_0 - reference length [m]; ξ_0 = 1.50×10^{-10} m

$\Delta\widetilde{\chi}$ - auxiliary function [-] (q.v. eq. (5.47))

Γ - constant [-]; Γ = 0.052

ν - constant [-]; ν =0.630

γ - constant [-]; γ =1.2415

$$\Delta\tilde{\chi} = \tilde{\chi}(\rho,T) - \tilde{\chi}(\rho,T_r)\frac{T_r}{T} \qquad (5.47)$$

$\tilde{\chi}$ - symmetrised compressibility [-] (q.v. eq. (5.49))

T_r - reference temperature [K] (q.v. eq. (5.48))

$$T_r = 1.5\,T_c \qquad (5.48)$$

T_c - critical temperature of CO_2 [K]

$$\tilde{\chi} = \frac{p_c}{\rho_c^2 T_c}\rho T\left(\frac{\partial\rho}{\partial p}\right)_T \qquad (5.49)$$

p_c - critical pressure of CO_2 [Pa]

ρ_c - critical density of CO_2 [Pa]

$\left(\frac{\partial\rho}{\partial p}\right)_T$ - specially defined compressibility [kg / (m³ Pa)] (q.v. “comments”)

$$\tilde{\Omega} = \frac{2}{\pi}\left[\left(\frac{c_p - c_v}{c_p}\right)\arctan\left(\tilde{q}_D\xi\right) + \frac{c_v}{c_p}\left(\tilde{q}_D\xi\right)\right] \qquad (5.50)$$

c_v - isochoric heat capacity [J/(kg K)] (q.v. eq. (5.56))

$\tilde{q}_D$ - constant [m]; $\tilde{q}_D$ =1/3.6×10^{-10} 1/m

$$\tilde{\Omega}_0 = \frac{2}{\pi}\left[1 - e^{-\frac{1}{\frac{1}{(\tilde{q}_D\xi)} + \frac{1}{3}\left(\frac{\tilde{q}_D\xi\rho_c}{\rho}\right)^2}}\right] \qquad (5.51)$$

Range of validity:

temperature: 200 K < T < 450 K

pressure: 0 MPa < p < 100 MPa

density: 25 kg/m³ < ρ < 1000 kg/m³

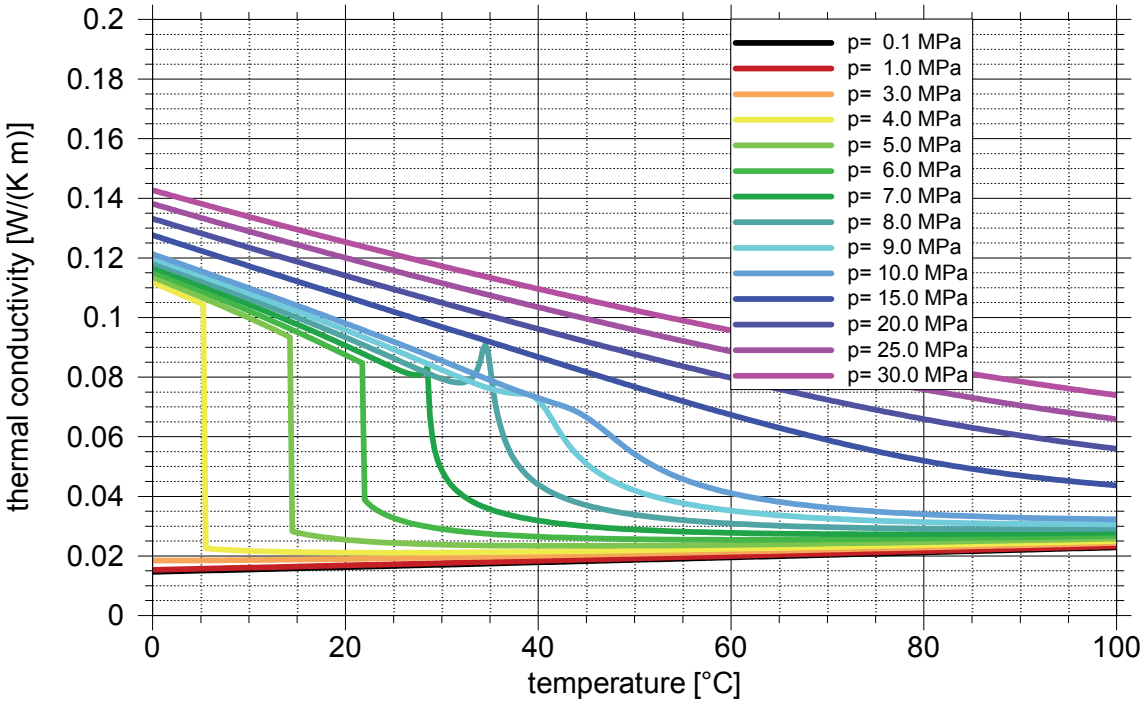

Fig. 5.4 Thermal conductivity for CO_2 as a function of temperature; after [39].

Comments: As discussed in the comments to section 5.3.1 referring to the formulations in [39], [13] does not provide an equation for the back calculation of the density as a function of temperature and pressure. In the framework of the formulations presented here, Eq. (5.49) can therefore not provided exactly but only by means of iteration as described in Appendix B and by calculating the derivative numerically.

Conclusions: Eq. (5.39) is a reliable formulation within the ranges (1.1).

5.5.2 Thermal conductivity of CO_2 with dissolved H_2O

Comments: We are not aware of formulations concerning the thermal conductivity of CO_2 with dissolved H_2O.

5.6 Enthalpy

5.6.1 Enthalpy of pure CO_2

Source: [39]

Formulation:

$$\frac{h}{R_{CO_2}T} = 1 + \tau\left(\Phi_\tau^0 + \Phi_\tau^r\right) + \delta\,\Phi_\delta^r \qquad (5.52)$$

h - enthalpy of carbon dioxide [J/kg]

R_{CO2} - specific gas constant for CO_2 [J/(kg K)] (c.f. Appendix B)

T - Temperature [K]

δ - standardised density [-] (c.f. eq. (5.5))

τ - inverse standardised temperature [-] (c.f. eq. (5.6))

$\Phi_\tau^0, \Phi_\tau^r, \Phi_\delta^r$ - partial derivatives of the dimensionless Helmholtz energy Φ, (c.f. eqs. (5.12), (5.21), (5.14))

Range of validity:

temperature: 216 K < T < 1100 K

pressure: 0 MPa < p < 800 MPa

Comments: Formulation (5.52) is valid over an exceptional range of pressure and temperature. However, it is too complex to be used in a numerical code. Instead, interpolation of discrete data is often used.

Conclusions: Eq. (5.52) is a reliable formulation within the ranges (1.1).

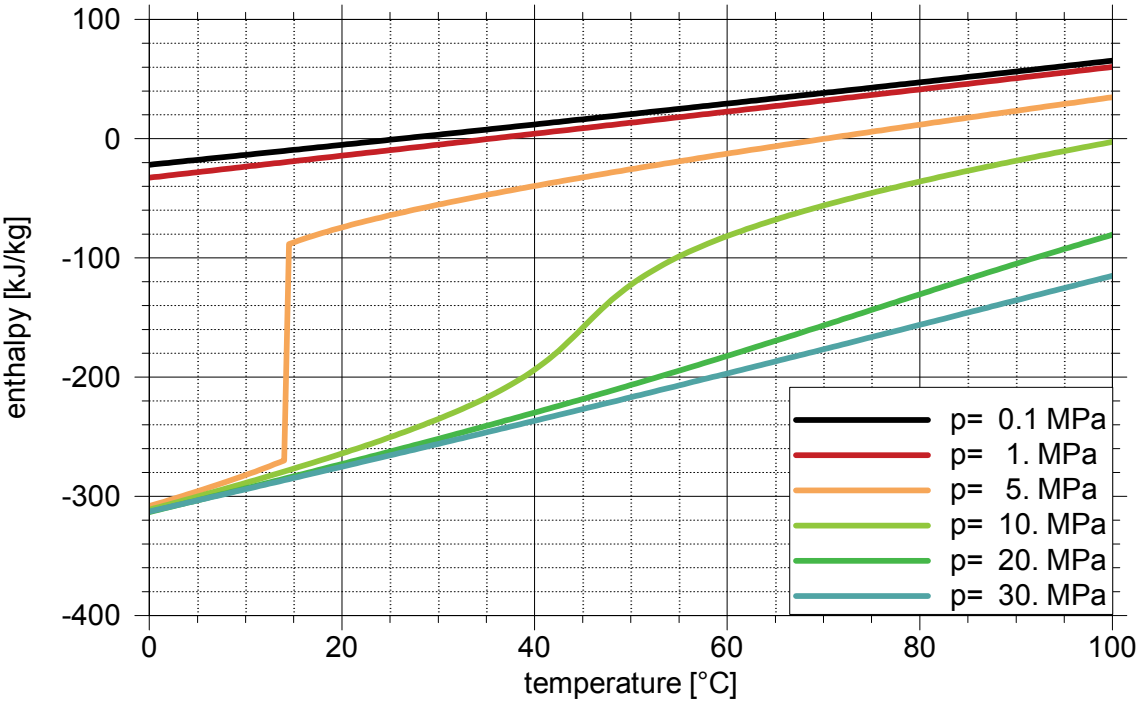

Fig. 5.5 Enthalpy for CO_2 as a function of temperature; after [39].

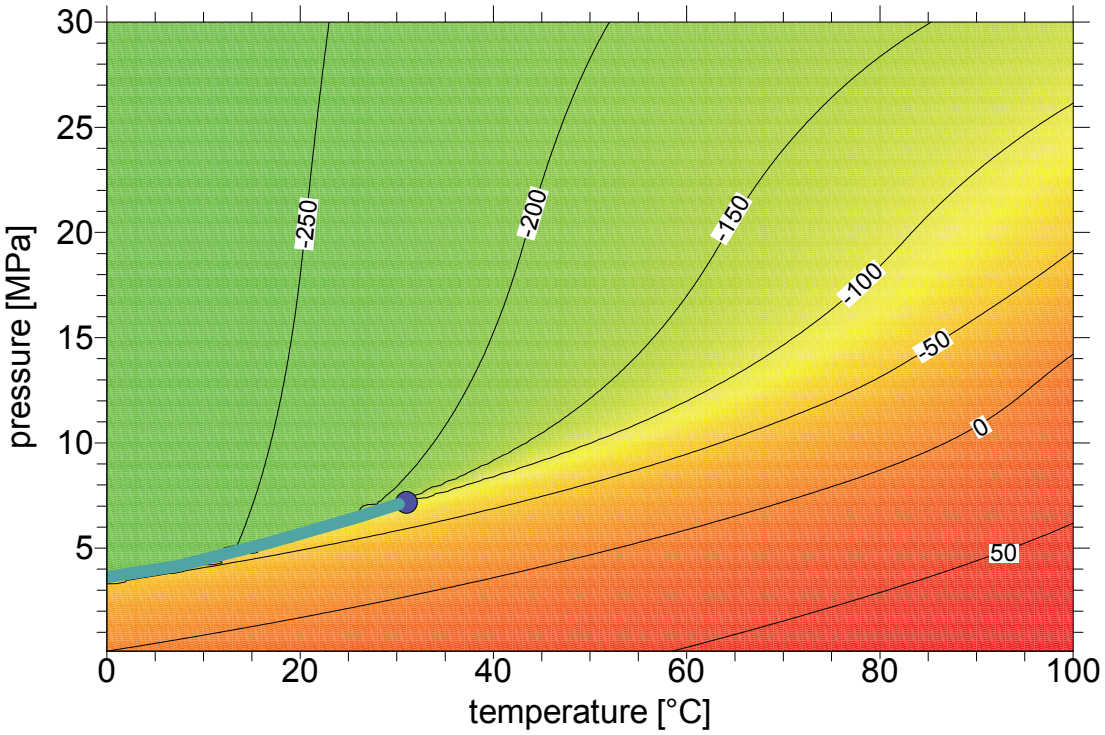

Fig. 5.6 Enthalpy for CO_2 as a function of temperature and pressure; after [39].

5.6.2 Enthalpy of CO_2 with water

5.6.2.1 Enthalpy of gaseous CO_2 with water

Source: [4]

Formulation:

$$h = X_{CO_2}^{CO_2} h^{CO_2} + X_{CO_2}^{H_2O} h^{H_2O} \qquad (5.53)$$

h - enthalpy of the mixture of gaseous CO_2 and water vapour [J/kg]

h^{CO_2} - enthalpy of gaseous CO_2 [J/kg] (q.v. eq.(5.52))

h^{H_2O} - enthalpy of water vapour [J/kg] (q.v. eq.(4.36))

$X_{CO_2}^{CO_2}$ - mass fraction of CO_2 in the gas phase [-]

$X_{CO_2}^{H_2O}$ - mass fraction of water vapour in the gas phase [-]

Comments: At single gas phase conditions the enthalpy of a mixture of water vapour and carbon dioxide is assumed to be mass proportional.

Conclusions: Apparently, no measurements are known to back up approach (5.53).

5.6.2.2 Enthalpy of liquid CO_2 with water

Source: -

Formulation:

$$h_{CO_2} = X_{CO_2}^{CO_2} h^{CO_2} + X_{CO_2}^{H_2O} h^{H_2O} + X_{CO_2}^{H_2O} \Delta h_{CO_2}^{H_2O} \qquad (5.54)$$

h - enthalpy of the mixture of liquid CO_2 and water [J/kg]

h^{CO2} - enthalpy of liquid CO_2 [J/kg] (q.v. eq.(5.52))

h^{H2O} - enthalpy of liquid water [J/kg] (q.v. eq.(4.36))

$X_{CO_2}^{CO_2}$ - mass fraction of CO_2 in the liquid CO_2-phase [-]

$X_{CO_2}^{H_2O}$ - mass fraction of water in the liquid CO_2-phase [-]

$\Delta h_{CO_2}^{H_2O}$ - enthalpy of dissolution of water in liquid CO2 [J/kg]

Comments:

– (5.54) is an analogon to (4.46), the enthalpy of water with dissolved CO_2.
– At the time we are not aware of formulations describing the solution enthalpy for water in CO_2.

Conclusions: Even being theoretically correct formulation (5.54) is not ready for use because of the missing formulation for the solution enthalpy for water in CO_2.

5.7 Heat capacity

5.7.1 Heat capacity of CO_2

Source: [39]

Formulation:

– Isobaric heat capacity

$$\frac{c_p}{R} = -\tau^2\left(\Phi_{\tau\tau}^0 + \Phi_{\tau\tau}^r\right) + \frac{\left(1 + \delta\Phi_\delta^r - \delta\tau\Phi_{\delta\tau}^r\right)^2}{1 + 2\delta\Phi_\delta^r + \delta^2\Phi_{\delta\delta}^r} \qquad (5.55)$$

c_p - isobaric heat capacity [J/(kg K)]

R - specific gas constant for CO_2 [J/(kg K)] (c.f. Appendix B)

δ - standardised density [-] (c.f. eq. (5.5))

τ - inverse standardised temperature [-] (c.f. eq. (5.6))

$\Phi_{\tau\tau}^{\ 0}$, $\Phi_{\tau\tau}^{\ r}$, $\Phi_\delta^{\ r}$, $\Phi_{\delta\delta}^{\ r}$, $\Phi_{\delta\tau}^{\ r}$ - partial derivatives of the dimensionless Helmholtz energy Φ, (c.f. eq.s (5.13), (5.24), (5.14), (5.17), (5.27))

– Isochoric heat capacity

$$\frac{c_v}{R} = -\tau^2\left(\Phi_{\tau\tau}^0 + \Phi_{\tau\tau}^r\right) \qquad (5.56)$$

c_v - isochoric heat capacity [J/(kg K)]

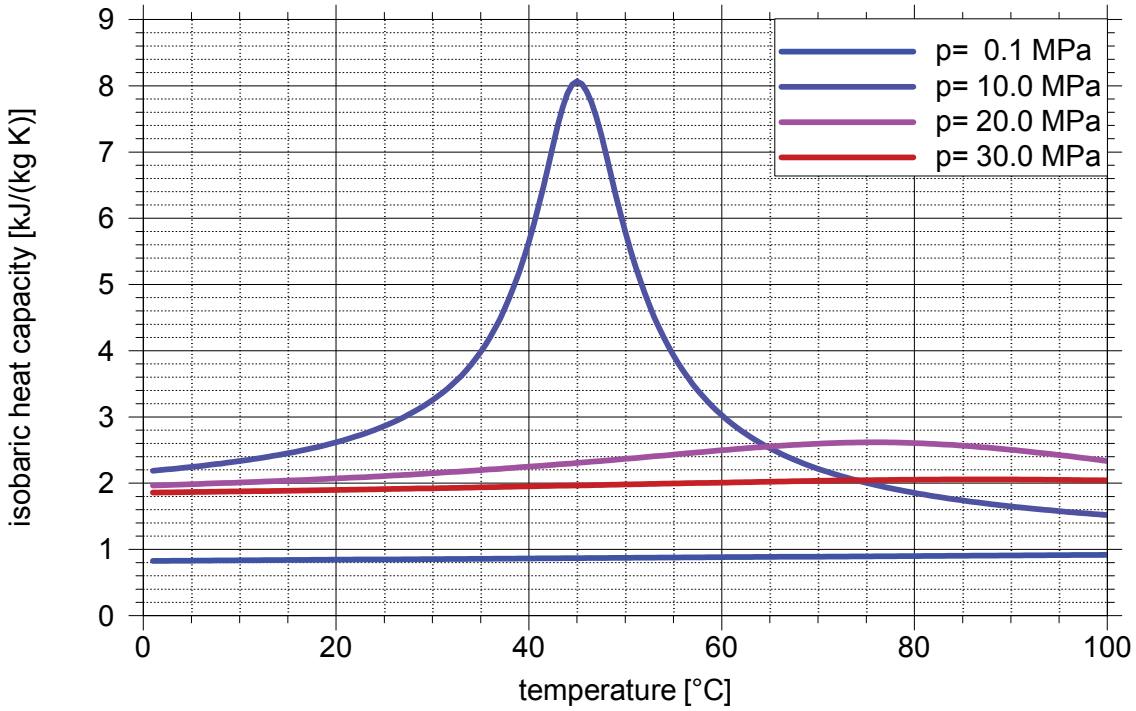

Fig. 5.7 Isobaric heat capacity of CO_2; after [39].

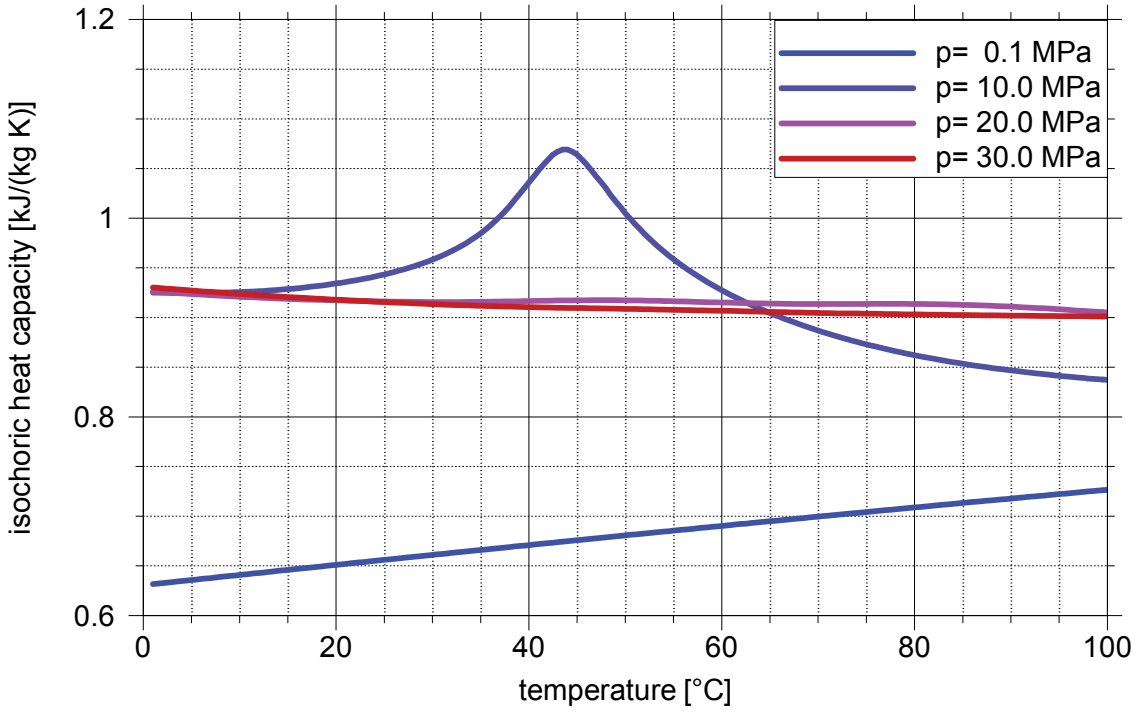

Fig. 5.8 Isochoric heat capacity of CO_2; after [39]; other scale than Fig. 5.7.

Comments: Formulation (5.52) is valid over an exceptional range of pressure and temperature. However, it is too complex to be used in a numerical code. Instead, interpolation of discrete data is often used.

Conclusions: Eq.s (5.55) and (5.56) are a reliable formulations within the ranges (1.1).

5.7.2 Heat capacity of CO_2 with water

Comments: We are not aware of formulations concerning the heat capacity of CO_2 with dissolved H_2O.

5.8 Solubility

5.8.1 Solubility of NaCl in CO_2

Source: [4]

Formulation:

$$L_{CO_2}^{NaCl} \cong 0 \qquad (5.57)$$

$L_{CO_2}^{NaCl}$ - solubility of NaCl in water CO_2 [kg/kg]

Comments: For thermodynamic reasons every substance is soluable in an other substance at temperatures above 0 °C [47]. For practical purposes some of these solubilities are negligibly small. While salt is well soluble in polar liquids like water solubility in non-polar substances like liquid carbon dioxide is very low. Salt solubility in CO_2 is thus commonly neglected as in [4].

Conclusions: Solubility of NaCl in CO_2 is negligible within the ranges (1.1).

5.8.2 Solubility of water in CO_2

Source: [41]

Formulation: (q.v. eq. (4.65))

Range of validity:

temperature: 12 °C < T < 100 °C

pressure: 0 MPa < p < 60 MPa

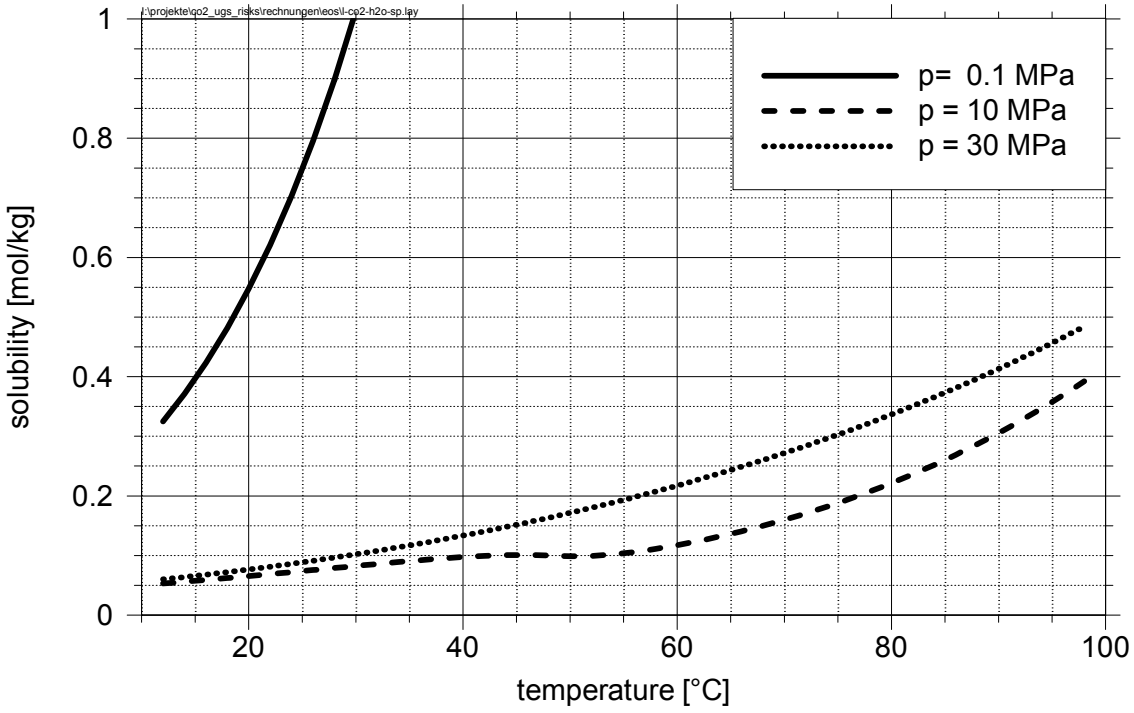

Fig. 5.9 Solubility of water in CO_2; after [41].

Comments: The solubility of water in CO_2 is calculated as part of the formulation (4.63) for the solubility of CO_2 in water.

Conclusions: Eq. (4.65) is a reliable formulation within the ranges (1.1) (see section 4.7.2).

5.8.3 Solubility of water from a NaCl-solution in CO_2

Source: [40]

Formulation:

$$\hat{L}_{CO_2}^{H_2O} = A\left(1 - \hat{L}_{H_2O}^{CO_2} - x_{H_2O}^{NaCl}\right) \qquad (5.58)$$

$\hat{L}_{CO_2}^{H_2O}$ - Solubility of H_2O in CO_2-phase [mol/mol] (q.v. eq. (5.60))

$\hat{L}_{H_2O}^{CO_2}$ - Solubility of CO_2 in the water-phase [mol/mol] (q.v. eq. (4.89))

A - (q.v. eq. (4.67))

$x_{H_2O}^{NaCl}$ - mole fraction of NaCl in the water-phase [mol/mol] (q.v. eq. (5.59))

$$x_{H_2O}^{NaCl} = \frac{\upsilon m_{H_2O}^{NaCl}}{55.508 + \upsilon m_{H_2O}^{NaCl} + L_{H_2O}^{CO_2}} \qquad (5.59)$$

υ - stoichiometric number of ions contained in the dissolved salt [-];
$\upsilon = 2$ in case of NaCl

$m_{H_2O}^{NaCl}$ - molality of NaCl in the water-phase [mol/kg]

$L_{H_2O}^{CO_2}$ - Solubility of CO_2 in the water-phase [mol/kg] (q.v. eq. (4.88))

Conversion of solubility $\hat{L}_{H_2O}^{CO_2}$ to molality:

$$L_{H_2O}^{CO_2} = \frac{\hat{L}_{H_2O}^{CO_2}\left(\upsilon m_{H_2O}^{NaCl} + 55.508\right)}{\left(1 - \hat{L}_{H_2O}^{CO_2}\right)} \qquad (5.60)$$

$L_{H_2O}^{CO_2}$ - Solubility of CO_2 in the water-phase [mol/kg]

Range of validity:

temperature: 12 °C < T < 100 °C

pressure: 0 MPa < p < 60 MPa

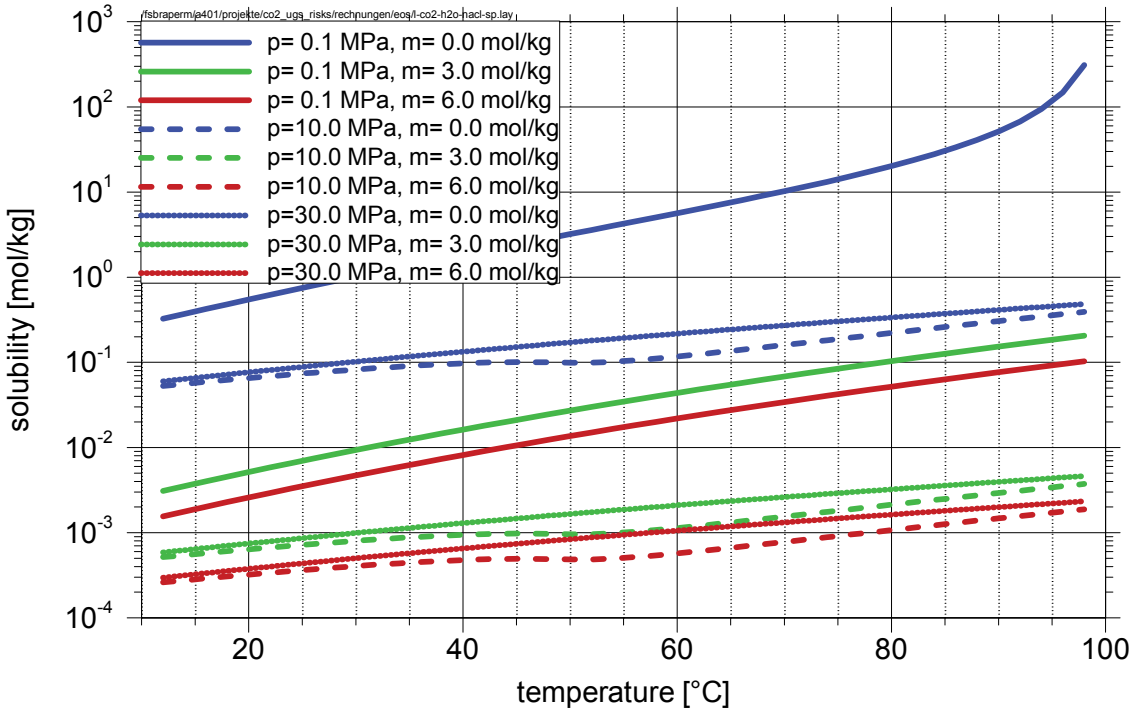

Fig. 5.10 Solubility of water from a NaCl-solution in CO_2, after [40], p=0.1 MPa (solid lines), 10 MPa (dashed lines) and 30 MPa (dotted lines); $m_{H_2O}^{NaCl}$ = 0 mol/kg (blue lines), 3 mol/kg (green lines), 6 mol/kg (red lines).

Comments: (see section 4.7.3)

Conclusions: (see section 4.7.3)

5.9 Diffusivity

Source: [28]

Formulation: -

Comments: We are not aware of a formulation for the self-diffusivity of CO_2 as a function of temperature and pressure. However, a good compilation of measured data exists.

Apparently, the values for self-diffusivity of supercritical CO_2 lie between the values for gaseous and liquid CO_2 in the ranges (1.1).

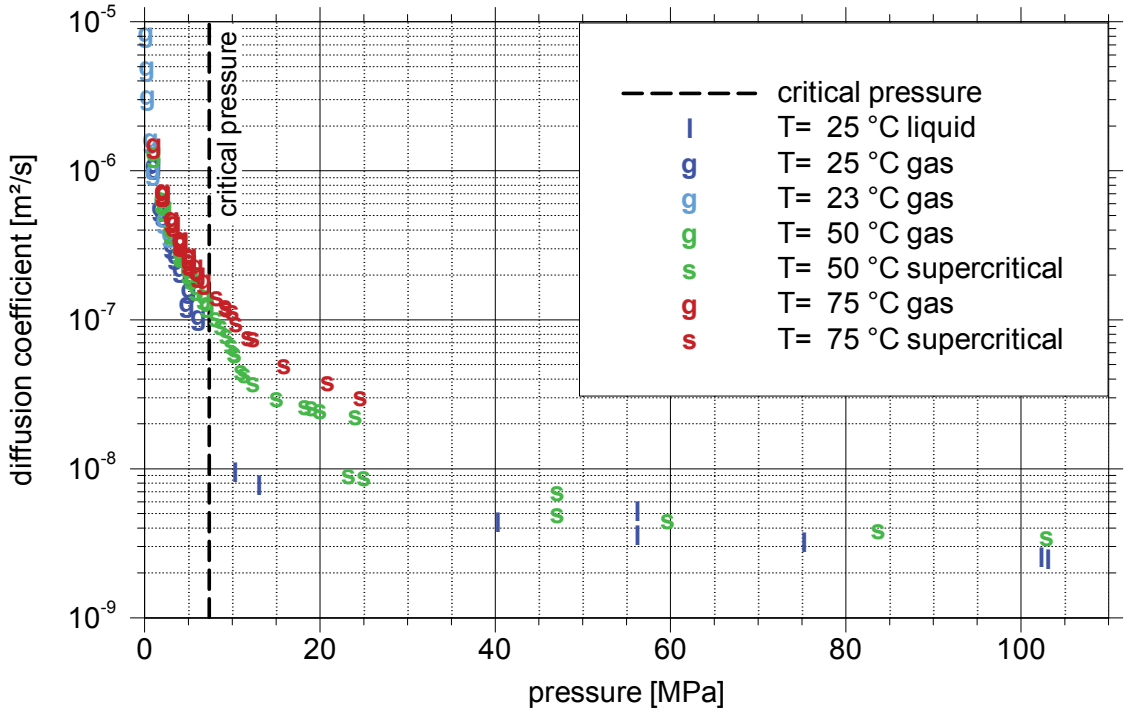

Fig. 5.11 Self-diffusivity of CO_2 for different temperatures and phase states; data from [28].

More appropriate would have been data on diffusivity of water in CO_2. Since we haven't found such data self-diffusivity indicates at least the order of magnitude for this value.

Conclusions: Only a rough estimate for the diffusion coefficient of water in supercritical CO_2 can be provided.

6 Properties of sodium chloride

6.1 Density of NaCl

Generally, the NaCl density is depending on pressure and temperature:

$$\rho = \rho(p,T) \qquad (6.1)$$

ρ - density of sodium chloride[kg/m³]

p - pressure [Pa]

T - temperature [K]

However, the density of NaCl is only rarely considered (e.g. [34]). Density of solid NaCl changes only in the range of tenths of percent with temperatures between 0 °C and 100 °C as shown in Fig. 6.1. Due to the high Young modulo of at least 10 GPa for rock salt the same applies to the dependency on pressure. A constant value of ρ = 2165 kg/m³ appears therefore adequate in case of the CO_2-sequestration.

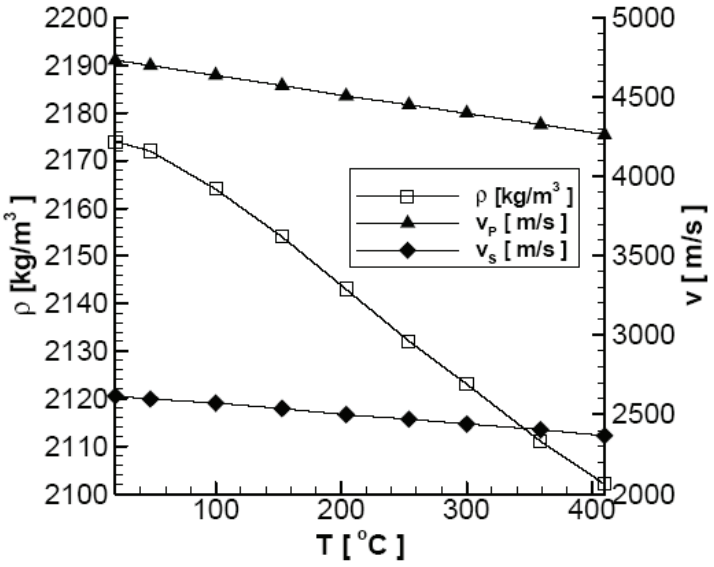

Fig. 6.1 Temperature-dependent density of rock salt; from [26], cited in [51].

6.2 Enthalpy of NaCl

Source: [30], [12]

Formulation:

from [30]:

$$h = \left[-0.83624\,10^{-3} T^3 + 0.16792\,T^2 - 25.9293\,T \right] \frac{4.184}{58.44} \qquad (6.2)$$

from [12]:

$$h = \frac{36710 \cdot T + 62.77 \cdot T^2/2 - 0.06667 \cdot T^3/3 + 0.000028 \cdot T^4/4}{58440} - 204.5698 \qquad (6.3)$$

h - enthalpy of pure NaCl [kJ/kg]

T - temperature [°C]

Range of validity is not specified, but secondary literature gives hints:

temperature: 0 °C < T < 350 °C

salinity: 0 to full NaCl saturation (as in the tabulated data from [21])

Comments: In comparison the correlation for the enthalpy of salt h_2 looks wrong. Following eq. (6.2) the enthalpy of pure salt actually decreases with temperature which it shouldn't do. The formulation from [12] shows instead an increasing enthalpy that is in the order of the values from the formulation from [30]. While several typos in [30] are corrected in [20] this has not been reported.

Conclusions: Formulation (6.3) is valid within the ranges (1.1).

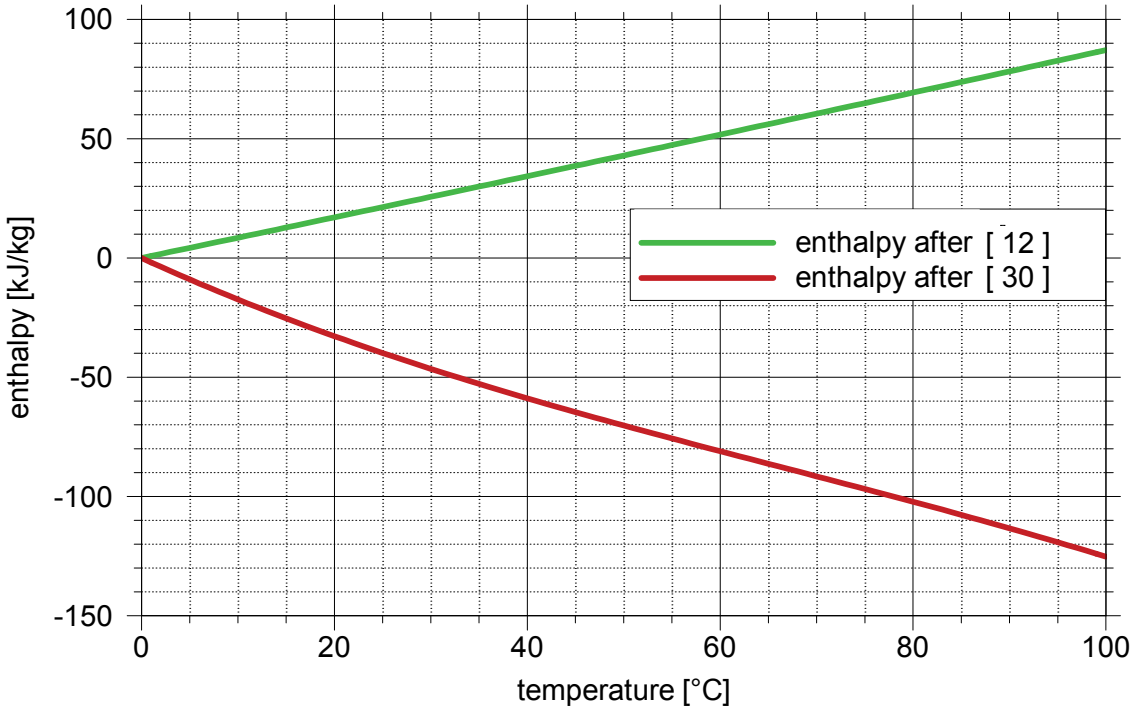

Fig. 6.2 Enthalpy of NaCl; after [30] and [12].

6.3 Heat capacity of NaCl

Source: using [12] from section 6.2

$$c = \frac{\partial h_{NaCl}}{\partial T} = \frac{36710 + 62.77 \cdot T - 0.06667 \cdot T^2 + 0.000028 \cdot T^3}{58440} \qquad (6.4)$$

Formulation:

c - heat capacity of NaCl [kJ/(kg K)]

h_{NaCl} - enthalpy of pure salt [kJ/kg] (q.v. eq. (6.3))

T - temperature [°C]

Range of validity:

(see section 4.5.2)

Comments: Heat capacity can be derived from the enthalpy as the partial derivative with respect to temperature (c.f. section 4.6). Here, the formulation of the NaCl-enthalpy from [12] is used.

Conclusions:

– (see section 4.5.2)

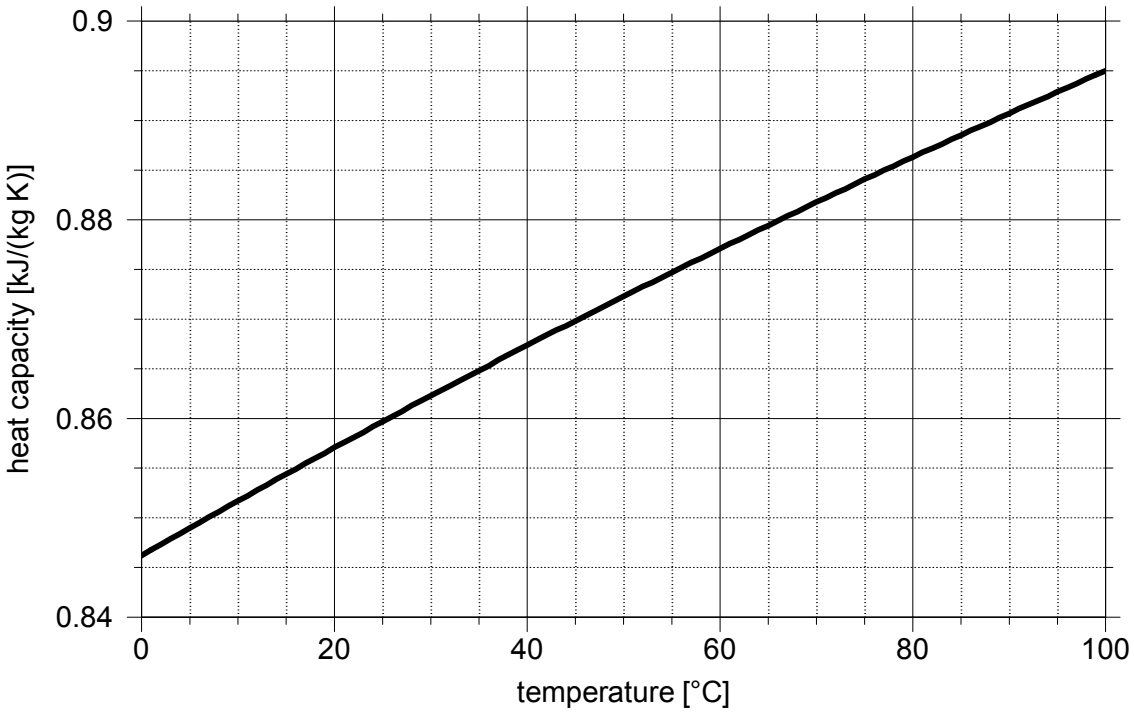

Fig. 6.3 Heat capacity of NaCl; derived from [12].

7 Phase state

7.1 Phase diagram for pure substances

The state of a substance or the phase in which it resides can be characterised by three state variables: pressure p, temperature t and volume V. “State” means here not only the three basic states of aggregation “solid”, “liquid” and “gaseous” but also the coexisting states like “solid-liquid” or “liquid-gaseous”.

Each combination of the state variables is related to a specific state. But only two of the three state variables are independent from each other. A plot of all possible states in a three-dimensional p-V-T-diagram yields thus a complex area with a special property: projections of this area along each axis yield a diagram of two independent state variables (p-T, p-V or T-V), in which the phase state is uniquely defined. The two- or three-dimensional drawings are called “phase diagrams”. Two examples for a 3-D phase diagram of a pure substance are given in Fig. 7.1. Diagram a) from [42] visualises most clearly the three-dimensional plane in the p-V-T-coordinate system while diagram b) from [6] points out the three possible projections on the p-T-, p-V- or T-V-plane, respectively, which helps greatly to understand these otherwise hardly comprehensible plots.

In the p-T-diagram of Fig. 7.1 a) some parts of the three-dimensional plane are just seen as lines due to the projection along the V-axis. These lines represent states of two coexisting phases. Fig. 7.2 shows a p-T-diagram for carbon dioxide, in which the lines are drawn in colour. Two characteristic states are highlighted as well: the triple point at which even three phases coexist and the critical point at the end of the red vapour pressure curve.

a)

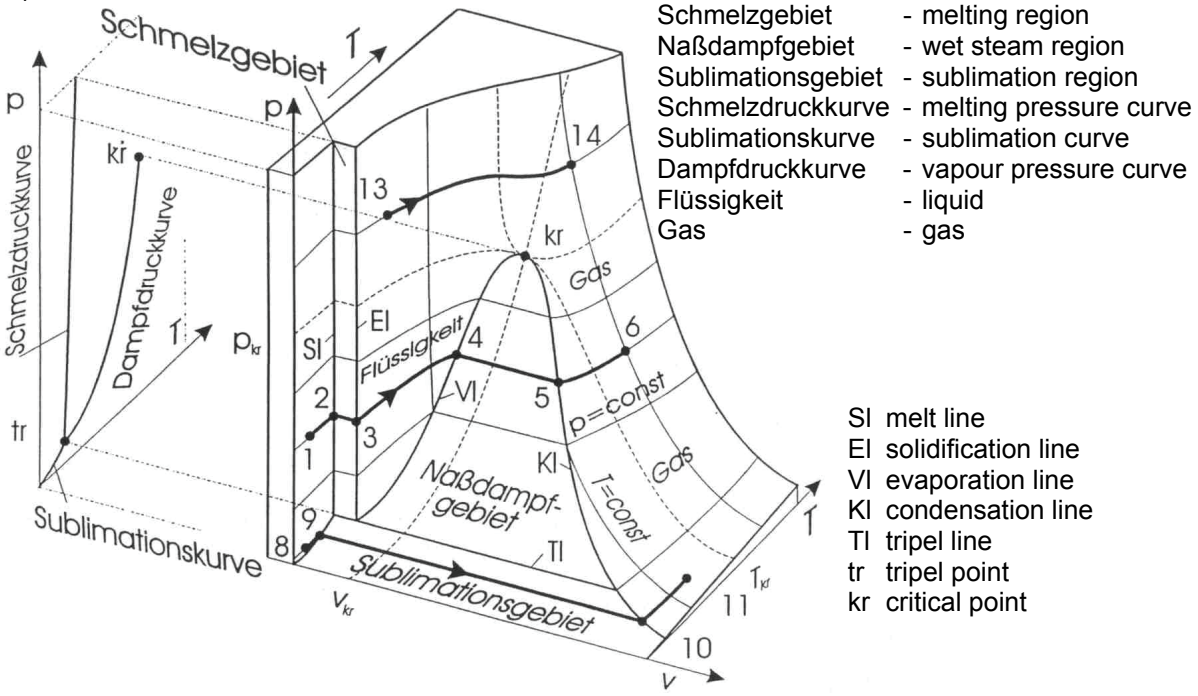

b)

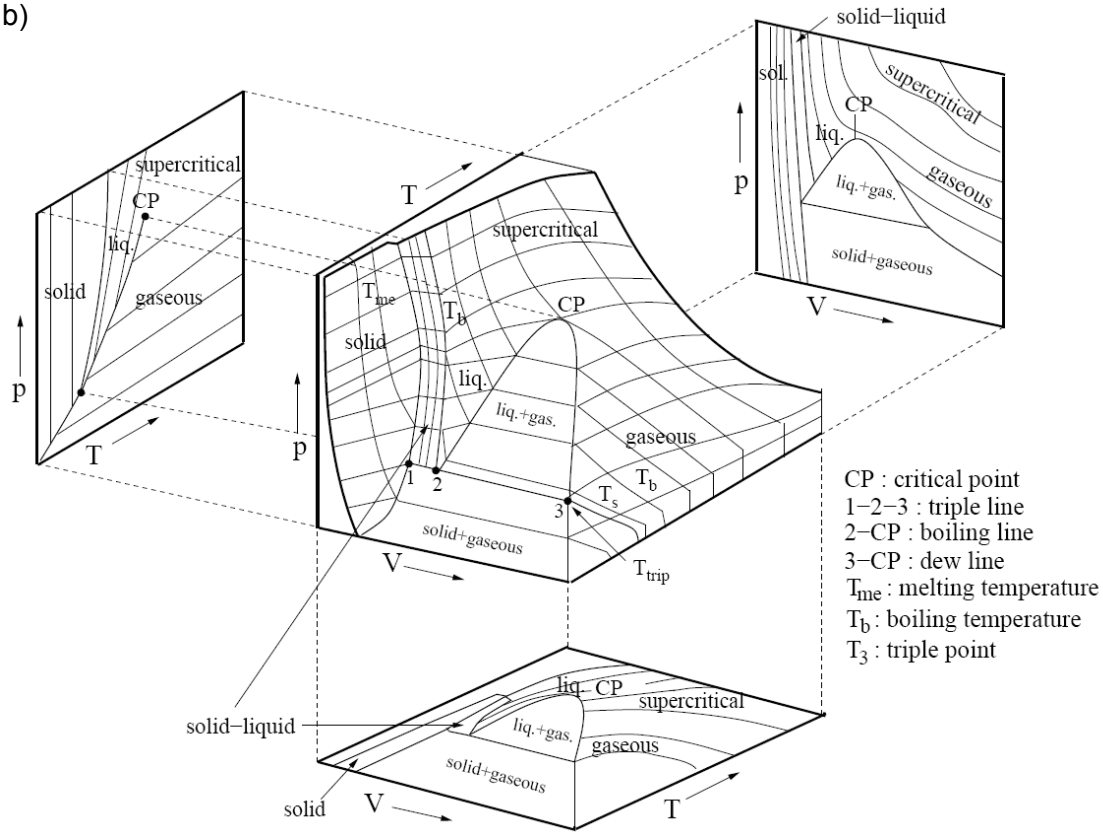

Fig. 7.1 Phase diagrams of a pure substance, a) after [42] and b) from [6].

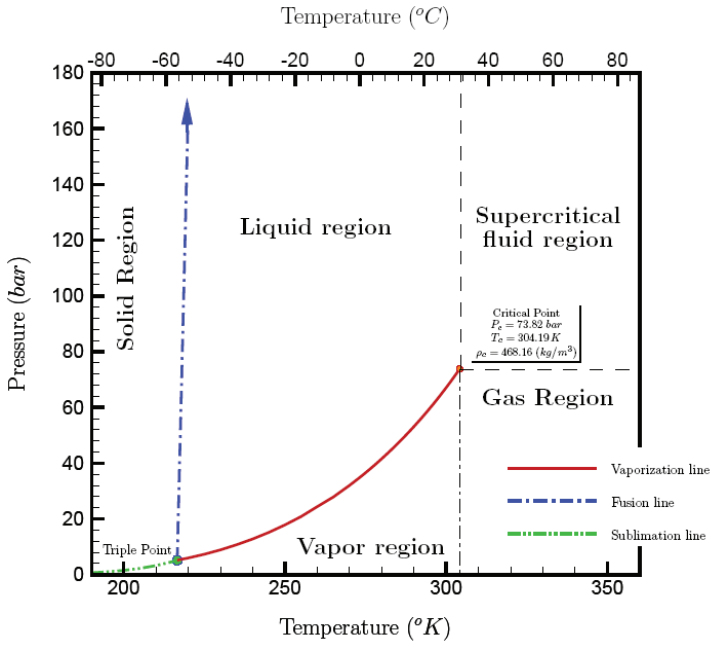

Fig. 7.2 p-T-diagram for carbon dioxide; from [17].

The critical point of a substance can be reached owing to pressure increase in the gas phase as well as owing to temperature increase in the liquid phase. At the critical point the difference between density of the liquid and density of the gas vanishes. Increase of temperature or pressure beyond this point means change into the supercritical state where the distinction between liquid and gas cease to exist. The supercritical state is often described as a state in which gas cannot be liquefied by any pressure increase. Pressure, temperature and density at the critical point for water and carbon dioxide are compiled in Tab. 7.1.

Tab. 7.1 Values of the state variables for CO_2 and H_2O at the critical point.

	temperature [°C/K]	pressure [Mpa]	density [kg/m³]
water	374,15 / 647,3	22,12	317
carbon dioxide	31,04 / 304,2	7,38	468,16

The supercritical state can be reached either from the liquid phase or from the gaseous phase. The transition is continuous as shown for carbon dioxide in Fig. 5.2, Fig. 5.3 and

Fig. 5.6 with respect to density, viscosity and enthalpy. Therefore the supercritical state is not clearly defined in a phase diagram and does not constitute an own phase. This means that, curiously, a liquid can be transformed in to a gas without an actual phase change. However, in the literature the boundary to the supercritical state is often assumed to coincide with parallels to the axes in a p-T-diagram starting at the critical point (e.g. Fig. 7.2). This approach is adopted in the following.

7.2 Phase diagram for mixtures of H_2O and CO_2

Phase diagrams exist for mixtures of two substances or components, too, only an additional state variable x is required that defines the mass fractions of the components. In this case three state variables are independent from each other so that a graphical representation of the phase states of a binary mixture has to be truly three-dimensional. Other than in the p-V-T-diagram for a pure substance where only a complicated area is constructed in space, every point in a p-T-x-space is defined.

The effort to compile the data and to plot a comprehensible diagram in space is considerable. One of the very few three-dimensional phase diagrams for a H_2O-CO_2-mixture is provided by [43] and shown in Fig. 7.3. According to [43] the diagram is distorted, though, to underline certain properties of the H_2O-CO_2-mixture:

– The spatial three-phase zone marked in yellow is strongly magnified in Fig. 7.3.
– In contrast to reality the critical pressure of water has about the same value as carbon dioxide.
– The temperature axis is not to scale and compresses the supercritical zone between the three-phase zone and the critical temperature for water.

The temperature in Fig. 7.3 lies between 20 °C and 370 °C, the pressure is given up to 350 MPa. The bold lines represent the vapour pressure curves of the pure components which end in the critical points C_{H2O} and C_{CO2}, respectively. The fine lines represent isotherms. The critical curves connecting the critical point of the respective component with horizontal tangents of the isotherms are drawn as dashed lines. The critical curves do not lie in planes but are curved in space. For the more volatile component the critical curve is often called “lower critical curve LC”. LCEP marks the lower critical end point.

The original figure in [43] is only a line drawing which is not easy to interpret. Therefore some characteristic areas representing different phase states have been coloured in the present figure. But not every phase state has been pointed out in Fig. 7.3. This becomes apparent by looking at the red marked area more closely. For high temperatures and pressures it represents a state where water does not exist as a separate phase but is totally dissolved in the supercritical CO_2. But if the pressure is lowered below the vapour pressure of the water, water vapour evolves and changes the single-phase carbon dioxide into a binary gas mixture. This phase change is not displayed in Fig. 7.3 but indicated by fading from red to cyan.

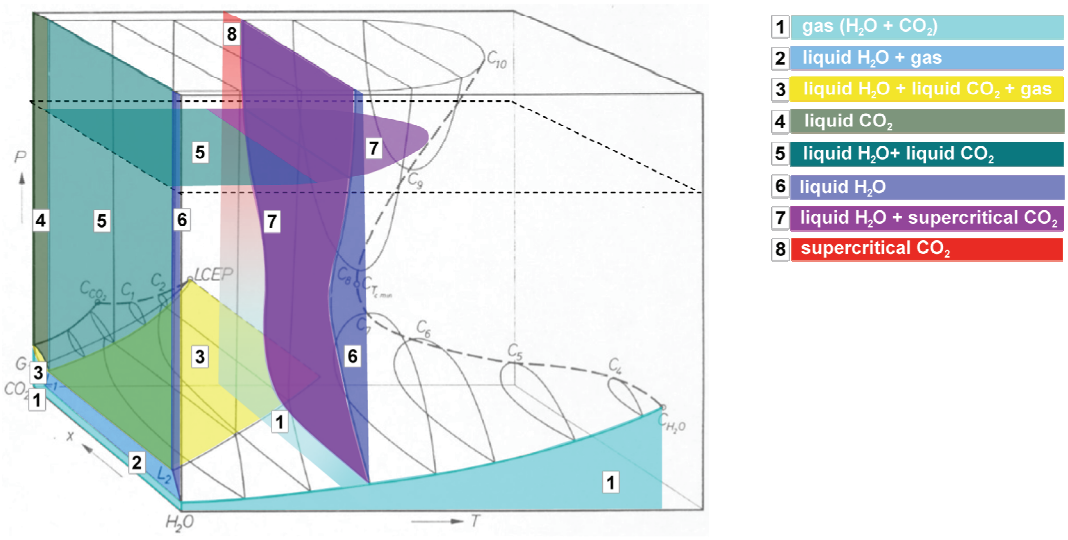

Fig. 7.3 Phase diagram for a H_2O-CO_2 mixture, not to scale; from [43]. Selected areas are coloured to improve understanding.

The colour coding used in Fig. 7.3 is applied for Fig. 7.4, Fig. 7.5 and Fig. 7.6, too. Fig. 7.4 shows two cross-sections in the p-T-plane. Unfortunately, the mass fraction x is not given in either case. The temperature range apparently exceeds the range covered in Fig. 7.3. Below 10 °C to 12 °C the diagrams show white areas where a CO_2-hydratrate phase forms. Included is even the temperature range where ice is formed. In order to avoid problems arising from hydrate formation [41] choses 12 °C to be a lower temperature boundary for developing formulations for mutual solubilities of water and carbon dioxide.

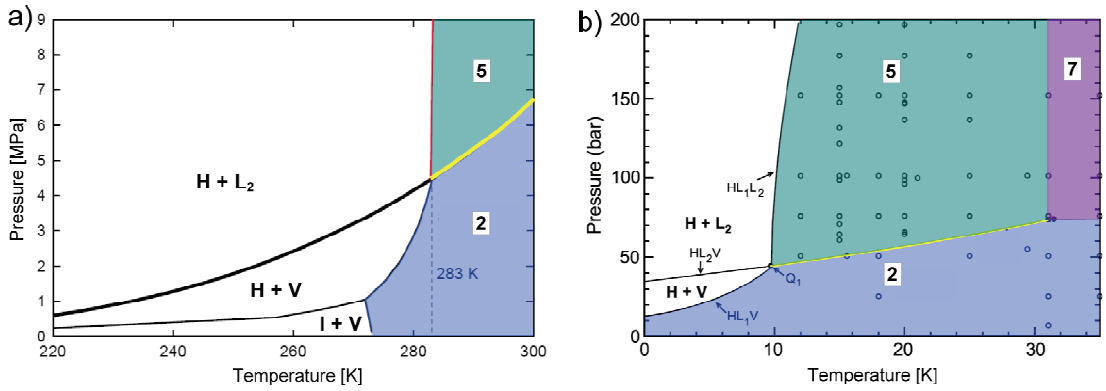

Fig. 7.4 p-T phase diagrams for a H_2O-CO_2 mixture; a) after [19] (cited in [44]), b) after [41]. Colour coding corresponds to Fig. 7.3; I – Ice(H_2O), H – CO_2-hydrate, L_1 – liquid H_2O, L_2 – liquid CO_2, V – gas phase, Q_1 – quadruple point; circles in b) represent measured data from the literature.

The phase diagram in Fig. 7.5 is given as a p-x-plane at a temperature level of 25 °C. At about 64 bar and a very low H_2O mole fraction the spatial, yellow marked three-phase zone of Fig. 7.3 can be found again. A cut-out of this region is given in this figure as well. It shows that the size of this region are actually very small, about 3‰ in x-direction and 0,3 bar in p-direction. [41] concludes that the spatial three-phase region is not relevant in case of CO_2-sequestration because of its size and of its position in the p-T-x-diagram.

Fig. 7.6 finally shows two cross-sections in T-x-plane for very high pressures, 20 MPa and 35 MPa. The first one lies below, the other one above the critical point for water. Due to the high temperatures considered the carbon dioxide is mainly in the supercritical state. However, here in the diagrams it is called “vapour”[5].

[5] Apparently, labelling of the supercritical state is ambiguously done in the literature.

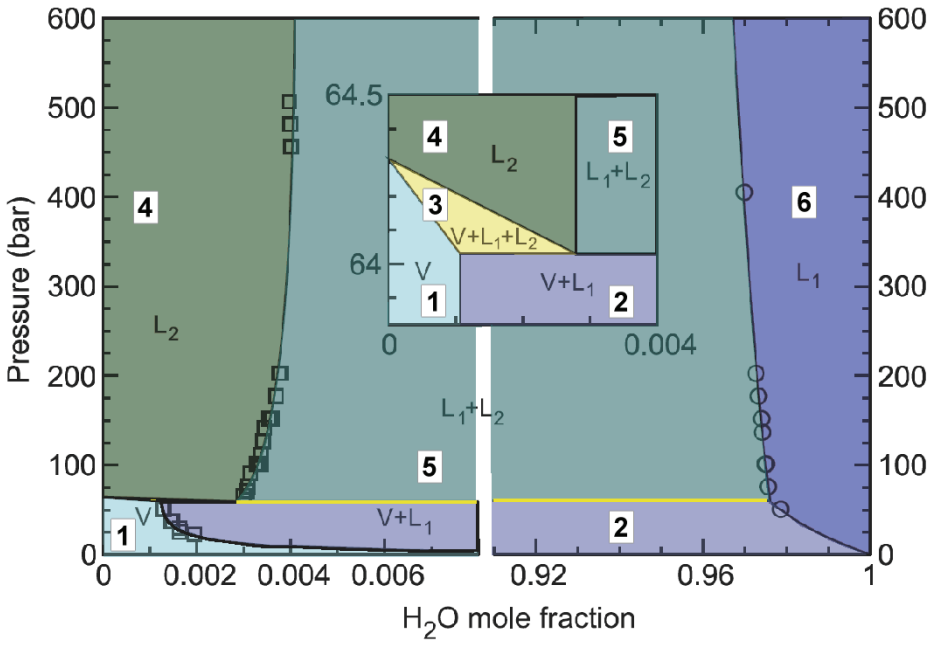

Fig. 7.5 p-x phase diagram for a H_2O-CO_2 mixture at 25 °C; after [41]. Colour coding corresponds to Fig. 7.3; for the explanation of abbreviations, see Fig. 7.4; symbols represent measured data from the literature.

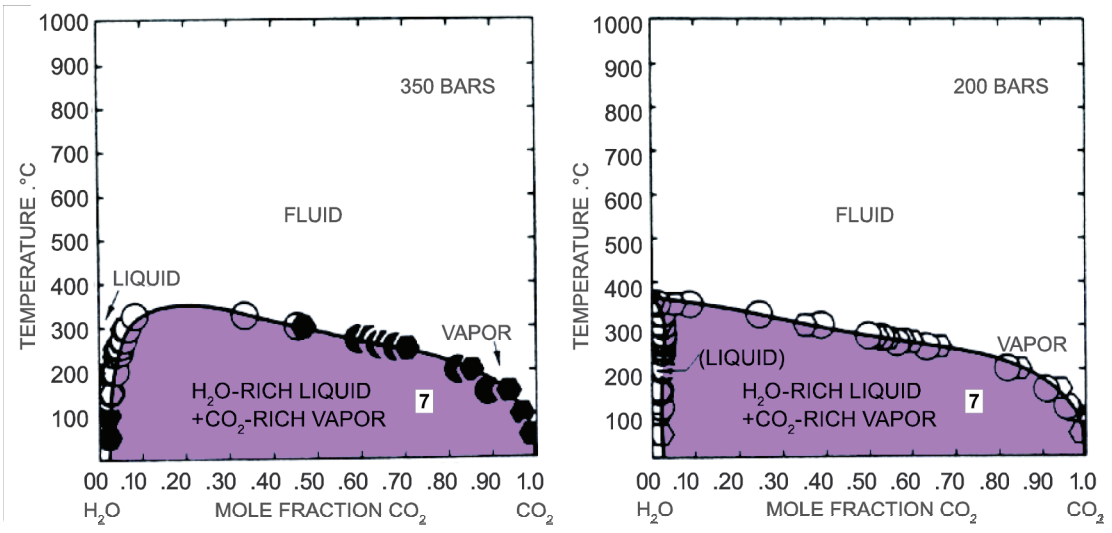

Fig. 7.6 T-x phase diagram for a H_2O-CO_2 mixture at 200 and 350 bars; after [7] (cited in [17]). Colour coding corresponds to Fig. 7.3; symbols represent measured data from the literature.

7.3 Phase diagnostics

7.3.1 Preliminary remarks

A mathematical model for the multiphase-multicomponent flow requires information on the local phase state of the mixture as discussed in detail in section 7.3.2. In the framework of the CO_2-sequestration the solid phases of water and carbon dioxide including hydrate phases are not of interest and will not be discussed here. In order to avoid forming of solid phases only temperatures above 12 °C are considered here as suggested by [41].

Since the local phase state may change with time the thermodynamic conditions of the flow have to be monitored during model calculations. This monitoring is often called “phase diagnostics” in the American literature. Relevant criteria for the phase diagnostics are compiled in sections 7.3.3 and 7.3.4.

7.3.2 Primary and secondary variables

According to Gibbs’ phase rule a non-isothermal multiphase-multicomponent system consisting of K components has K+1 degrees of freedom. Each degree of freedom requires a primary variable in the mathematical model. Primary variables for the description of the two-phase–two-component flow for instance could be pressure, saturation and temperature. Depending on the local phase composition different combinations of primary variables are relevant in the mathematical model.

Changes in the local thermodynamic conditions may let an additional phase evolve (e. g. by condensation) or an existing phase disappear (e. g. by evaporation). For two-phase–two-component flow two different conditions have to be considered:

– Two phases coexist.
– Only one phase exists.

Usually, each phase is quantitatively dominated by one component. In case of two coexisting phases a certain mass fraction of one component is dissolved in the phase

dominated by the other component. As a rule mathematical models assume local thermodynamic equilibrium so that the amount of dissolved mass is depending on other state variables like pressure or temperature. The mass fraction of the dissolved component is therefore a secondary variable.

If only one phase exists locally, the dissolved component i can be transported freely within the phase-dominating component j. The mass fraction of the dissolved component (or concentration) becomes an independent variable. In terms of the mathematical model this means: if component i dominates phase α and component j dominates phase β and if phase α disappears then a transport equation for the component i in the β-phase has to be solved instead of a flow equation for the α-phase. The saturation S_α^i becomes 0 - is no variable anymore - and the mass fraction X_β^i becomes a primary variable instead.

Salt behaves differently because it forms a solid phase if the concentration exceeds the solubility. A solid salt phase is assumed to be immobile. In this case the referring balance equation is reduced to a storage term and a source term. As discussed in section 2.3 precipitation or dissolution of salt in the pore space changes porosity and permeability in the other balance equations.

7.3.3 Phase diagnostics for a one-component flow

Depending on pressure and temperature there exist three possible phase states for one-component flow: single-phase liquid, single-phase gas and coexisting gas and liquid. The processes leading to phase changes from the liquid phase to the gas phase and vice versa are evaporation and condensation, respectively. The incidence of these processes is controlled by the ratio of the vapour saturation pressure p_{sat} and the actual pressure p. Depending on the phase state pressure p is either the pressure of the liquid p_l or the gas pressure p_g. The conditions on that evaporation or condensation commence are:

evaporation: $p_l \leq p_{sat}$

condensation: $p_g \geq p_{sat}$ (7.1)

p_{sat} - vapour saturation pressure [Pa]

p_l - pressure of the liquid [Pa]

p_g - gas pressure [Pa]

Calculation of the vapour saturation pressure of water, brine and carbon dioxide is discussed in sections 4 and 5.1.1. Detecting phase changes from a single-phase state to the two-phase state needs monitoring whether one of the pressure conditions (7.1) becomes fulfilled. The same applies to the reverse change from the two-phase state to the single liquid phase because this is a pressure controlled process. A change from the two-phase state to the single gas phase can simply and pragmatically be detected by monitoring the mass of the liquid in terms of the water. If evaporation lets the saturation S_l (defined in section 3.1) drop down to zero the liquid phase has vanished. The complete set of conditions and processes for a one-component flow system is illustrated in Fig. 7.7.

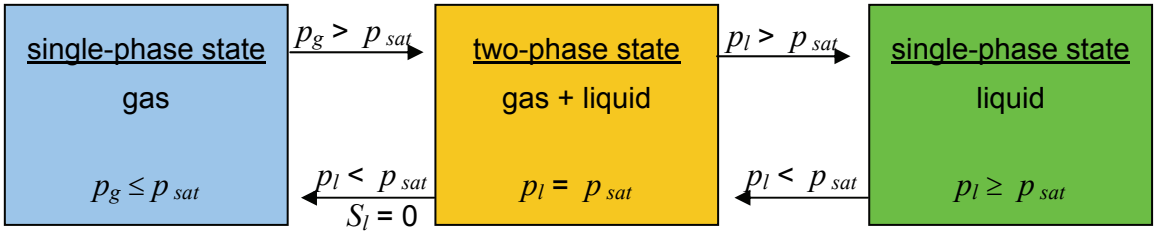

S_α - Saturation of the α-phase [-]

Fig. 7.7 Phase state and phase change conditions of an one-component system.

7.3.4 Phase diagnostics for the two-component flow of H_2O and CO_2

7.3.4.1 Possible phase states during normal and altered evolution

According to the currant view an aquifer suitable for CO_2-sequestration has to have a depth of at least 800 m. This depth corresponds to a water pressure of about 8 MPa and to a temperature of about 36 °C based on the geothermal gradient given in section 2.5. Temperature and pressure exceed therefore barely but maybe sufficiently the critical values for carbon dioxide (c.f. Tab. 7.1) at this depth. In this case CO_2 will not undergo phase changes.

While carbon dioxide is in the supercritical state when sequestered in the underground water doesn't reach the critical temperature at reasonable depths. It exists therefore only in the subcritical state. An additional water vapour phase could theoretically evolve if the vapour pressure exceeds the fluid pressure. In pure water a vapour pressure of 8 MPa is reached at 290 °C (c.f. Fig. 4.2). For NaCl-solutions this value even increases. Forming of a vapour phase from liquid water will therefore not take place either.

During the normal evolution of a CO_2-sequestration there are two phases to be expected at most: a liquid water phase and a supercritical CO_2-phase. Of course, water may always be dissolved within the carbon dioxide dominated phase and vice versa.

During an altered evolution carbon dioxide rises due to the lower density in comparison to the water. While rising, pressure and temperature decrease and fall below the critical values for CO_2. Supercritical CO_2 fades either into the gaseous or into the liquid state depending on temperature and pressure conditions. Water pressure as well as rock temperature correlate with depth. These correlations can be plotted into a phase diagram for CO_2 thereby giving an hint into which phase state the carbon dioxide falls during its ascend. In Fig. 7.8 such a curve is plotted assuming that

– temperature and pressure increase linearly with depth,
– the average water density relates to a 2 percent NaCl-solution,
– a surface temperature and a geothermal gradient typical for Germany (cf. section 2.5) are applied and
– carbon dioxide always has the temperature of the undisturbed rock.

These conditions result in a linear function between pressure and temperature. Fig. 7.8 shows that the rising carbon dioxide would change directly from the supercritical into the gaseous state. The altered evolution could then be described as a two-phase flow like in the case of normal evolution because the change from supercritical to subcritical conditions is continuous and the same applies to the fluid properties.

However, Fig. 7.8 shows, too, that the depth dependent temperature-pressure curve (in violet) passes the critical point rather closely. Little changes in the assumptions may steepen or bend this curve sufficiently to let it cross the liquid region. In this case supercritical carbon dioxide changes first into a subcritical liquid. When the pressure has

dropped down to the vapour pressure evaporation starts forming a three-phase system of liquid and gaseous CO_2 as well as water. Temporarily, a liquid and a gas phase of CO_2 coexist until the liquid is completely vaporised.

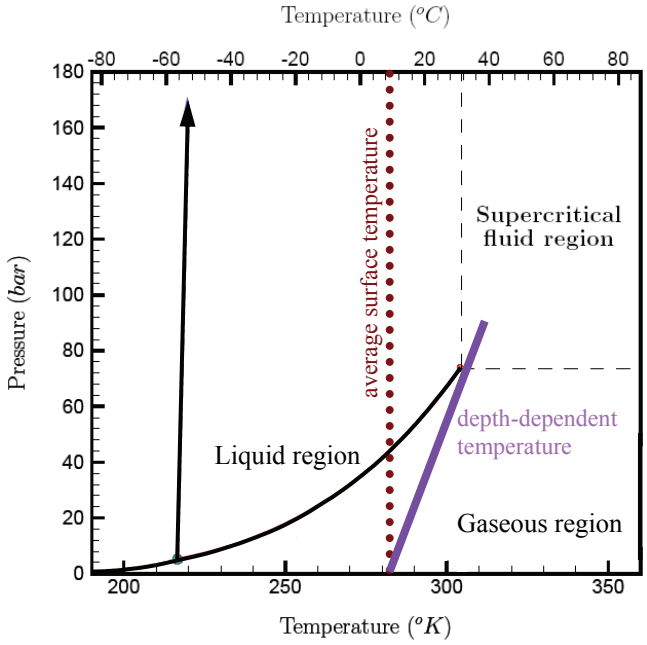

Fig. 7.8 Phase diagram for pure CO_2 including a depth dependent temperature-pressure relationship for an undisturbed geosphere typical for Germany; modified from [17].

Model calculations including heat effects caused by depressurisation and boiling have shown that boiling of CO_2 can cool the water down to freezing conditions. Depressurisation of gaseous CO_2 results in a rising specific enthalpy and thus may cause cooling effects to such an extent that in turn a three-phase zone evolves [35].

A complete mathematical description for the altered evolution is therefore certainly more complex than for the normal evolution. It comprises not only two possible phase states of CO_2 but also phase changes from liquid water to ice or water hydrates.

7.3.4.2 Phase diagnostics for normal evolution

In case of normal evolution no more than two coexisting phases - a water phase and a phase dominated by supercritical CO_2 - are to be expected as discussed in the previous

section. In Fig. 7.3, the phase diagram for a H_2O-CO_2 mixture, this covers the space above the critical temperature (right of the yellow three-phase zone) except for the single gas-phase zone - marked in cyan - in the lowest part of the diagram.

Supercritical fluids in general behave like liquids referring to dissolution. The CO_2-phase can therefore be treated like subcritical liquid CO_2 in this respect. The following applies therefore analogously to the zone above the yellow three-phase zone in the phase diagram (Fig. 7.3).

Whether one or two phases are present is only controlled by the mass fractions of the components and the mainly temperature-dependent solubilities of component i in the β-phase as well as component j in the α-phase. The solubility of component j in the α-phase marks the maximum mass of component j that can be dissolved in the α-phase. Concerning CO_2 und H_2O the mutual solubilities are discussed in sections 4.7 and 5.8. Three phase states are possible as illustrated in Fig. 7.9:

– If there is less water present than is dissolvable in the supercritical CO_2, the water-phase vanishes.
– If there is less carbon dioxide present than can be dissolved in the water, the CO_2-phase vanishes.
– If there is more water present than can be dissolved in the carbon dioxide and at the same time more carbon dioxide present than can be dissolved in the water both phases exist simultaneously. In this case concentration of the dissolved component always equals the solubility.

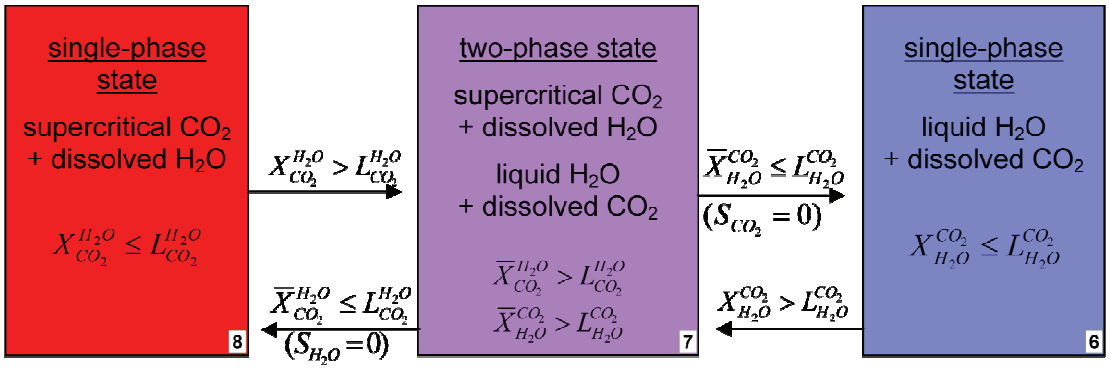

Fig. 7.9 Phase state conditions of a mixture of supercritical CO_2 and liquid H_2O; colour coding according to Fig. 7.3.

Evolving of a second phase from a single-phase state requires that the amount of solute mass exceeds the solubility

$$X_\beta^i > L_\beta^i \qquad (7.2)$$

X_β^i - mass fraction of component i in the β-phase [-];$i \triangleq H_2O, CO_2$, $\beta \triangleq CO_2, H_2O$

L_β^i - solubility of component i in the β-phase [-];$i \triangleq H_2O, CO_2$, $\beta \triangleq CO_2, H_2O$

Disappearing of one phase from a two-phase state can simply be detected monitoring the saturations S_α and S_β. A second option is to check whether the total mass m^i of component i can be dissolved in the total mass m^j of component j and vice versa. For this purpose a theoretical mass fraction $\overline{X}_\beta^i$ must be calculated that would result if only one phase were present:

$$\overline{X}_\beta^i = \frac{m^i}{m^i + m^j} \qquad i \triangleq H_2O, CO_2, \beta \triangleq CO_2, H_2O \qquad (7.3)$$

$\overline{X}_\beta^i$ - theoretical mass fraction of component i in the β-phase [-]

m^i, m^j - mass of components i and j (c.f. eq. (7.4)) [kg]

with

$$m^i = X_\alpha^i m_\alpha + X_\beta^i m_\beta, \qquad m^j = X_\alpha^j m_\alpha + X_\beta^j m_\beta \qquad (7.4)$$

m_α, m_β - mass of the α- and the β-phase [kg]

Phase change conditions (7.2) can thus be supplemented by

$$\overline{X}_\beta^i \le L_\beta^i \qquad i \triangleq H_2O, CO_2, \beta \triangleq CO_2, H_2O \qquad (7.5)$$

7.3.4.3 Phase diagnostics for altered evolution

In an altered evolution scenario CO_2 can appear in supercritical, liquid and gaseous form while water is still mainly present in liquid form for reasons discussed in section 7.3.4.1. That a gaseous state of CO_2 has to be considered in addition to the supercritical/liquid state complicates the phase diagnostics considerably because

– there are now seven possible phase states[6] in comparison to the three states discussed in the previous section,
– phase changes are involved here and
– dissolution of gases in liquids follows different principles than mutual dissolution of liquids. While for condensed phases (solids and liquids) the pressure dependence of solubility is typically weak and usually neglected in practice, Henrys law or any refined version of this law states a strong relation between pressure and concentration of a gas dissolved in a liquid.

A discussion of possible phase states below the three-phase zone of the phase diagram in Fig. 7.3 as well as a discussion of phase changes of CO_2 are thus required.

Phase states below the three-phase zone

For one-component flow the phase state is controlled by the ratio of fluid pressure to vapour saturation pressure as discussed in section 7.3.3. The criteria for phase changes in a two-component flow look similar. The vapour saturation pressure $p_{sat}{}^{i}$ of the component i in the liquid α-phase is just to be increased by the partial pressure $p_{\beta}{}^{j}$ of the component j that is dissolved in the α-phase[7]. The reason is that mixtures of two components a gas phase always contain both components simultaneously[8]. The sum of

[6] if no difference is made between liquid and supercritical state

[7] If a gaseous β-phase already exists the partial pressure p_{β}^{j} is in equilibrium with the mass fraction X_{α}^{j} of the component j dissolved in the α-phase. The partial pressure can be calculated as a function of the mass fraction X_{α}^{j} with the help of the solubility models described in sections 4.7.3 and 5.8.3. If there is no β-phase the partial pressure is only hypothetical. Nevertheless, the solubility models provide a value and it can be used to calculate the bubble pressure.

[8] This is why vaporous water can appear in an altered evolution despite the reasoning in section 7.3.4.1.

$p_{sat}{}^{i}$ and $p_{\beta}{}^{j}$ is often called “bubble pressure” $p_{b\,\alpha}$ because small bubbles of a binary gas mixture are formed at the beginning of evaporation:

$$p_{b\,\alpha} = p_{sat}^{i} + p_{gas}^{j} \qquad (7.6)$$

$p_{b\,\alpha}$	-	bubble pressure in the α-phase [Pa]
$p_{sat}{}^{i}$	-	vapour saturation pressure of component i [Pa]
$p_{gas}{}^{j}$	-	partial pressure of component j in the β-phase [Pa]

If the liquid pressure decreases down to the bubble pressure bubbles evolve and form a separate gas phase. The gas pressure equals the liquid pressure except for the forces at the phases interface. If the gas and liquid pressure decrease a little bit further more gas evolves until a new equilibrium is reached by increasing the gas pressure and/or by decreasing the mass of dissolved gas. In this equilibrium partial pressure $p_{\beta}{}^{i}$ equals the vapour saturation pressure $p_{sat}{}^{i}$ and partial pressure $p_{\beta}{}^{j}$ depends on the mass fraction X_{α}^{j}. If the pressure drops finally below the vapour saturation pressure $p_{sat}{}^{i}$ component i becomes completely gaseous.

Quite the opposite happens when the gas pressure increases again assuming here, that the vapour pressure of component i is lower than the vapour pressure of component j. When the vapour saturation pressure $p_{sat}{}^{i}$ of component i is exceeded it condensates and forms a separate liquid phase. Immediately, an appropriate amount of gaseous component j is dissolved in the liquid phase. Increasing the pressure further increases dissolution until the bubble pressure is reached and the gas phase disappears again.

In case of gaseous carbon dioxide being dissolved in a water phase the phase state changes as intuitively expected: from a single liquid water phase to two phases, liquid water and a binary gas, and finally to a single gas phase as shown in Fig. 7.10. This is due to the fact that the bubble pressure is dominated by the partial pressure of the dissolved carbon dioxide. At the same temperature the vapour pressure for carbon dioxide is far above the vapour pressure of water (cp. Fig. 4.1 and Fig. 5.1). If the pressure decreases carbon dioxide forms a gas phase long before the water can completely vaporise.

Note, that a single gas phase will not appear in the context of CO_2-sequestration. For the sake of completeness it will nevertheless be discussed in the following. However, the range of very low pressures where pure water vaporises is excempt from consideration.

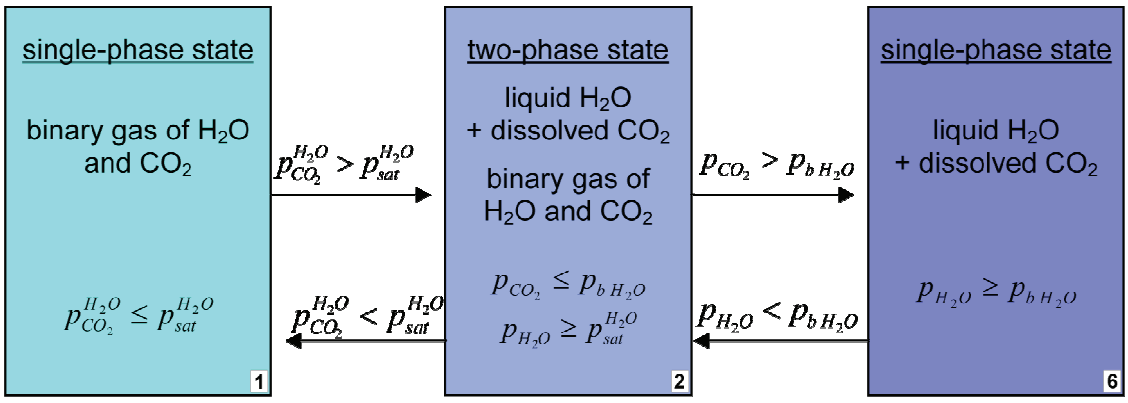

X_α^i - mass fraction of component i in the α-phase [-];

indices: $i \triangleq H_2O, CO_2$; $\alpha \triangleq$ (liquid) H_2O, (binary) gas

Fig. 7.10 Phase state conditions of a mixture of gaseous CO_2 and liquid H_2O; colour coding according to Fig. 7.3.

Phase states due to phase changes of CO_2

The process of a phase change of one component was explained in section 7.3.3. If this component was CO_2 the situation is more complicated if water is additionally present. The number of possible phase states doubles in this case since a separate water phase may be present or not. The connection of all possible states that could take part in a phase change is graphically illustrated in Fig. 7.11.

The situation is straightforward for the transition from the two-phase state - liquid or gaseous CO_2 and water - to the three-phase state with water and liquid CO_2 and gaseous CO_2. Evolving of an additional gas phase in a two-phase system of liquid water and liquid CO_2 due to decreasing pressure is independently of the water mass fraction as can be seen in Fig. 7.5. The same applies to evolving of an additional liquid phase in a two-phase system of liquid water and liquid CO_2. The process is dominated by the CO_2-rich phase because the vapour pressure of carbon dioxide is so much higher than the vapour pressure of water.

But the three-phase state can be reached directly from single-phase states as well. In a single water phase pressure and CO_2-concentration must be coincide in such a way that a gaseous CO_2-phase evolves at the vapour saturation pressure $p_{sat}^{CO_2}$ of CO_2. These are conditions that are hard to match so this case has a low practical relevance.

If the pressure in a single phase of liquid CO_2 with dissolved water is lowered to the bubble pressure a separate phase of a binary gas evolves. This is what happens in liquid water as well. But in addition to the gas phase a liquid water phase forms, too, because the partial pressure of the water in the newly formed gas phase $p_{gas}^{H_2O}$ is still higher than the vapour pressure of water $p_{gas}^{H_2O}$. So, two additional phases evolve at the same time.

If the pressure in the single-phase gas is increased there are to possible courses of development depending on the local mass fraction of water. Above a certain amount of water vapour the water-component of the gas begins to condensate and forms a two-phase state consisting of liquid water and gas which in turn can reach three-phase state as discussed above. But if the gas contains very little water the saturation partial pressure of carbon dioxide can be exceeded before the partial pressure of water is reached. In that case liquid carbon dioxide evolves first. Since a part of the gaseous CO_2 changes into liquid CO_2 partial pressure of water vapour increases, and a liquid water phase is formed again. Only in case of practically no water present in the CO_2-phase a two-phase state consisting of a liquid and a gaseous CO_2-phase can be reached.

7.3.4.4 Combination of phase diagnostics for normal and altered evolution

The different possible phase states, characteristic conditions for a stable state as well as for a change of the phase state as presented in Fig. 7.9 to Fig. 7.11 are combined in Fig. 7.12. As in the previous figures each coloured box represents a phase state. The colours are chosen to match the colour coding of Fig. 7.3. The arrows connecting the boxes indicate possible changes of the phase state. Despite the fact that a supercritical state doesn't pose an own condition of aggregation it is considered separately in Fig. 7.12 in order to relate this figure to the discussion of the normal evolution.

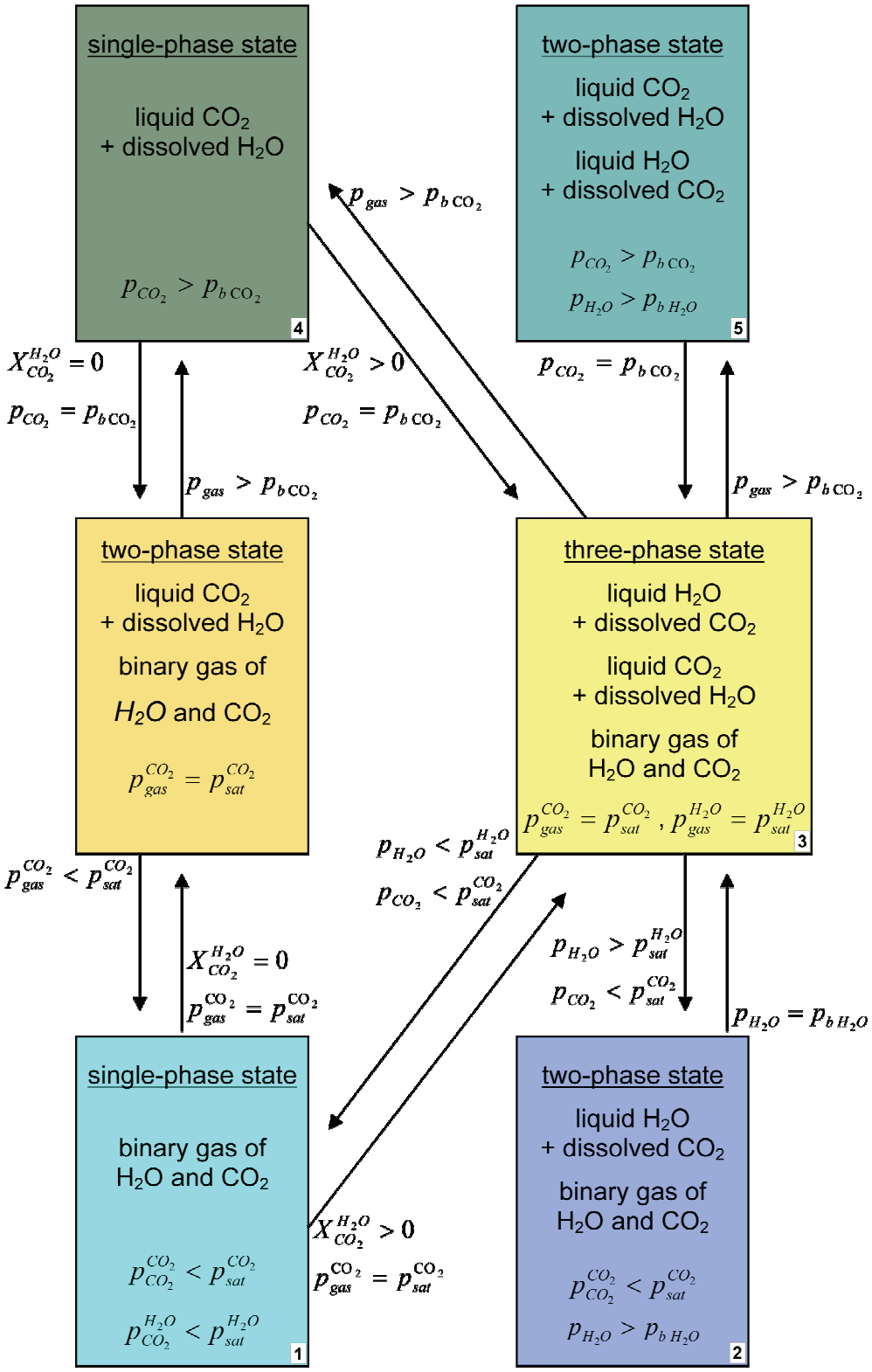

Fig. 7.11 Phase state conditions of a H_2O-CO_2-mixture due to phase changes; colour coding according to Fig. 7.3.

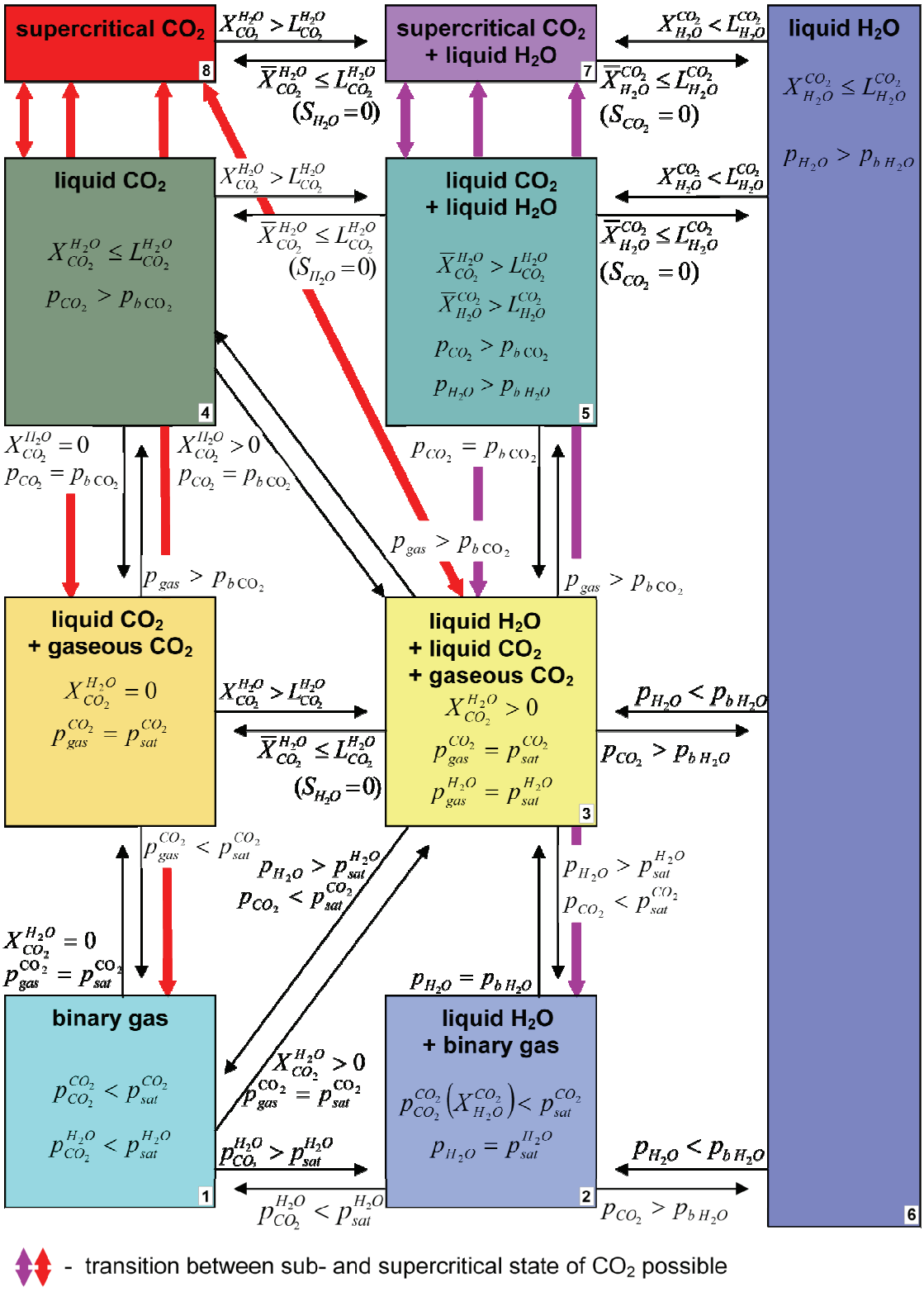

Fig. 7.12 Possible phase states and criteria for the phase changes; colour coding according to Fig. 7.3.

7.3.5 Phase diagnostics for a NaCl-component

Since solubilities of NaCl in water vapour and in CO_2 in general are negligible (c.f. sections 4.7.1.2 and 5.8.1) only the case of NaCl dissolved in liquid water has to be considered. If the concentration of NaCl amounts to less than the salt solubility the dissolved salt is transported in the water-phase subject to advection, diffusion, dispersion and density-driven flow. If more salt is present than allowed by the solubility precipitation commences and solid salt evolves. In this case the variable salt concentration adopts the equilibrium value and the amount of solid salt becomes variable. In any phase state without water the salt component can be present only as solid precipitate.

8 Need for further research

8.1 Normal and altered evolution

It appears to be useful, to subdivide the problem of CO_2-storage in the underground into the normal evolution of a CO_2-repository and into altered evolutions because the physics involved in a normal evolution of a deep storage of CO_2 are less demanding than those in the altered evolutions. While the mathematical description as a two-phase flow of brine and supercritical CO_2 is sufficient in case of the normal evolution three-phase conditions can occur in an altered evolution scenario if CO_2 rises to higher aquifers. In the latter case

– an additional balance equation,
– more sophisticated phase diagnostics,
– formulations including phase transitions and the properties of subcritical CO_2 and
– more complicated and up to now mostly unknown EOS for the three-phase system

are required. Additionally, the range of validity for the formulations must also cover lower temperatures (down to 10 °C) and lower pressures (down to atmospheric pressure) in contrast to the normal evolution where temperatures above 35 °C and pressures above 8 MPa suffice to keep the CO_2 supercritical.

Beyond the scope of this report but certainly relevant for further altered evolution modelling is the matter of even lower temperatures leading to the transition from liquid to solid phases due to the Joule-Thomson effect of rising CO_2. Forming solid obstacles of CO_2-hydrates means retardation and dispersion of the CO_2-plume [35] with all the implications for safety assessment. However, the extension to include phase change from fluid to solid state is edge of research at the time and not yet ready for application.

8.2 Two-phase flow properties

Recent investigations have shown that the hydrogeologic characterisation of strata with a view to two-phase flow is not only depending on the properties of the rock matrix but also - via the fluid properties - on the prevailing in-situ conditions. Since the fluid combination of brine and CO_2 in the deep underground is only investigated over the last

few years, only a very limited amount of measurements and of experience in the appropriate choice of the EOS exists up to now.

From a mathematical point of view accurate EOS are of high importance since the two-phase flow equations are highly non-linear which can easily lead to unreliable model predictions. An important aspect regarding CO_2-storage poses the description of the residual CO_2-saturation. On one hand, this value determines the amount of physical trapping of CO_2 in the wake of the CO_2-plume after shutdown of injection and consequently the mobility of the remaining plume. On the other hand, it is subject to changes of the local in-situ conditions. An appropriate choice is therefore difficult. For altered evolution scenarios where CO_2 escapes to higher strata, the problem intensifies. Note, that apparently no data exists for EOS should a three-phase flow system evolve during the rise of CO_2.

Keeping in mind the complexity of the flow processes involved and the uncertainties introduced by heterogeneities over the large model areas that come into question the geohydrological characterisation with regard to two-phase flow needs to be addressed in the future with high priority.

8.3 Densitiy-driven flow

During the last few years it has become an acknowledged fact that dissolution of CO_2 and subsequent transport in the aqueous phase is a relevant effect increasing the long-term safety of CO_2-storage in the underground. After the injected CO_2 has pooled up below the bottom of the upper aquitard, dissolution into the brine phase increases brine density slightly but significantly. This effect leads to an unstable layering of heavier over lighter brine. In this situation the slightest perturbation triggers density-driven brine flow in form of downwards lengthening fingers. This is a self-sustaining phenomenon because CO_2-saturated brine pushes less saturated brine upwards where CO_2-dissolution feeds the convection cells.

Apparently, this fingering is an extremely delicate process thus being massively influenced by three types of factors:

– the physical parameters
  - dispersion
  - diffusion
– the domain geometry
– the numerical parameters, especially the grid

Since density differences between pure brine and CO_2-saturated brine amount only to a few kilograms per cubic metre the introduced advective flow velocities will be rather low. Accordingly, the influence of diffusion in comparison to the influence of hydrodynamic dispersion will be rather high. A very good representation of both phenomena in the model is therefore highly advisable. If the diffusion coefficient turns out to be a sensitive constant more data covering the conditions in the deep underground is required.

Convective flow patterns depend strongly on the layer thickness and in case of laterally bounded domains also on the width of the domain [50]. While this phenomenon is extensively investigated for a large variety of different convection problems complexity of the density-dependent flow can be highly increased by inhomogeneities of the solid matrix.

Finally, it is always a challenging task to reproduce a situation with unstable physical conditions with numerical tools because of the inherent chaotic behaviour of such a system. A big problem in this case may be to demonstrate that the model solution is independent of the used grid since it needs extremely fine grids to resolve convections cells with sufficient accuracy. Also, to find a measure to compare growth and intensity of the fingers may prove to be difficult.

All in all, there are many difficulties involved in modelling transport of dissolved CO_2 and to provide means of reliable model calculations is still subject of intensive research.

8.4 Thermodynamic fluid properties

The properties of the three components water, carbon dioxide and sodium chloride considered in this report are - not surprisingly - far better known for the pure components than for mixtures. However, the formulation for the thermal conductivity of pure water is

only valid for temperatures above 20 °C (s. tables C.1, C.5 and C.7, appendix C) and thus not totally appropriate for altered evolution simulations.

Quite well described are NaCl-solutions, too, even if there are gaps that might be relevant for very high salinities or low temperatures (s. table C.2, appendix C). Uncertainties exist referring to formulation for the heat of dissolution but the relevance of this term is not completely clear.

Apparently, only little can be found in the literature concerning formulations for a CO_2-phase with dissolved water [6] (q.v. table C.6, appendix C). For the gaseous CO_2-phase density, enthalpy and heat capacity can be taken as the mass weighed sum of the referring quantity of the components. Additionally, the solubility of water in CO_2 is well described. In all other cases formulations are based on assumptions that are not confirmed by laboratory data. Since the solubility of water in CO_2 is low the impact of dissolved water on the CO_2-properties is sometimes neglected in numerical models e.g. [6]. But the relevance or irrelevance of this assumption has still to be demonstrated.

Formulations for the properties of pure water or aqueous NaCl-solutions containing CO_2 are also scarce [17] (q.v. tables C.4 and C.5, appendix C). Especially the impact of CO_2 on the viscosity of water or brine at high pressures is apparently unknown. The only known source is valid only for deep sea conditions and can certainly not be used for CO_2-storage in the underground. But also the influence of CO_2 on thermal conductivity and vapour pressure needs to be clarified.

It is not at all clear, whether all those data or formulations missing are relevant in the end. Even if they can be produced it still may turn out that the influence of a particular dependency is indeed negligible. A physical quantity like the enthalpy of dissolution could be varying largely but being insignificant in comparison to the variability caused by a varying mixture composition. On the other hand, as pointed out by [2], where delicate processes like density-driven flow or fingering are involved it is important to use the best possible formulations even if a property like the density is not varying much at all. In the light of the physically and mathematically highly complex and non-linear problems that are stated in the framework of CO_2-storage in the deep underground this should be made certain.

9 References

[1] Altunin, V.V.: Thermophysical properties of carbon dioxide (in russisch). Publishing House of Standards, Moskau, 1975.

[2] Adams, J. J. and Bachu, S.: Equations of state for basin geofluids: algorithm review and intercomparison for brines. Geofluids (2002) 2, 257–271, 2002.

[3] Bachu, S., Bennion, B.: Effects of in-situ conditions on relative permeability characteristics of CO_2-brine systems. Environmental Geology, DOI 10.1007/s00254-007-0946-9, Springer Verlag, 2007.

[4] Batistelli, A., Calore, C., Pruess, K.: The simulator TOUGH2/EWASG for modelling geothermal reservoirs with brines and non-condensable gas. Geothermics, Vol. 26, No. 4, 1997.

[5] Batzle, M. and Wang, Z.:Seismic properties of pore fluids. Geophysics, 57, 1396-1408, 1992.

[6] Bielinski, A.: Numerical Simulation of CO2 Sequestrationin Geological Formations. PhD thesis, Heft 155, Eigenverlag, Institut für Wasserbau, Universität Stuttgart, 2007.

[7] Bowers, T.S.: Calculation of the Thermodynamic and Geochemical Consequences of Nonideal Mixing in the System H2O-CO2-NaCl on Phase Relations in Geologic Systems. PhD thesis, University of California at Berkeley, 1982.

[8] Brooks, A.N. and Corey, A.T.: Hydraulic Properties of Porous Media. Hydrol. Pap. Vol.3, Fort Collins, Colorado State University, 1964.

[9] Chou, I.M.: Phase relations in the system NaCl-KCl-H_2O. III: solubilities of halite in vapour-saturated liquids above 445 °C and redetermination of phase equilibrium properties in the system NaCl-H_2O. Geochimica et Cosmochimica Acta 51, 1987.

[10] Cygan, R.T.: The solubility of Gases in NaCl Brine and a Critical Evaluation of Available Data. Sandia Report SAND90-2848 UC-721, Sandia National Laboratories, Albuquerque, 1991.

[11] D'ans Lax: Taschenbuch für Chemiker und Physiker. Band 1 Physikalisch-chemische Daten. Springer Verlag, 4. Auflage, 1992.

[12] Daubert, T. E. and Danner, R. P.: Physical and thermodynamic properties of pure chemicals: data compilation. Design Institute for Physical Property Data, 1989.

[13] Deutscher Kälte- und Klimatechnischen Verein e.V. – DKV: Kohlendioxid - Besonderheiten und Einsatzchancen als Kältemittel. DKV-Statusreport Nr. 20 (3rd revised edition 2006), DKV-Geschäftsstelle, Stuttgart, 2006.

[14] Duan, Z. and Sun, R.: An improved model calculating CO_2 solubility in purewater and aqueous NaCl solutions from 273 to 533 k and from 0 to 2000 bar. Chemical Geology, (193):257–271, 2003.

[15] Fenghour, A., Wakeman, W.A., Vesovic, V.: The viscosity of carbon dioxide. GJ. Phys. Chem. Ref. Data, 27(1):31-44, 1998.

[16] Garcia, J.E.: Density of aqueous solutions of CO_2. Technical Report LBNL-49023, Lawrence Berkeley National Laboratory, Berkeley, CA, 2001.

[17] Garcia, J.E.: Fluid Dynamics of Carbon Dioxide Disposal into Saline Aquifers. Dissertation, University of California, Berkeley, 2003.

[18] Van Genuchten, M.T.: A Closed-Form Equation for Predicting the Hydraulic Conductivity of Unsaturated Soils. Soil Sci. Soc. Am. J., 44:892-898, 1980.

[19] Gmelin, L.: Gmelins Handbuch der Anorganischen Chemie, 8. Edition, Kohlenstoff TeilC3. Verlag Chemie, Weinheim, 1973.

[20] Gudmundsson, J.-S., Thrainsson, H.: Power potential of two-phase geothermal wells. Geothermics, (18):357-366, 1989.

[21] Haas, J.L.: Physical Properties of the Coexisting Phases and Thermochemical Properties of the H_2O Component in Boiling NaCl Solutions. USGS, Geological Survey Bulletin 1421-A, Washington D.C., 1976.

[22] Helmig, R.: Multiphase Flow and Transport Processes in the Subsurface. Springer, 1997.

[23] International Association for Properties of Water and Steam: Release on the IAPWS Industrial Formulation 1997 for the Thermodynamic Properties of Water and Steam. 1997. Homepage: http://www.iapws.org.

[24] The International Association for the Properties of Water and Steam: Revised Release on the IAPS Formulation 1985 for the Viscosity of Ordinary Water Substance. 2003. Homepage: http://www.iapws.org.

[25] IFC: A formulation of thermodynamic properties of ordinary water substance. International Formulation Committee Secretariat, Düsseldorf, 1967.

[26] Kern, H.: Elastic wave velocity in crustal and mantle rocks at high pressure and temperature: the role of High-low quartz transition and of dehydration reactions. Phys. Earth. Planet. Inter. 29, 1982.

[27] Kumagai, A., Yokoyama, Ch.: Viscosities of Aqueous NaCL Solutions Containing CO_2 at High Pressures. J. Chem. Eng. Data, 44, 227-229, 1999.

[28] Landolt-Börnstein: Zahlenwerte und Funktionen aus Physik * Chemie * Astronomie * Geophysik und Technik; 2. Band Eigenschaften der Materie in ihren Aggregatzuständen; 5. Teil Transportphänomene * Kinetik * homogene Gasgleichgewichte; Bandteil a Transportphänomene I (Viskosität und Diffusion). Springer-Verlag, 1969.

[29] Leverett, M.C.: Capillary behaviour in Porous Solids. Transactions of the AIME, 142:152-169, 1941.

[30] Michaelides, E.E.: Thermodynamics properties of geothermal fluids. Geothermal Resources Council Transactions, (5):361-364, 1981.

[31] Phillips, S.L., Igbene, A., Fair, J.A., Ozbek, H., Tavana, M.: A Technical Databook for Geothermal Energy Utilization. Lawrence Berkeley Laboratory, University of California, LBL-12810, 1981.

[32] Potter, R.W., II, Brown, D.L.: The Volumetric Properties of Aqueous Sodium Chloride Solutions from 0° to 500°C at Pressures up to 2000 Bars Based on Regression of Available Data in the Literature. USGS, Geological Survey Bulletin 1421-A, Washington D.C., 1977.

[33] Potter, R.W., II, Babcock, R.S., Brown, D.L.: A new method for determining the solubility of salts in aqueous solutions at elevated temperatures. J. Research U.S. Geol. Surv. 5, no.3, 1977.

[34] Pruess, K., Garcia, J.: Multiphase flow dynamics during CO_2 disposal into saline aquifers. Environmental Geology, 42:282-295, 2002.

[35] Pruess, K.: Numerical Simulation of CO2 Leakage from a Geologic Disposal Reservoir, Including Transitions from Super- to Sub-Critical Conditions, and Boiling of Liquid CO_2. Technical Report LBNL-52423, Lawrence Berkeley National Laboratory, Berkeley, CA, 2003.

[36] Scheidegger, A.E.: General Theory of Dispersion in Porous Media. Journal of Geophysical Research, Vol. 66, No. 10, October, 1961.

[37] Silvester, L.F. and Pitzer, K.S.: Thermodynamics of Geothermal Brines. Part I. Technical Report LBNL-4456, Lawrence Berkeley National Laboratory, Berkeley, CA, 1976.

[38] Span, R. und Flacke, N.: Thermophysikalische Eigenschaften von CO_2. In: DKV-Statusbericht Nr. 20 „Kohlendioxid - Besonderheiten und Einsatzchancen als Kältemittel“, (3. überarbeitete Ausgabe 2006), Deutscher Kälte- und Klimatechnischer Verein e.V. - DKV , Stuttgart, 2006.

[39] Span, R., Wagner, W.: A new equation of state for carbon dioxide covering the fluid region from the triple-point temperature to 1100 K at pressures up to 800 Mpa. J. Phys. Chem. Ref. Data, 25(6):1509-1596, 1996.

[40] Spycher, N.F., Pruess, K.: CO2-H2O Mixtures in the Geological Sequestration of CO2. II. Partitioning in Chloride Brines at 12-100°C and up to 600 bar. Geochimica Cosmochim. Acta, in press. (LBNL-56334), 2005.

[41] Spycher, N.F., Pruess, K., Ennis-King, J.: CO_2-H_2O mixtures in the geological sequestration of CO_2. I. Assessment and calculation of mutual solubilities from 12 to 100 °C and up to 600 bar. Geochimica et Cosmochimica Acta, 67 (16): 3015-3031, 2003.

[42] Technische Universität Darmstadt, Fachgebiet Technische Thermodynamik, 2005. Homepage: http://www.tu-darmstadt.de/fb/mb/ttd.

[43] Tödheide, K., Franck, E. U.: Das Zweiphasengebiet und die kritische Kurve im System Kohlendioxid-Wasser bis zu Drucken von 3500 bar. Zeitschrift für Physikalische Chemie Neu Folge, (37):387–401, 1963.

[44] Ullrich, A., Eggers, R.: Hydratbildung bei Entspannung von feuchtem CO_2. In: Jahresbericht 2001/02 zum Max-Buchner-Forschungsstipendium, 2002.

[45] Verma, A., Pruess, K.: Thermohydrological Conditions and Silica Redistribution Near High-Level Nuclear Wastes Emplaced in Saturated Geological Formations. Journal of Geophysical Research, Vol. 93, No. 83, 1988.

[46] Vesovic, V., Wakeham, W.A., Olchowy, G.A., Sengers, J.V., Watson, J.T.R., Millat, J.: The Transport properties of Carbon Dioxide. J. Phys. Chem. Ref. Data, Vol. 19, No. 3, 1990.

[47] Wikipedia – Die freie Enzyklopädie. Homepage: http://de.wikipedia.org

[48] Xu, T., Apps, J.A., Pruess, K.: Analysis of mineral trapping for CO_2 disposal in deep aquifers. Paper LBNL-46992, Lawrence Berkeley National Laboratory, 2001.

[49] Yusufova, V.D., Pepinov, R.I., Nikolaev, V.A., Guseinov, G.M.. Inzh.-Fiz. Zh., 29, 600,1975.

[50] Zierep, J. and Oertel jr., H. (eds.): Convective Transport and INstability Phenomena. Verlag G. Braun, Karlsruhe, 1982.

[51] Zimmer, U.: Quantitative Untersuchung zur Mikrorissigkeit aus akustischen Gesteinseigenschaften am Beispiel von Steinsalz und Anhydrit. Dissertation, Fakultät VI – Bauingenieurwesen und Angewandte Geowissenschaften der Technischen Universität Berlin, 1991.

Table of Figures

List of Tables

Appendix C

Appendix A - Iterative scheme for calculating CO_2-density

Temperature and pressure are usually primary variables in a numerical model. Graphical illustrations of secondary variables are therefore most helpful if they are shown depending on these quantities. In case of the density of CO_2 there is no function given for the density depending on temperature and pressure, as mentioned in section 5.3. Therefore an iteration scheme is described here for calculating the density. This helps only for plotting purposes, though, but not in a numerical model.

Fig. A1 shows a diagram illustrating the iteration procedure. The relations required for this procedure are the vapour pressure $p_s(T)$ given in eq. (5.1) and the pressure of carbon dioxide $p(T,\rho)$ given in eq. (5.30). Additionally, the functions for the densities of liquid CO_2 $\rho'(T)$ and gaseous CO_2 $\rho''(T)$ in the two-phase domain as given in [39] are used:

$$\ln\left(\frac{\rho'}{\rho_c}\right) = \sum_{i=1}^{4} a_i \left(1 - \frac{T}{T_c}\right)^{t_i} \qquad \text{(A.1)}$$

ρ' - saturated liquid density [kg/m³]

ρ_c - density of carbon dioxide at the critical point [kg/m³]
(c.f. 0, eq. (5.5))

T - temperature [K]

T_c - temperature at the critical point [K] (c.f. 0, eq. (5.1))

a_i, t_i- constants:

a_1= 1.9245108	t_1= 0.34
a_2=-0.62385555	t_2= 0.50
a_3=-0.32731127	t_3= 10/6
a_4= 0.39245142	t_4= 11/6

$$\ln\left(\frac{\rho''}{\rho_c}\right) = \sum_{i=1}^{5} a_i \left(1 - \frac{T}{T_c}\right)^{t_i} \qquad \text{(A.2)}$$

ρ'' - saturated vapour density [kg/m³]

a_i, t_i- constants:

a_1= -1.7074879 t_1= 0.34

a_2= -0.82274670 t_2= 0.50

a_3= -4.6008549 t_3= 1

a_4= -10.111178 t_4= 7/3

a_4= -29.742252 t_4= 14/3

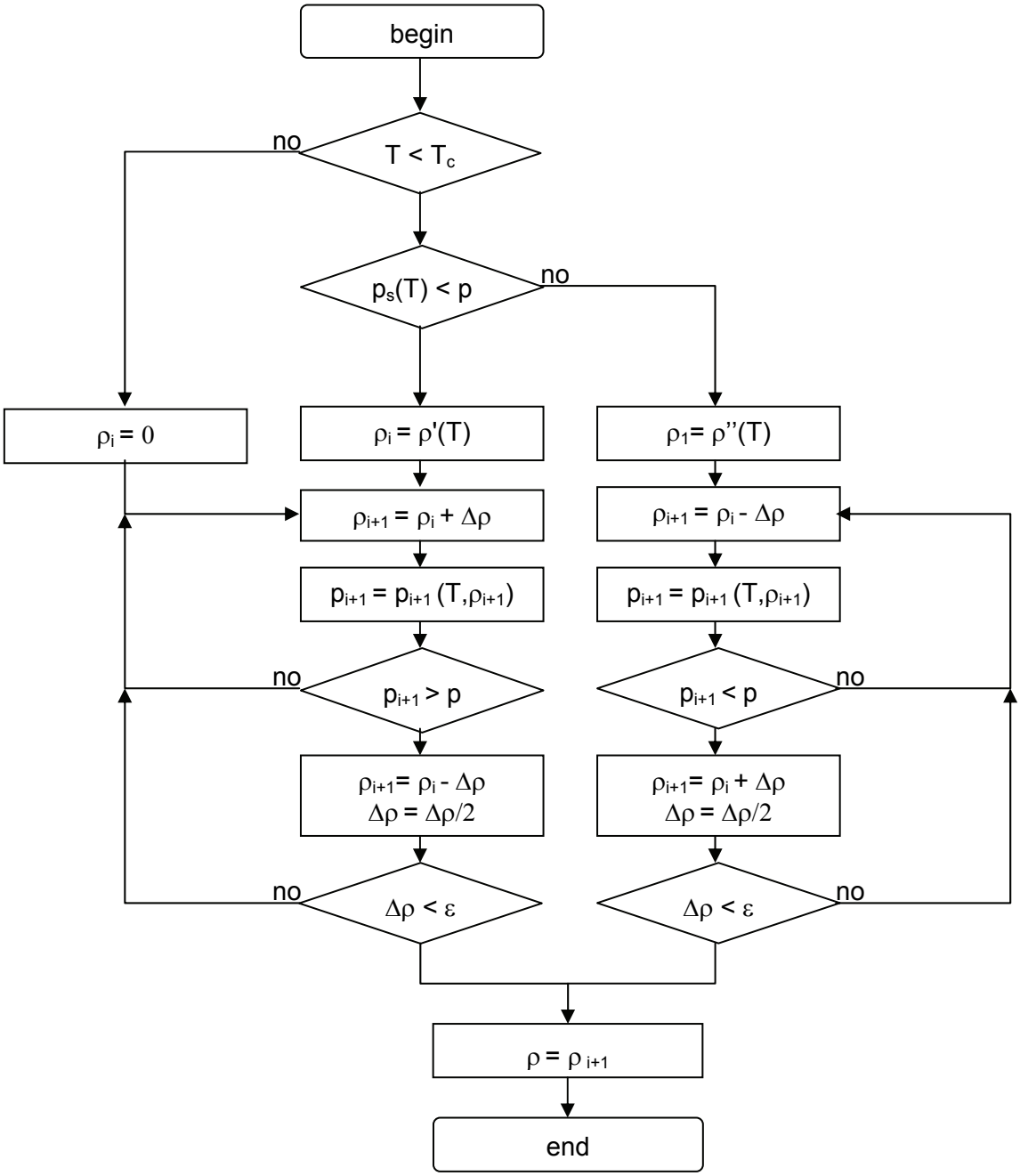

Fig. A.1 Iterative scheme for calculating the CO_2-density.

Appendix B - Constants

General constants

R - general gas constant: 8.314 J/(mol K)
m^{H_2O} - molecular weight of H_2O: 0.01801528 kg/mol
m^{CO_2} - molecular weight of CO_2: 0.044099 kg/mol
m^{NaCl} - molecular weight of NaCl: 0.05844 kg/mol
$T_{crit}^{CO_2}$ - critical temperature of CO_2: 304.1282 K
$p_{crit}^{CO_2}$ - critical pressure of CO_2: 7.3773 MPa
$\rho_{crit}^{CO_2}$ - critical density of CO_2: 467.6 kg/m³
$T_{crit}^{H_2O}$ - critical temperature of H_2O: 647.29 K
$p_{crit}^{H_2O}$ - critical pressure of H_2O: 22.085 MPa

Vapour pressure of pure water

Eq.s (4.1), (4.2), (4.3):

$p^* = 1$ MPa
$T^* = 1$ K

$n_1 = 0.116\,705\,214\,527\,67\ 10^4$
$n_2 = -0.724\,213\,167\,032\,06\ 10^6$
$n_3 = -0.170\,738\,469\,400\,92\ 10^2$
$n_4 = 0.120\,208\,247\,024\,70\ 10^5$
$n_5 = -0.323\,255\,503\,223\,33\ 10^7$
$n_6 = 0.149\,151\,086\,135\,30\ 10^2$
$n_7 = -0.482\,326\,573\,615\,91\ 10^4$
$n_8 = 0.405\,113\,405\,420\,57\ 10^6$
$n_9 = -0.238\,555\,575\,678\,49$
$n_{10} = 0.650\,175\,348\,447\,98\ 10^3$

Vapour pressure of water with dissolved NaCl

Eq.s (4.4), (4.7), (4.10), (4.11):

$a_1 = 5.935\,82\ 10^{-6}$
$a_2 = -5.193\,86\ 10^{-5}$
$a_3 = 1.231\,56\ 10^{-5}$

$b_1 = 1.154\,20\ 10^{-6}$
$b_2 = 1.412\,54\ 10^{-7}$
$b_3 = -1.924\,76\ 10^{-8}$
$b_4 = -1.707\,17\ 10^{-9}$
$b_5 = 1.053\,90\ 10^{-10}$

$e_0 = 12.508\,49\,100$
$e_1 = -4.616\,913\ 10^3$
$e_2 = 3.193\,455\ 10^{-4}$
$e_3 = 1.196\,500\ 10^{-11}$
$e_4 = -1.013\,137\ 10^{-2}$
$e_5 = -5.714\,8\ 10^{-3}$
$e_6 = 2.937\,0\ 10^5$

Density of liquid water

Eq. (4.13), (4.14), (4.15), (4.16):

$p^* = 16.53$ MPa

$T^* = 1386$ K

$R^{H_2O} = 0.461526$ kJ/(kg K)

i	I_i	J_i	n_i
1	0	-2	0.146 329 712 131 67 10^{0}
2	0	-1	-0.845 481 871 691 14 10^{0}
3	0	0	-0.375 636 036 720 40 10^{1}
4	0	1	0.338 551 691 683 85 10^{1}
5	0	2	-0.957 919 633 878 72 10^{0}
6	0	3	0.157 720 385 132 28 10^{0}
7	0	4	-0.166 164 171 995 01 10^{-1}
8	0	5	0.812 146 299 835 68 10^{-3}
9	1	-9	0.283 190 801 238 04 10^{-3}
10	1	-7	-0.607 063 015 658 74 10^{-3}
11	1	-1	-0.189 900 682 184 19 10^{-1}
12	1	0	-0.325 297 487 705 05 10^{-1}
13	1	1	-0.218 417 171 754 14 10^{-1}
14	1	3	-0.528 383 579 699 30 10^{-4}
15	2	-3	-0.471 843 210 732 67 10^{-3}
16	2	0	-0.300 017 807 930 26 10^{-3}
17	2	1	0.476 613 939 069 87 10^{-4}
18	2	3	-0.441 418 453 308 46 10^{-5}
19	2	17	-0.726 949 962 975 94 10^{-15}
20	3	-4	-0.316 796 448 450 54 10^{-4}
21	3	0	-0.282 707 979 853 12 10^{-5}
22	3	6	-0.852 051 281 201 03 10^{-9}
23	4	-5	-0.224 252 819 080 00 10^{-5}
24	4	-2	-0.651 712228956 01 10^{-6}
25	4	10	-0.143 417299379 24 10^{-12}
26	5	-8	-0.405 169968601 17 10^{-6}
27	8	-11	-0.127 343017416 41 10^{-8}
28	8	-6	-0.174 248712306 34 10^{-9}
29	21	-29	-0.687 621312955 31 10^{-18}
30	23	-31	0.144 783078285 21 10^{-19}
31	29	-38	0.263 357816627 95 10^{-22}
32	30	-39	-0.119 476226400 71 10^{-22}
33	31	-40	0.182 280945814 04 10^{-23}
34	32	-41	-0.935 370872924 58 10^{-25}

Density of water vapour

Eq. (4.17), (4.18), (4.19):

$p^* = 1$ MPa, $T^* = 540$ K, $R^{H_2O} = 0.461526$ kJ/(kg K)

i	I_i	J_i	n_i
1	1	0	-0.177 317 424 732 13 10^{-2}
2	1	1	-0.178 348 622 923 58 10^{-1}
3	1	2	-0.459 960 136 963 65 10^{-1}
4	1	3	-0.575 812 590 834 32 10^{-1}
5	1	6	-0.503 252 787 279 30 10^{-1}
6	2	1	-0.330 326 416 702 03 10^{-4}
7	2	2	-0.189 489 875 163 15 10^{-3}
8	2	4	-0.393 927 772 433 55 10^{-2}
9	2	7	-0.437 972 956 505 73 10^{-1}
10	2	36	-0.266 745 479 140 87 10^{-4}
11	3	0	0.204 817 376 923 09 10^{-7}
12	3	1	0.438 706 672 844 35 10^{-6}
13	3	3	-0.322 776 772 385 70 10^{-4}
14	3	6	-0.150 339 245 421 48 10^{-2}
15	3	35	-0.406 682 535 626 49 10^{-1}
16	4	1	-0.788 473 095 593 67 10^{-9}
17	4	2	0.127 907 178 522 85 10^{-7}
18	4	3	0.482 253 727 185 07 10^{-6}
19	5	7	0.229 220 763 376 61 10^{-5}
20	6	3	-0.167 147 664 510 61 10^{-10}
21	6	16	-0.211 714 723 213 55 10^{-2}
22	6	35	-0.238 957 419 341 04 10^{2}
23	7	0	-0.590 595 643 242 70 10^{-17}
24	7	11	-0.126 218 088 991 01 10^{-5}
25	7	25	-0.389 468 424 357 39 10^{-1}
26	8	8	0.112 562 113 604 59 10^{-10}
27	8	36	-0.823 113 408 979 98 10^{1}
28	9	13	0.198 097 128 020 88 10^{-7}
29	10	4	0.104 069 652 101 74 10^{-18}
30	10	10	-0.102 347 470 959 29 10^{-12}
31	10	14	-0.100 181 793 795 11 10^{-8}
32	16	29	-0.808 829 086 469 85 10^{-10}
33	16	50	0.106 930 318 794 09
34	18	57	-0.336 622 505 741 71
35	20	20	0.891 858 453 554 21 10^{-24}
36	20	35	0.306 293 168 762 32 10^{-12}
37	20	48	-0.420 024 676 982 08 10^{-5}
38	21	21	-0.590 560 296 856 39 10^{-25}
39	22	53	0.378 269 476 134 57 10^{-5}
40	23	39	-0.127 686 089 346 81 10^{-14}
41	24	26	0.730 876 105 950 61 10^{-28}
42	24	40	0.554 147 153 507 78 10^{-16}
43	24	58	-0.943 697 072 412 10 10^{-6}

Brine density

Eq.s (4.20), (4.21):

A = -3.033 405 a_1= -0.004 539 c_1=-9.9595
B =10.128 163 a_2= -0.000 163 8 c_2= 7.0845
C = -8.750 567 a_3= 0.000 025 51 c_3= 3.9093
D = 2.663107

(a_1= -0.005 vapour saturated value)

Viscosity of pure water

Eq.s (4.26), (4.27), (4.28):

T^* = 647.226 K
ρ^* = 317.763 kg/m³
η^* = 55.071 10^{-6} Pa s

H_0 = 1.000 000
H_1 = 0.978 197
H_2 = 0.579 829
H_3 =-0.202 354

i	j	H_{ij}
0	0	0.513 204 7
1	0	0.320 565 6
4	0	-0.778 256 7
5	0	0.188 544 7
0	1	0.215 177 8
1	1	0.731 788 3
2	1	1.241 044
3	1	1.476 783
0	2	-0.281 810 7
1	2	-1.070 786
2	2	-1.263 184
0	3	0.177 806 4
1	3	0.460 504 0
2	3	0.234 037 9
3	3	-0.492 417 9
0	4	-0.041 766 10
3	4	0.160 043 5
1	5	-0.015 783 86
3	6	-0.003 629 481

(coefficients omitted from this list are equal to zero)

Viscosity of water with dissolved NaCl

Eq. (4.30)

a = 0.0816
b = 0.0122
c = 0.000 128
d = 0.000 629
k =-0.7

Viscosity water with dissolved NaCl and CO_2

Eq. (4.31)

a = 3.85971
b = 1.32561 10^{-2}
c = -5.37539
d = 1.90621 10^{-2}
e = 8.79552
f = -3.17229 10^{-2}
g = -7.22769
h = 2.64498 10^{-2}
i = -1.69956 10^{-3}

Enthalpy of pure water

Eq. (4.36), (4.37):

R^{H_2O}, T^*,I_i, J_i, n_i (see density of pure water)

Enthalpy of water with dissolved NaCl

Eq. (4.44):

i	j	a_{ij}	
0	0	+9633.6	Correction from [20]: a_{00} = -9633.6
0	1	-4080.0	
0	2	286.49	
1	0	166.58	
1	1	68.577	
1	2	-4.6856	
2	0	-0.90963	
2	1	-0.36524	
2	2	0.249667 10^{-1}	
3	0	0.17965 10^{-2}	
3	1	0.71924 10^{-3}	
3	2	-0.4900 10^{-4}	

Enthalpy of water with dissolved CO_2

Eq. (4.47):

c_1 = 28.944 770 6
c_2 = -0.035 458 176 8
c_3 = -4770.670 77
c_4 = 1.027 827 68 10^{-5}
c_5 = 33.812 609 8
c_6 = 9.040 371 40 10^{-3}
c_7 = -1.149 340 31 10^{-3}
c_8 = -0.307 405 726
c_9 = -0.090 730 148 6
c_{10}= 9.327 133 93 10^{-4}

Enthalpy of water with dissolved CO_2 and NaCl

Eq.s (4.51), (4.52):

$B(0)$= 7.836 66 10^{7}
$B(1)$= 1.960 25 10^{6}
$B(2)$= 8.205 74 10^{4}
$B(3)$=-7.406 74 10^{2}
$B(4)$= 2.183 80
$B(5)$=-2.209 99 10^{-3}

$C(0)$= 1.197 84 10^{-1}
$C(1)$=-7.178 23 10^{-4}
$C(2)$= 4.938 54 10^{-6}
$C(3)$=-1.038 26 10^{-8}
$C(4)$= 1.082 33 10^{-11}

Heat capacity of pure water

Eq.s (4.54), (4.55)

R^{H_2O}, T^*,I_i, J_i, n_i (see density of pure water)

Solubility of NaCl in liquid water

Eq. (4.61)

M^{NaCl}=0.05844 kg/mol

Solubility of CO_2 in water

Eq.s (4.67), (4.69), (4.71):

$\overline{V}^{H_2O} = 18.5$ cm³/mol after [41]

$\overline{V}^{CO_2}$ = 32.1 cm³/mol after [41]

$a_{H_2O-CO_2} = 7.89\,10^7$ bar cm^6 K$^{0.5}$ mol^{-2}

$b_{CO_2} = 27.86$ cm³/mol

$b_{H_2O} = 18.10$ cm³/mol

Eq. (4.68)

a=-2.215
b= 3.162 10^{-2}
c=-1.294 10^{-4}
d= 4.187 10^{-7}
e=-7.331 10^{-10}

Eq. (4.70)

gaseous and supercritical CO_2:
a= 1.188
b= 1.307 10^{-2}
c=-5.445 10^{-5}

liquid CO_2:

a= 1.168
b= 1.361 10^{-2}
c=-5.135 10^{-5}

Solubility of CO_2 in water with dissolved NaCl

Eq.(4.82) (coefficients omitted from this list are equal to zero):

for $\mu_{CO_2}^{1(0)} / RT$:

c_1 = 28.944 770 6
c_2 = -0.035 458 176 8
c_3 = -4770.670 77
c_4 = 1.027 827 68 10^{-5}
c_5 = 33.812 609 8
c_6 = 9.040 371 40 10^{-3}
c_7 = -1.149 340 31 10^{-3}
c_8 = -0.307 405 726
c_9 = -0.090 730 148 6
c_{10}= 9.327 133 93 10^{-4}
c_{11}= 0.0

for λ_{CO_2-Na}:

c_1 = -0.411 370 585
c_2 = 6.076 320 13 10^{-4}
c_3 = 97.534 770 8
c_8 = -0.023 762 2469
c_9 = 0.017 065 623 6
c_{11} = 1.413 358 34 10^{-5}

for $\zeta_{CO_2-Na-Cl}$:

c_1 = 3.363 897 23 10^{-4}
c_2 = -1.982 989 80 10^{-5}
c_8 = 2.122 208 30 10^{-3}
c_9 = -5.248 733 03 10^{-3}

Eq.s (4.83) and (4.86)

a_1 = 8.992 884 97 10^{-2}
a_2 = -4.947 831 27 10^{-1}
a_3 = 4.779 222 45 10^{-2}
a_4 = 1.038 088 83 10^{-2}
a_5 = -2.825 168 61 10^{-2}
a_6 = 9.498 875 63 10^{-2}
a_7 = 5.206 008 80 10^{-4}
a_8 = -2.935 409 71 10^{-4}
a_9 = -1.772 651 12 10^{-3}
a_{10} = -2.511 019 73 10^{-5}
a_{11} = 8.933 534 41 10^{-5}
a_{12} = 7.889 985 63 10^{-5}
a_{13} = -1.667 270 22 10^{-2}
a_{14} = 1.398 0
a_{15} = 2.960 000 00 10^{-2}

Vapour pressure of CO_2

Eq. (5.1)

a_1=-7.0602087	t_1=1.0
a_2= 1.9391218	t_2=1.5
a_3=-1.6463597	t_3=2.0
a_4=-3.2995634	t_4=4.0

Helmholtz energy for CO_2

Eq. (5.2)

R_{CO_2} = 188.9241 [J/(kg K)]

Eq. (5.4), (5.12), (5.13)

i	a_0^i	θ_0^i
1	8.373 044 56	0.0
2	-3.704 543 04	0.0
3	2.500 000 00	0.0
4	1.994 270 42	3.151 63
5	0.621 052 48	6.111 90
6	0.411 952 93	6.777 08
7	1.040 289 22	11.323 84
8	0.083 276 78	27.087 92

Eq.s (5.7), (5.8), (5.10), (5.14) through to (5.29):

i	n_i	d_i	t_i	c_i	a_i	b_i
1	0.388 568 232 031 61	1	0.00			
2	0.293 854 759 427 40 10^{1}	1	0.75			
3	-0.558 671 885 349 34 10^{1}	1	1.00			
4	-0.767 531 995 924 77	1	2.00			
5	0.317 290 055 804 16	2	0.75			
6	0.548 033 158 977 67	2	2.00			
7	0.122 794 112 203 35	3	0.75			
8	0.216 589 615 432 20	1	1.50	1		
9	0.158 417 351 097 24	2	1.50	1		
10	-0.231 327 054 055 03	4	2.50	1		
11	0.581 169 164 314 36 10^{-1}	5	0.00	1		
12	-0.553 691 372 053 82	5	1.50	1		
13	0.489 466 159 094 22	5	2.00	1		
14	-0.242 757 398 435 01 10^{-1}	6	0.00	1		
15	0.624 947 905 016 78 10^{-1}	6	1.00	1		
16	-0.121 758 602 252 46	6	2.00	1		
17	-0.370 556 852 700 86	1	3.00	2		
18	-0.167 758 797 004 26 10^{-1}	1	6.00	2		
19	-0.119 607 366 379 87	4	3.00	2		
20	-0.456 193 625 087 78 10^{-1}	4	6.00	2		
21	0.356 127 892 703 46 10^{-1}	4	8.00	2		
22	-0.744 277 271 320 52 10^{-2}	7	6.00	2		
23	-0.173 957 049 024 32 10^{-2}	8	0.00	2		
24	-0.218 101 212 895 27 10^{-1}	2	7.00	3		
25	0.243 321 665 592 36 10^{-1}	3	12.00	3		
26	-0.374 401 334 234 63 10^{-1}	3	16.00	3		
27	0.143 387 157 568 78	5	22.00	4		
28	-0.134 919 690 832 86	5	24.00	4		
29	-0.231 512 250 534 80 10^{-1}	6	16.00	4		
30	0.123 631 254 929 01 10^{-1}	7	24.00	4		
31	0.210 583 219 729 40 10^{-2}	8	8.00	4		
32	-0.339 585 190 263 68 10^{-3}	10	2.00	4		
33	0.559 936 517 715 92 10^{-2}	4	28.00	5		
34	-0.303 351 180 556 46 10^{-3}	8	14.00	6		
35	-0.213 654 886 883 20 10^{-3}	2	1.00	1		
36	0.266 415 691 492 72 10^{-5}	2	0.00	0		
37	-0.240 272 122 045 57 10^{-5}	2	1.00	1		
38	-0.283 416 034 239 99 10^{-3}	3	3.00	3		
39	0.212 472 844 001 79 10^{-3}	3	3.00	3		
40	-0.666 422 765 407 51				3.5	0.875
41	0.726 086 323 498 97				3.5	0.925
42	0.550 686 686 128 42 10^{-1}				3.0	0.875

i	α_i	β_i	γ_i	ε_i	A_i	B_i	C_i	D_i
35	25	325	1.16	1				
36	25	300	1.19	1				
37	25	300	1.19	1				
38	15	275	1.25	1				
39	20	275	1.22	1				
40		0.3			0.7	0.3	10.0	275
41		0.3			0.7	0.3	10.0	275
42		0.3			0.7	1.0	12.5	275

Viscosity of pure CO_2

Eq.s (5.33), (5.36), (5.37):

a_0 = 0.235 156	d_{11} = 0.407 111 9 10^{-2}	e_1 = 5.5930 10^{-3}
a_1 = -0.491 266	d_{21} = 0.719 803 7 10^{-4}	e_2 = 6.1757 10^{-5}
a_2 = 5.211 155 10^{-2}	d_{64} = 0.241 169 7 10^{-16}	e_3 = 0
a_3 = 5.347 906 10^{-2}	d_{81} = 0.297 107 2 10^{-22}	e_4 = 2.6430 10^{-11}
a_4 = -1.537 102 10^{-2}	d_{82} = -0.162 788 8 10^{-22}	

(coefficients omitted from this list are equal to zero)

Thermal conductivity of CO_2

Eq.s (5.41), (5.42), (5.44)

b_0= 0.4226159			
b_1= 0.6280115	c_1= 2.387869×10^{-2}	d_1= 2.447164×10^{-2}
b_2= -0.5387661	c_2= 4.350794	d_2= 8.705605×10^{-5}
b_3= 0.6735941	c_3= -1.033404×10^{1}	d_3= -6.547950×10^{-8}
b_4= 0	c_4= 7.981590	d_4= 6.594919×10^{-11}
b_5= 0	c_5= -1.940558	
b_6= -0.4362677		
b_7= 0.2255388		

Appendix C - Currant knowledge about formulations

The following tables summarise the state of knowledge concerning the state equations that are required for modelling the CO_2-sequestration. „✓“ depicts a reliable formulation within the ranges (1.1). A convention shortly describing the degree of need for further research is used in the tables:

- no need for further research
0 the formulation does not fully cover the required p-T-m-range
1 the formulation should be checked against measured data
2 apparently no measured data exists to validate the formulation
3 apparently neither measured data nor formulations exist

Tab. C. 1 Parameters for pure water

parameter	range of validity	need for research	sources	section
density	✓	-	[23]	4.2.1
viscosity	✓	-	[23]	4.3.1
thermal conductivity	T > 20°C	0	[49] cited in [31]	4.4
enthalpy	✓	-	[23]	4.5.1
heat capacity	✓	-	[23]	4.6.1
vapour pressure	✓	-	[23]	4.1.1
diffusivity	✓	-	[28], [11]	4.8

[11] D’ans Lax: Taschenbuch für Chemiker und Physiker. Band 1 Physikalisch-chemische Daten. Springer Verlag, 4. Auflage, 1992.

[23] International Association for Properties of Water and Steam: Release on the IAPWS Industrial Formulation 1997 for the Thermodynamic Properties of Water and Steam. 1997. Homepage: http://www.iapws.org.

[28] Landolt-Börnstein: Zahlenwerte und Funktionen aus Physik * Chemie * Astronomie * Geophysik und Technik; 2. Band Eigenschaften der Materie in ihren Aggregatzuständen; 5. Teil Transportphänomene * Kinetik * homogene Gasgleichgewichte; Bandteil a Transportphänomene I (Viskosität und Diffusion). Springer-Verlag, 1969.

[49] Yusufova, V.D., Pepinov, R.I., Nikolaev, V.A., Guseinov, G.M.. Inzh.-Fiz. Zh., 29, 600,1975.

[31] Phillips, S.L., Igbene, A., Fair, J.A., Ozbek, H., Tavana, M.: A Technical Databook for Geothermal Energy Utilization. Lawrence Berkeley Laboratory, University of California, LBL-12810, 1981.

Tab. C. 2 Parameters for water with dissolved NaCl

parameter	range of validity	need for research	sources	section
density	0.25 – 5 mol/kg	0	[21], [31]	4.2.2
viscosity	0 – 5 mol/kg	0	[31]	4.3.2
thermal conductivity	0 – 5 mol/kg T>20 °C	0	[49] cited in [31]	4.4.2
enthalpy	✓	1[9]	[30],[23],[12]	4.5.2
heat capacity	✓	1[9]	[30],[23],[12]	4.6.2
solubility of NaCl	✓	-	[33] cited in [9], [21]	4.7.1
vapour pressure	✓	1[10]	[21], [4], [25]	4.1.2
diffusivity	0 – 5 mol/kg[11]	3	[28]	4.8

[4] Batistelli, A., Calore, C., Pruess, K.: The simulator TOUGH2/EWASG for modelling geothermal reservoirs with brines and non-condensable gas. Geothermics, Vol. 26, No. 4, 1997.

[9] Chou, I.M.: Phase relations in the system NaCl-KCl-H2O. III: solubilities of halite in vapour-saturated liquids above 445 °C and redetermination of phase equilibrium properties in the system NaCl-H2O. Geochimica et Cosmochimica Acta 51, 1987.

[12] Daubert, T. E. and Danner, R. P.: Physical and thermodynamic properties of pure chemicals: data compilation. Design Institute for Physical Property Data, 1989.

[21] Haas, J.L.: Physical Properties of the Coexisting Phases and Thermochemical Properties of the H2O Component in Boiling NaCl Solutions. USGS, Geological Survey Bulletin 1421-A, Washington D.C., 1976.

[23] International Association for Properties of Water and Steam: Release on the IAPWS Industrial Formulation 1997 for the Thermodynamic Properties of Water and Steam. 1997. Homepage: http://www.iapws.org.

[25] IFC: A formulation of thermodynamic properties of ordinary water substance. International Formulation Committee Secretariat, Düsseldorf, 1967.

[28] Landolt-Börnstein: Zahlenwerte und Funktionen aus Physik * Chemie * Astronomie * Geophysik und Technik; 2. Band Eigenschaften der Materie in ihren Aggregatzuständen; 5. Teil Transportphänomene * Kinetik * homogene Gasgleichgewichte; Bandteil a Transportphänomene I (Viskosität und Diffusion). Springer-Verlag, 1969.

[30] Michaelides, E.E.: Thermodynamics properties of geothermal fluids. Geothermal Resources Council Transactions, (5):361-364, 1981.

[31] Phillips, S.L., Igbene, A., Fair, J.A., Ozbek, H., Tavana, M.: A Technical Databook for Geothermal Energy Utilization. Lawrence Berkeley Laboratory, University of California, LBL-12810, 1981.

[33] Potter, R.W., II, Babcock, R.S., Brown, D.L.: A new method for determining the solubility of salts in aqueous solutions at elevated temperatures. J. Research U.S. Geol. Surv. 5, no.3, 1977.

[49] Yusufova, V.D., Pepinov, R.I., Nikolaev, V.A., Guseinov, G.M.. Inzh.-Fiz. Zh., 29, 600,1975.

[9] referring to the enthalpie of mixing//referring to heat of dissolution

[10] accuracy of correction for NaCl-content is unclear

[11] not sufficient data on varying temperature and/or pressure

Tab. C. 3 Parameters for water with dissolved CO_2

parameter	range of validity	need for research	sources	section
density	unclear[12]	0	[16]	4.2.3
viscosity	-	3	-	0
thermal conductivity	-	3	-	4.4.3
enthalpy	✓	-	[14] [13]	4.5.3
heat capacity	✓	-	-	4.6.3
solubility of CO_2	✓	-	[41]	4.7.2
vapour pressure	-	3	-	4.1.3
diffusivity	-	3[14]	[28]	4.8

[14] Duan, Z. and Sun, R.: An improved model calculating CO2 solubility in purewater and aqueous NaCl solutions from 273 to 533 k and from 0 to 2000 bar. Chemical Geology, (193):257–271, 2003.

[16] Garcia, J.E.: Density of aqueous solutions of CO_2. Technical Report LBNL-49023, Lawrence Berkeley National Laboratory, Berkeley, CA, 2001.

[28] Landolt-Börnstein: Zahlenwerte und Funktionen aus Physik * Chemie * Astronomie * Geophysik und Technik; 2. Band Eigenschaften der Materie in ihren Aggregatzuständen; 5. Teil Transportphänomene * Kinetik * homogene Gasgleichgewichte; Bandteil a Transportphänomene I (Viskosität und Diffusion). Springer-Verlag, 1969.

[41] Spycher, N.F., Pruess, K., Ennis-King, J.: CO_2-H_2O mixtures in the geological sequestration of CO_2. I. Assessment and calculation of mutual solubilities from 12 to 100 °C and up to 600 bar. Geochimica et Cosmochimica Acta, 67 (16): 3015-3031, 2003.

[12] probably ok
[13] [14] provides a sufficient formulation for the enthalpy of dissolution.
[14] No data on varying temperature and/or pressure

Tab. C. 4 Parameters for water with dissolved NaCl and CO_2

parameter	range of validity	need for research	sources	section
density	unclear[12]	0	[17]	4.2.4
viscosity	totally out of range	3	[27]	4.3.4
thermal conductivity	-	3	-	4.4.4
enthalpy	✓	1 (as in 4.5.2)	[4]	4.5.4
heat capacity	✓	1 (as in 4.5.2)		4.6.4
solubility of NaCl and CO2	✓	-	[40],[14]	4.7.3
vapour pressure	-	3	-	4.1.4
diffusivity	-	3	-	4.8

[4] Batistelli, A., Calore, C., Pruess, K.: The simulator TOUGH2/EWASG for modelling geothermal reservoirs with brines and non-condensable gas. Geothermics, Vol. 26, No. 4, 1997.

[14] Duan, Z. and Sun, R.: An improved model calculating CO2 solubility in purewater and aqueous NaCl solutions from 273 to 533 k and from 0 to 2000 bar. Chemical Geology, (193):257–271, 2003.

[17] Garcia, J.E.: Fluid Dynamics of Carbon Dioxide Disposal into Saline Aquifers. Dissertation, University of California, Berkeley, 2003.

[27] Kumagai, A., Yokoyama, Ch.: Viscosities of Aqueous NaCL Solutions Containing CO_2 at High Pressures. J. Chem. Eng. Data, 44, 227-229, 1999.

[40] Spycher, N.F., Pruess, K.: CO2-H2O Mixtures in the Geological Sequestration of CO2. II. Partitioning in Chloride Brines at 12-100°C and up to 600 bar. Geochimica Cosmochim. Acta, in press. (LBNL-56334), 2005.

Tab. C. 5 Parameters for pure CO_2

parameter	range of validity	need for research	sources	section
density	✓	-	[39]	5.3.1
viscosity	✓	-	[15], [46]	5.4.1
thermal conductivity	✓	-	[46], [38]	5.5.1
enthalpy	✓	-	[39]	5.6.1
heat capacity	✓	-	[39]	5.7.1
vapour pressure	✓	-	[39]	5.1.1
diffusivity	✓	3[15]	[28]	5.9

[15] Fenghour, A., Wakeman, W.A., Vesovic, V.: The viscosity of carbon dioxide. GJ. Phys. Chem. Ref. Data, 27(1):31-44, 1998.

[28] Landolt-Börnstein: Zahlenwerte und Funktionen aus Physik * Chemie * Astronomie * Geophysik und Technik; 2. Band Eigenschaften der Materie in ihren Aggregatzuständen; 5. Teil Transportphänomene * Kinetik * homogene Gasgleichgewichte; Bandteil a Transportphänomene I (Viskosität und Diffusion). Springer-Verlag, 1969.

[38] Span, R. und Flacke, N.: Thermophysikalische Eigenschaften von CO_2. In: DKV-Statusbericht Nr. 20 „Kohlendioxid - Besonderheiten und Einsatzchancen als Kältemittel“, (3. überarbeitete Ausgabe 2006), Deutscher Kälte- und Klimatechnischer Verein e.V. - DKV , Stuttgart, 2006.

[39] Span, R., Wagner, W.: A new equation of state for carbon dioxide covering the fluid region from the triple-point temperature to 1100 K at pressures up to 800 Mpa. J. Phys. Chem. Ref. Data, 25(6):1509-1596, 1996.

[46] Vesovic, V., Wakeham, W.A., Olchowy, G.A., Sengers, J.V., Watson, J.T.R., Millat, J.: The Transport properties of Carbon Dioxide. J. Phys. Chem. Ref. Data, Vol. 19, No. 3, 1990.

[15] formulation required

Tab. C. 6 Parameters for CO_2 with dissolved H_2O

parameter	range of validity	need for research	sources	section
density	?	gas: 2, liquid: 3	[4], [17]	5.3.2
viscosity	?	gas: 2, liquid: 3	[4]	5.4.2
thermal conductivity	-	3	-	5.5.2
enthalpy	?	gas: 2, liquid: 3	[4]	5.6.2
heat capacity	?	gas: 2, liquid: 3	-	5.7.2
solubility of H_2O	✓	-	[41]	5.8.3
vapour pressure	-	3	-	5.1.2
diffusivity	-	3	-	5.9

[4] Batistelli, A., Calore, C., Pruess, K.: The simulator TOUGH2/EWASG for modelling geothermal reservoirs with brines and non-condensable gas. Geothermics, Vol. 26, No. 4, 1997.

[17] Garcia, J.E.: Fluid Dynamics of Carbon Dioxide Disposal into Saline Aquifers. Dissertation, University of California, Berkeley, 2003.

[41] Spycher, N.F., Pruess, K., Ennis-King, J.: CO_2-H_2O mixtures in the geological sequestration of CO_2. I. Assessment and calculation of mutual solubilities from 12 to 100 °C and up to 600 bar. Geochimica et Cosmochimica Acta, 67 (16): 3015-3031, 2003.

Tab. C. 7 Parameters for NaCl

parameter	range of validity	need for research	sources	section
density	✓	-	[26] cited in [51]	6.1
enthalpy	?	?	[12]	6.2
heat capacity	?	?	[12]	6.3

[12] Daubert, T. E. and Danner, R. P.: Physical and thermodynamic properties of pure chemicals: data compilation. Design Institute for Physical Property Data, 1989.

[26] Kern, H.: Elastic wave velocity in crustal and mantle rocks at high pressure and temperature: the role of High-low quartz transition and of dehydration reactions. Phys. Earth. Planet. Inter. 29, 1982.

[51] Zimmer, U.: Quantitative Untersuchung zur Mikrorissigkeit aus akustischen Gesteinseigenschaften am Beispiel von Steinsalz und Anhydrit. Dissertation, Fakultät VI – Bauingenieurwesen und Angewandte Geowissenschaften der Technischen Universität Berlin, 1991.

Gesellschaft für Anlagen- und Reaktorsicherheit (GRS) mbH

Schwertnergasse 1
50667 Köln
Telefon +49 221 2068-0
Telefax +49 221 2068-888

Forschungsinstitute
85748 Garching b. München
Telefon +49 89 32004-0
Telefax +49 89 32004-300

Kurfürstendamm 200
10719 Berlin
Telefon +49 30 88589-0
Telefax +49 30 88589-111

Theodor-Heuss-Straße 4
38122 Braunschweig
Telefon +49 531 8012-0
Telefax +49 531 8012-200

www.grs.de

ISBN 978-3-939355-10-6